UNIVERSITY OF CALIFORNIA SAN DIEGO

Nucleolar Stress and RNA Toxicity in C9ORF72 Amyotrophic Lateral Sclerosis and Frontotemporal Dementia

A dissertation submitted in partial satisfaction of the
requirements for the degree of
Doctor of Philosophy

in

Neurosciences

by

Olubankole Aladesuyi Arogundade

Committee in charge:

Professor John Ravits, Chair
Professor Susan Ackerman
Professor Don Cleveland
Professor Robert Rissman
Professor Eugene Yeo

2020

The Dissertation of Olubankole Aladesuyi Arogundade is approved, and it is acceptable in quality and form for publication on microfilm and electronically:

Chair

University of California San Diego

2020

DEDICATION

In recognition to all the teachers of my past who have tried, no matter how difficult I may have made it, to teach me everything that I now know; for encouraging me to persevere through every difficulty; for challenging me to surpass my limitations, this thesis is dedicated to my educators and friends.

EPIGRAPH

Progress is the attraction that moves humanity.

—Marcus Garvey

TABLE OF CONTENTS

LIST OF FIGURES

LIST OF TABLES

ACKNOWLEDGEMENTS

I would like to acknowledge Professor John Ravits for his support as the chair of my committee and for his phenomenal guidance as my mentor. I would also like to acknowledge the Neurosciences Graduate Program of 2014-2020 for providing the environment and resources that have enabled me to complete this dissertation. Their support has inspired me to grow in immeasurable ways. Most importantly, I would like to acknowledge the patients and families that have contributed to this research and whose goal it is to find a cure for amyotrophic lateral sclerosis and frontotemporal dementia. Their eagerness to facilitate progress has been a constant motivation in completing this work.

Chapter 1, in part, has been submitted for publication of the material as it may appear in The Development of Neurotherapeutics in the Era of Translational Medicine, 2020. Aladesuyi Arogundade, Olubankole; Jiang, Jie; Ravits, John, Elsevier, 2020. The dissertation author was the coauthor of this chapter.

Chapter 2, in full, is a reformatted reprint of the material as it appears in Aladesuyi Arogundade, Olubankole; Stauffer, Jennifer; Saberi, Shahram; Diaz Garcia, Sandra; Malik, Sahana; Basilim, Hani; Rodriguez, Maria; Ohkubo, Takuya; Ravits, John. Acta Neuropathologica, 2019. The dissertation author was the coauthor of this paper.

Chapter 3, in part is currently being prepared for submission for publication of the material. Aladesuyi Arogundade, Olubankole; Nguyen, Sandra; Leung, Ringo; Wainio, Danielle; Rodriguez, Maria; Ravits, John. The dissertation author was the primary author of this material.

VITA

2014	Bachelor of Sciences, University of Illinois, Urbana Champaign
2015, 2018	Teaching, Academic Connections University of California, San Diego
2020	Doctor of Philosophy, University of California San Diego

PUBLICATIONS

Aladesuyi Arogundade, Olubankole; Stauffer, Jennifer; Saberi, Shahram; Diaz Garcia, Sandra; Malik, Sahana; Basilim, Hani; Rodriguez, Maria; Ohkubo, Takuya; and Ravits, John, "Antisense RNA foci are associated with nucleoli and TDP-43 mislocalization in C9orf72-ALS/FTD: A quantitative study". *Acta Neuropathologica*, vol.137(3), 527-530 2019.

Aladesuyi Arogundade, Olubankole, Jiang, Jie , and Ravits, John, "Unravelling the molecular biology of C9ORF72 repeat expansions in amyotrophic lateral sclerosis-frontotemporal dementia: implications for therapy". *Neurotherapeutics in the Era of Translational Medicine*, Elseiver, 2020 (*in press*).

Aladesuyi Arogundade, Olubankole; Nguyen, Sandra; Leung, Ringo; Wainio, Danielle; Rodriguez, Maria; and Ravits, John, "Biphasic nucleolar stress in C9orf72 and sporadic ALS spinal motor neurons correlates with TDP-43 mislocalization". *Acta Neuropathologica Communications*, 2020 (*in preparation*).

ABSTRACT OF THE DISSERTATION

Nucleolar Stress and RNA Toxicity in C9ORF72 Amyotrophic Lateral Sclerosis and Frontotemporal Dementia

by

Olubankole Aladesuyi Arogundade

Doctor of Philosophy in Neurosciences

University of California San Diego, 2020

Professor John Ravits, Chair

In 2011, two independent groups discovered that hexanucleotide repeat expansion in C9orf72 cause amyotrophic lateral sclerosis and frontotemporal dementia (C9-ALS/FTD). Since this paramount discovery, a race has ensued to understand the mechanisms underlying neurodegeneration and develop a cure for this fatal disease. Bidirectional transcription of C9orf72 complicates gain of function toxicity and treatment. Both sense and antisense RNA can be toxic as repeat-containing RNA and when translated into dipeptide repeat proteins (DPRs). Perhaps due to the gap between identifying C9orf72 repeat expansion and bidirectional transcription, the field has mainly focused on unravelling disease mechanisms involving toxicity from sense RNA

and sense-encoded DPRs, and contributions from antisense RNA are less well understood.

However, the relatively few studies that have investigated the role of antisense RNA in disease have found evidence that it is important in toxicity and perhaps an important target for effective treatment. Both sense and antisense RNA form peri-nucleolar RNA foci, but unlike sense RNA, peri-nucleolar antisense RNA foci are intrinsically related to pathology. Peri-nucleolar antisense but not sense RNA foci are significantly increased in regions vulnerable to neurodegeneration and correlate with clinical symptoms of FTD. Moreover, increased peri-nucleolar antisense but not sense RNA foci correlate with TAR DNA binding protein (TDP-43) mislocalization, the hallmark proteinopathy of C9-ALS/FTD. Additionally, morphological alterations comprising shrunken nucleoli, nuclei and cytoplasm occur in C9-ALS and sporadic ALS spinal motor neurons, but perplexingly, these alterations occur in the absence of peri-nucleolar antisense RNA foci or TDP-43 mislocalization. This raises the possibility that nucleolar antisense RNA foci formation and TDP-43 mislocalization occur later in disease following morphological abnormalities. Nevertheless, antisense RNA may be toxic before forming peri-nucleolar RNA foci and may remain a key target for effective therapy. Thus, disease-relevant phenotypes in cellular models, such as C9orf72 patient fibroblasts, may prove useful to measure the benefits of reducing potential gain of function toxicity from the C9orf72 sense and antisense strands.

Introduction

Hexanucleotide repeat expansion in C9orf72 is the leading cause of amyotrophic lateral sclerosis and frontotemporal dementia. Loss of function and gain of function mechanisms have been proposed to contribute to toxicity. Bi-directional transcription of the repeat expansion further complicates mechanisms underlying gain of function toxicity. The few years gap between the discovery of C9orf72 repeat expansion in 2011 and the first publications acknowledging possible gain of function toxicity from antisense RNA and antisense encoded dipeptide repeat proteins have generated a bias in the focus of research and subsequent knowledge of gain of function toxicity. Most research has focused on the sense strand and has neglected to investigate how gain of function toxicity may occur from the antisense strand, particularly toxicity resulting from antisense RNA. The relatively few studies that have alluded to antisense strand-related toxicity suggest that the antisense strand may be a necessary target for effective therapy. Thus, the purpose of this thesis is to increase understanding of how antisense RNA correlate to neuropathology and provide insight to whether the antisense strand is an important target for therapy.

The aim of the first chapter is to provide a broad overview of what is known about the mechanisms and disease pathways involved in C9-ALS/FTD and to discuss current and future efforts aimed at producing an effective therapy.

The aim of the second chapter is to introduce novel key aspects of how the nucleolar localization of C9orf72 antisense RNA transcripts correlate to clinical and neuropathological aspects of C9-ALS/FTD. Significantly, we show that peri-nucleolar antisense RNA foci are increased in regions of neurodegeneration and are intrinsically related to TDP-43 mislocalization.

The third chapter extends the findings of the second chapter to previously uncharacterized neuropathology involving nucleolar stress in C9-ALS and sporadic ALS spinal motor neurons. We have shown that the nucleolar localization of antisense RNA transcripts is important to disease, and now demonstrate that neuropathology occurs at the nucleolus and correlates with peri-nucleolar antisense RNA transcripts and TDP-43 mislocalization.

The fourth chapter provides insight to methods testing the hypothesis that antisense RNA transcripts are integral in disease and are an important target for therapy. In this chapter, the disease-relevant phenotype involving nucleolar stress in C9orf72 patient fibroblasts is presented along with two approaches that aim to mitigate toxicity from C9orf72 sense and antisense RNA: antisense oligonucleotides and CRISPR interference.

Chapter 1

Unravelling the molecular biology of C9ORF72 repeat expansions in amyotrophic lateral sclerosis-frontotemporal dementia: implications for therapy

1.1 INTRODUCTION

The literature bringing together amyotrophic lateral sclerosis (ALS) and frontotemporal dementia (FTD), two devastating, adult-onset neurodegenerative disorders with distinct clinical presentations, can be traced nearly to their original descriptions. ALS was first described by the French neurologist Jean-Martin Charcot in 1869 and is the most common motor neuron disease. It is characterized by rapid progression of muscle weakness leading to paralysis and respiratory failure caused by the loss of upper and lower motor neurons and is usually fatal within 3-5 years (Taylor et al., 2016). FTD was first described by Arnold Pick in 1892 and was originally called Picks Disease, a term now reserved for cases with pathological verification of abnormal tau aggregates called Pick bodies. FTD is characterized by behavioral and personality changes, deficits in executive functions, and/or language impairments due to the degeneration of neurons in the frontal and temporal lobes (Olney et al., 2017). While most cases of either ALS or FTD are sporadic, about 10 or more percent of each occur in families, almost always in a

dominant pattern (Ling et al., 2013). Some of the genes that cause ALS, notably SOD1, usually do not cause dementia and some of the kinships that have FTD, notably caused by granulin (GRN) mutations, infrequently have ALS. But a large group of families with either ALS or FTD or overlap ALS-FTD in an autosomal genetic pattern have been identified and found to be caused by a hexanucleotide repeat expansion in the C9orf72 (abbreviated from its genomic loci in chromosome 9 open reading frame 72) gene, the most common genetic cause of both ALS and FTD (Dejesus-hernandez et al., 2011; Gijselinck et al., 2012; Renton et al., 2011). This mutation accounts for 40% of familial ALS, 5–10% of sporadic ALS, 12–25% of familial FTD, and 6–7% of sporadic FTD cases (Nguyen et al., 2018). It is now recognized that ALS and FTD belong to a continuous disease spectrum with clinical, pathological and genetic overlaps.

Identification of the C9orf72 locus added ALS/FTD (referred to as C9-ALS/FTD hereafter) to more than 40 other repeat expansion disorders (e.g., myotonic dystrophy, Huntington's disease, and several spinocerebellar ataxias) (La Spada AR and JP, 2010). Based on lessons learned from these other repeat expansion disorders and initial pathological characterization of C9orf72 postmortem tissues, three disease mechanisms have been proposed: (1) loss of C9orf72 function, (2) toxicity from repeat containing RNAs, which are bidirectionally transcribed, form foci, and perhaps sequester key RNA binding proteins (RBPs), and (3) toxicity from production of dipeptide repeat (DPR) proteins through a non-canonical repeat-associated non-AUG dependent (RAN) translation which also happens bidirectionally. Although the C9orf72 mutation was only identified 8 years ago, research progress has been rapid, and significantly influenced current thinking about the pathogenesis and treatment of neurological disorders. A number of trials directed at C9-ALS/FTD are now underway or in early stages of development.

1.2 PATHOGENIC MECHANISMS of C9-ALS/FTD

1.2.1 C9orf72 hexanucleotide repeat expansions

The hexanucleotide repeat expansion is localized in the first intron of the C9orf72 gene (Fig. 1.1a). The size of the repeats vary dramatically among C9orf72 patients. The threshold pathogenic repeat size is unknown, but 30 is used in most publications. Healthy individuals have typically fewer than 11 repeats, whereas most patients have several hundreds to thousands (Beck et al., 2013; Buchman et al., 2013; Dejesus-hernandez et al., 2011; Dobson-Stone et al., 2013; Hübers et al., 2014; Ishiura et al., 2012). A small percentage of patients have shorter expansions, 45–80 repeats (Gijselinck et al., 2016). Unlike Huntington's disease and other CAG repeat expansion disorders where a phenomenon called anticipation causes increased size and a more severe phenotype in offspring, increased C9orf72 repeat size in offspring is only reported in a few families (Proudfoot et al., 2014; Van Mossevelde et al., 2017). The correlation of the repeat size and clinical and pathological characteristics has also been explored, and the results are variable, depending on patient size, ethnic background, and tissues in which expansion size was measured (Beck et al., 2013; Benussi et al., 2014; Blitterswijk et al., 2013; Dols-Icardo et al., 2014; Gijselinck et al., 2016; Hübers et al., 2014; Nordin et al., 2014; Suh et al., 2015). Longer repeat sizes seem to be associated with a survival disadvantage (Blitterswijk et al., 2013) and an earlier onset of disease (Beck et al., 2013; Gijselinck et al., 2016; Hübers et al., 2014). Interestingly, individuals with an intermediate repeat length in blood or fibroblast DNAs have significant increases of repeat size (repeat instability) and variation in repeat size (mosaicism) in different regions of the central nervous system (Blitterswijk et al., 2013; Gijselinck et al., 2016; Nordin et al., 2014). The mechanisms of such instability and somatic mosaicism are not well understood, but need to be considered when using repeat size from peripheral blood and fibroblast cells for genetic counselling.

1.2.2 Loss of C9orf72 protein function

In the original discovery, C9ORF72 was described to have three transcript variants, variant 1 (NM_145005.6), variant 2 (NM_018325.5) and variant 3 (NM_001256054.2) although this naming scheme has been inconsistent in the literature (Fig. 1.1b). Transcript variants 2 and 3 are transcribed from two alternatively spliced exons, exon 1B and exon 1A, respectively, and encode a full-length C9orf72 protein with 481 amino acids. The expanded GGGGCC repeat is located in an intron between these two exons. Variant 1 comprising 5 of 11 exons produces a predicted "short isoform" protein of 222 amino acids, which harbors a unique lysine residue at the C-terminus. However, it remains controversial whether the predicted C9orf72 short isoform is expressed in nature. Xiao et al. developed antibodies that selectively detect either the full-length or the predicted short C9orf72 protein isoforms and showed that the full-length protein was expressed within the cytoplasm whereas the short isoform was preferentially expressed on the nuclear membrane (Xiao et al., 2015). However, using an antibody against the N-terminal region of C9orf72 that could recognize both the full-length and the predicted short isoform C9orf72, we demonstrated that C9orf72 is predominantly, if not exclusively, expressed as the full-length protein in human and mouse tissues (Saberi et al., 2017). This is further confirmed by another study using novel knock-out validated C9orf72 monoclonal rat and mouse antibodies (Frick et al., 2018).

While the expression of C9orf72 protein isoforms in human cells has yet to be unequivocally established, our understanding of the physiological function of the C9orf72 protein is emerging. Bioinformatic analysis shows that C9orf72 has high homology with the DENN (differentially expressed in normal and neoplastic cells) protein family, which function as guanine nucleotide exchange factors (GEFs) activating RAB GTPases to regulate membrane trafficking (Levine et al., 2013; Zhang et al., 2012). In agreement with this, C9orf72 interacts with Smith-Magenis syndrome chromosomal region candidate gene 8 (SMCR8) and WD repeat containing protein 41 (WDR41), and this complex possesses GEF activity for different Rab proteins and

plays a role in multiple steps of autophagy/lysosomal pathways (Amick et al., 2016; Farg et al., 2014; Jung et al., 2017; Sellier et al., 2016; Sullivan et al., 2016; Ugolino et al., 2016; Webster et al., 2016; Yang et al., 2016). Several Rab proteins are substrates of C9orf72, including Rab1, Rab3, Rab5, Rab7, Rab8a, Rab11 and Rab39(Farg et al., 2014; Sellier et al., 2016; Sullivan et al., 2016; Webster et al., 2016; Yang et al., 2016).

Early on, it was proposed that the presence of an enormous GGGGCC repeat expansion in the intron region may lead to abortive C9orf72 transcripts, thus depriving cells of an important player in autophagy/lysosomal functions and leading to neurodegeneration (Fig. 1.2a). Indeed, reduced transcript expression was the case for variants 2 and 3 as they were found to be attenuated in patient lymphoblast cells and frontal cortex (Dejesus-hernandez et al., 2011). Alternative explanations for reduced C9orf72 transcript expression have also been proposed. For example, it has been suggested that CpG island regions 5FL of GGGGCC repeats cause cytosine hypermethylation of CG dinucleotides and silencing of C9ORF72. This is similar to epigenetic silencing by CGG expansion in the 5'UTR of FMR1 causing fragile X mental retardation syndrome (Coffee et al., 1999). In C9orf72 patients, the CpG islands are hypermethylated (Xi et al., 2013), as is the repeat itself (Xi et al., 2015). Additionally, trimethylation of histones H3 and H4 at the C9orf72 locus has been detected in C9orf72 patient blood (Belzil et al., 2013), providing a third pathway contributing to downregulation of C9orf72 gene expression and loss of C9orf72 protein function.

Since the initial identification of reduced C9orf72 RNA transcripts in patient lymphoblasts and frontal cortex, many independent groups have extended these findings with one or more C9ORF72 transcript variants in other cell lines such as induced pluripotent stem (iPS) neurons and patient tissues, including cerebellum (Dejesus-hernandez et al., 2011; Gijselinck et al., 2012; van Blitterswijk et al., 2015). Several studies also suggest that, consistent with reduced RNAs, C9orf72 proteins are reduced in the frontal and temporal cortex in patients (Frick et al., 2018; Saberi et al., 2017; Waite et al., 2014). However, demonstrating reduced C9orf72 protein levels has been more challenging due to the low abundance of C9orf72 protein and a lack of antibodies

for its detection.

Assuming C9orf72 has an essential role in autophagy and lysosomal functions, one could reasonably conclude that impairment of these functions is involved in ALS and FTD. A growing body of literature, including studies in cellular and animal models as well as human trials, support this. In human cell lines and iPSC-derived neurons from C9orf72 patients, knockdown of C9orf72 inhibits the induction of autophagy, leading to accumulation of autophagy substrates, including P62 (Sellier et al., 2016; Webster et al., 2016). Accumulated P62, is also observed in spleens of C9orf72 knockout mice (Aoki et al., 2017). IPS neurons from C9orf72 patients also showed increased sensitivity to autophagy inhibition, suggesting that reductions in C9orf72 levels contribute to cellular stress (Almeida et al., 2013). Recently, Burberry et al., found that an environment with reduced abundance of immune-stimulating bacteria protects C9orf72-mutant mice from premature mortality and significantly ameliorates their underlying systemic inflammation and autoimmunity (Burberry et al., 2020). Additionally, inflammatory phenotypes in mutant mice can be suppressed by reducing the microbial burden with broad spectrum antibiotics or by transplanting gut microfora from a protective environment, suggesting C9orf72 functions to prevent microbiota from inducing a pathological inflammatory response (Burberry et al., 2020).

Studies in lower species model systems suggest that C9orf72 is critical for the development of motor systems and motor functions. In zebrafish, blocking C9orf72 translation or splicing with antisense morpholino oligonucleotides resulted in axonopathy and reduced mobility (Ciura et al., 2013). Overexpressing C9orf72 that lacks the complete DENN protein domain also mimics the morpholino experiment, suggesting the indispensability of the complete DENN protein domain (Yeh et al., 2018). Similarly, deletion of C9orf72 orthologue in Caenorhabditis elegans led to age-dependent motility deficits, paralysis, and increased susceptibility to environmental osmotic stress (Therrien et al., 2013). Primary hippocampal neurons cultured from C9orf72 knockout mice have reduced dendritic arborization and spinal density, suggesting its role in neuronal morphogenesis (Ho et al., 2019).

Despite evidence supporting the importance of C9orf72 in human cells and lower organisms, much evidence counters that loss of function is the main disease driver for C9-ALS/FTD. Only one sporadic ALS patient has ever been found to carry a splice site mutation potentially causing a heterozygous loss of function, and it is unclear whether this mutation is the cause of disease or a variant of undetermined significance (Harms et al., 2013; F. Liu et al., 2016). Further, one would expect that patients homozygous for C9orf72 repeat expansions (and thus with less C9orf72 than heterozygotes) will have more severe symptoms of disease, but this is not the case (Fratta et al., 2013). Although not conclusive, these human studies do not support a loss of function as the disease-driving mechanism.

Additionally, sustained reduction of mouse C9orf72 to 30–40% of its normal level throughout the CNS using antisense oligonucleotides (ASOs) is well tolerated, producing no behavioral or pathological features characteristic of ALS/FTD (Lagier-Tourenne et al., 2013). Several ubiquitous or neuronal/glial-specific C9orf72 knockout mice have also been characterized and none of these mice produced any ALS/FTD-like pathological or behavioral phenotypes (Atanasio et al., 2016; Burberry A, Suzuki N, Wang JY, Moccia R, Mordes DA, 2016; Koppers et al., 2015; Lagier-Tourenne et al., 2013; O'Rourke et al., 2016; Sudria-Lopez et al., 2016; Sullivan et al., 2016; Ugolino et al., 2016). Interestingly, global C9orf72 knockout mice develop a proinflammatory/autoimmune phenotype with enlarged spleen and lymph nodes, consistent with the observation that C9orf72 ALS/FTD patients also show an increased prevalence of autoimmune disease (Miller et al., 2016). These findings are particularly noteworthy, given growing appreciation of the role of the immune system in a variety of neurodegenerative diseases (Molteni and Rossetti, 2017), yet it is thought that C9orf72 loss-of-function alone is not the main ALS/FTD disease driver in mice.

Overall, C9orf72 loss of function by itself is insufficient to precipitate disease, and intriguingly, reduced expression of the mutant C9orf72 allele might actually be protective, potentially by decreasing the transcription of toxic repeat-containing C9orf72 RNAs (Liu et al., 2014; McMillan et al., 2015; Russ et al., 2015). Alternatively, given the role of C9orf72 in

autophagy and microglial function, pathways implicated in ALS and FTD, haploinsufficiency might contribute to the disease process in synergy with the gain-of-toxicity mechanism.

1.2.3 Gain of function: DPR protein-mediated toxicity

Despite being in an intronic region, the hexanucleotide repeat of bidirectionally transcribed C9orf72 RNA transcripts can be translated through an unusual mechanism, RAN translation, in every reading frame to produce five different dipeptide repeat (DPR) proteins [poly(GA), poly(GP), poly(GR), poly(PR) and poly(PA)]. These might drive toxicity in C9-ALS/FTD. Poly(GA) and poly(GR) are uniquely translated from the sense GGGGCC RNA; poly(PR) and poly(PA) are uniquely translated from the antisense CCCCGG RNA, and poly(GP) can be translated from both sense and antisense directions (Fig. 1.2b). Accumulations of DPR proteins have been detected using either immunohistochemical assays for DPR inclusions or immunoblotting and ELISA-based assays for the soluble form (Ash et al., 2013; Gendron et al., 2013; Mori et al., 2013; Mori et al., 2013a; Zu et al., 2013). DPR inclusions are widely distributed throughout the brains of C9-ALS/FTD but, interestingly, are less frequent in the spinal cord (Ash et al., 2013; Gomez-Deza et al., 2015; Mackenzie et al., 2015; Schipper et al., 2016; Schludi et al., 2015). Of the five different types of DPRs, those encoded by the sense-strand, poly(GA), poly(GP), and poly(GR), form inclusions far more frequently than those encoded by the antisense-strand, poly(PA) and poly(PR), and they can co-occur in a same neuron (Mori et al., 2013a). Based on the staining patterns, they can be categorized into neuronal cytoplasmic inclusions, intranuclear inclusions, dystrophic neurites, and diffuse dendritic or cytoplasmic staining. So far, no DPR pathology has been reported in astrocytes, microglia, or oligodendrocytes. SDS-soluble poly(GA) and poly(GP) can also be detected in CSF and blood by immunoassay which could prove to be useful biomarkers specific to C9-ALS/FTD for current and future clinical trials (Floeter and Gendron, 2018; Lehmer et al., 2017; Su et al., 2014; Tania F. Gendron et al., 2017).

Several clinico-pathological studies have sought to determine whether or not DPR proteins are the primary culprit of C9-ALS/FTD. Mackenzie et al. showed moderate associations of

poly(GA)-positive dystrophic neurites with local degeneration in the frontal cortex (Mackenzie et al., 2015) and in another study by Davidson, et al., more abundant neural cytoplasmic inclusions of poly(GA) in cortical, hippocampal, and motor regions were associated with earlier age at symptom onset (Davidson et al., 2014). In a cohort of 40 C9-ALS/FTD cases, middle frontal gyrus inclusions of poly(GR) but not poly(GA) or poly(GP) were strongly correlated with neurodegeneration, supporting that DPRs containing the arginine residue are the most toxic (Sakae et al., 2018). Recently, we found that in C9orf72 ALS, poly(GR) inclusions were increased in areas of neurodegeneration, frontal and motor cortex and the anterior horn of the spinal cord, compared to areas that are spared from neurodegeneration (parietal and occipital cortex and the posterior horn of the spinal cord) (Saberi et al., 2017). Compared to the other DPR species, poly(GR) was also unique in colocalizing with phosphorylated TDP-43, a hallmark pathology observed in ALS/FTD. Eighty percent of poly(GR) dendritic inclusions also had phosphorylated TDP-43 whereas this co-occurrence was nearly unseen for poly(GA) and poly(GP)]. Notably, DPRs exclusively encoded by the C9orf72 antisense transcript, poly(PA) and poly(PR) were rarely seen in the brain and spinal cord.

To move from pathology to pathogenesis, several groups have expressed individual DPR proteins in isolation in yeast (Jovičič et al., 2015), mammalian cells (Kanekura et al., 2016; Lee et al., 2016; May et al., 2014; Tao et al., 2015; Wen et al., 2014; Yamakawa et al., 2015; Zhang et al., 2014; Zu et al., 2011), Drosophila (Boeynaems et al., 2016; Freibaum et al., 2015; Lee et al., 2016; Mizielinska et al., 2014; Wen et al., 2014; Yang et al., 2015a), zebrafish (Ohki et al., 2017; Swaminathan et al., 2018; Swinnen et al., 2018), and mice (Choi et al., 2019; Schludi et al., 2017; Yong-Jie Zhang et al., 2017; Zhang et al., 2019, 2016). Of all the DPR proteins, poly(GR) and poly(PR) containing the arginine residue have proven to be the most toxic. Synthetic 20-mer poly(GR) and poly(PR) can cause rapid death of U2OS cells and cultured human astrocytes when added exogenously (Kwon et al., 2014). These DPR proteins also consistently show toxicity when overexpressed in several different cell lines, such as HEK293T cells, NSC-34 cells, and iPSC-derived neurons (Lee et al., 2016; Tao et al., 2015;

Wen et al., 2014). In Drosophila, targeted expression of poly(GR) or (PR) resulted in eye degeneration, motor deficits, and reduced survival (Boeynaems et al., 2016; Freibaum et al., 2015; Lee et al., 2016; Mizielinska et al., 2014; Wen et al., 2014; Yang et al., 2015a). Finally, AAV-mediated or transgenic expression of poly(GR) and poly(PR) in mice caused age-dependent neurodegeneration, brain atrophy, and motor/memory deficits (Choi et al., 2019; Hao et al., 2019; Yong-Jie Zhang et al., 2017; Zhang et al., 2019). To a lesser extent, poly(GA) has also been shown to exert toxicity. When synthetic poly(GA) is exogenously applied to human cells or primary neurons, there is decreased survivability within two days (Flores et al., 2016). While the remaining DPR proteins, poly(PA) and poly(GP), are less likely to be the toxic species driving disease, poly(GA) has continually been shown to be toxic through overexpression in cultured cells and primary neurons (May et al., 2014; Zhang et al., 2014), zebrafish (Ohki et al., 2017; Swaminathan et al., 2018), Drosophila (Mizielinska et al., 2014), and mouse brains (Schludi et al., 2017; Zhang et al., 2016). These studies provide compelling evidence that certain DPR proteins are toxic. However, since individual DPR proteins were overexpressed, a key question remains: which (if any) of the DPR proteins are the main toxic species in C9-ALS/FTD when expressed at the endogenous levels in patients?

While DPRs have been demonstrated to be toxic in numerous animal and cellular models, many pathological studies have raised doubts about the pathogenicity of DPR inclusions, i.e. no obvious correlation exists between the abundance of these inclusions and neurodegeneration (Davidson et al., 2014; MacKenzie et al., 2013; Mackenzie et al., 2015; Schludi et al., 2015). Regions with the highest burden of DPR inclusions are cerebellum, hippocampus, and neocortex, where no significant loss of neurons occurs; and when DPRs are observed, most neurons lack TDP-43 pathology, the hallmark proteinopathy of C9-ALS/FTD. Also, DPR inclusions do not differ in the neuroanatomical distributions between FTD and ALS cases and DPR inclusions are rarely observed in spinal cord motor neurons. Countering this paucity of evidence found in pathological studies is the possibility that key factors underlying disease remain unknown. These pathological studies only detect aggregated, insoluble proteins, and it is possible that soluble DPR

species mediate toxicity. Most problematic is the lingering possibility that toxic DPR species, notably poly-PR which is all but absent in postmortem human tissues, have killed neurons, thus precluding their abundance and correlation with disease. Alternatively, CNS regions that have extensive DPR pathology but are unaffected by neurodegeneration might contain protective factors yet to be discovered. Another important issue is whether different DPR proteins, repeat RNA and DPR proteins act synergistically, potentially in conjunction with loss of function of C9orf72, to elicit downstream effects.

1.2.4 Gain of function: RNA foci-mediated toxicity

RNAs containing sense GGGGCC and antisense CCCCGG repeats are bidirectionally transcribed from the C9orf72 mutation. These repeat-containing RNAs may form complicated secondary structures, such as hairpins, i-motifs and G-quadruplexes (Fratta et al., 2012; Kovanda et al., 2015; Reddy et al., 2013), which in turn sequester RBPs into intranuclear RNA foci that can be experimentally visualized using fluorescence in situ hybridization with probes against the repeats. These RNA foci lead to depletion of the normal function of the sequestered RBPs and neuronal death. The RBP sequestration model is best demonstrated in the neuromuscular disease myotonic dystrophy 1, where the muscleblind family proteins are sequestered by the CTG repeats in the DMPK gene and cause downstream splicing changes (Rahimov and Kunkel, 2013). In C9-ALS/FTD patients, both sense and antisense RNA foci are detected in fibroblast, lymphoblast, iPSC-derived neurons, and several CNS regions of C9-ALS/FTD patients (Cooper-Knock et al., 2015; Donnelly et al., 2013; Gendron et al., 2013; Lagier-Tourenne et al., 2013; Mizielinska et al., 2013; Zu et al., 2013). RNA foci are most abundant in neurons, but also occur in astrocytes, microglia and oligodendrocytes (Gendron et al., 2013; Lagier-Tourenne et al., 2013; Mizielinska et al., 2013).

Several studies have overexpressed GGGGCC repeats with variable sizes and demonstrated deleterious phenotypes in cell culture (Wen et al., 2014), C. elegans (Wang et al., 2016), zebrafish (Swinnen et al., 2018) and Drosophila (Freibaum et al., 2015; Mizielinska et al., 2014;

Xu et al., 2013). Short or interrupted repeats are generally used, given the technical difficulties to obtain long and pure repeats. For example, adeno-associated viruses expressing 66 or 149 GGGGCC repeats were injected intraventricularly into newborn mice to induce somatic transgenesis. These mice accumulated nuclear RNA foci and inclusions of DPR proteins, and consequently exhibited hyperactivity, anxiety, antisocial behavior, and motor deficits (Chew et al., 2019, 2015). Four different groups, including ours, also generated transgenic mice expressing a bacterial artificial chromosome (BAC) that can accommodate genomic DNA from C9-ALS/FTD patients to express long repeats (up to 1000 repeats) in the context of the human gene. All of these mouse models produced sense and antisense RNA foci, as well as DPR proteins from the sense strand. Two transgenic models failed to produce neurodegeneration (O'Rourke et al., 2015; Peters et al., 2015), and our mice, expressing exons 1–5 of the human C9orf72 gene and 450 repeats, developed age-dependent increased anxiety and cognitive deficits, accompanied by the loss of hippocampal neurons, but no unusual motor phenotype (Jiang et al., 2016). In the last model expressing the full-length C9orf72 gene and 500 repeats, a subset of female mice developed an acute motor phenotype, including paralysis and decreased survival. Other females and males showed slower progression (Y. Liu et al., 2016). The reasons for differences in these mouse models are unknown but they feature different genetic backgrounds, repeat sizes, transgene insertion sites, and expression levels which can modulate induced toxicity. An in-depth comparison of all BAC models especially the accumulation of RNA foci and DPR proteins will provide insights to the toxic species leading to motor and/or cortical neuron death.

Expressing C9orf72 GGGGCC repeats in primary neurons (Wen et al., 2014), Drosophila (Xu et al., 2013; Zhang et al., 2015), and zebrafish (Swinnen et al., 2018), suggests that the toxicity arises from RNA foci because no DPR proteins were detected. However, the inability to detect DPR proteins in these studies is insufficient to exclude a role for these proteins. In two important studies, researchers generated Drosophila expressing either pure GGGGCC repeats or interrupted repeats of similar size, but with stop codons inserted in each reading frame to prevent the translation of the repeats into DPR proteins (Freibaum et al., 2015; Moens et al.,

2018). Both pure and interrupted repeats form similar levels of RNA foci. Expression of pure repeats caused toxicity and early lethality whereas the interrupted ones had no effect. In another study, Drosophila expressing 160 GGGGCC repeats in the intron formed abundant sense RNA foci in the nucleus but produced little DPR protein and no neurodegeneration, again suggesting that nuclear sense RNA foci are not sufficient to drive neurodegeneration in this model (Tran et al., 2015). There are, however, some caveats for interpreting these experiments, including whether the interrupted repeat RNAs have similar secondary structures to sequester the same key RBPs as the pure repeats, and whether RNA foci in humans may sequester RBPs that are not expressed in Drosophila.

A key to validating RNA foci-mediated toxicity is to identify the RBP(s) that are sequestered and thus lose function. Many proteins are proposed to interact with short, synthesized C9orf72 repeat RNAs in vitro, including hnRNPA1, hnRNPA3, hnRNP-H, hnRNP-H1/F, nucleolin, Pur-α, double-stranded RNA-specific editase B2 (ADARB2), RanGAP1, THO complex subunit 4 (ALYREF), serine/arginine-rich splicing factor 1 (SRSF1), SRSF2, and Zfp106 (Celona et al., 2017; Conlon et al., 2016; Donnelly et al., 2013; Haeusler et al., 2014; Lee et al., 2013; Mori et al., 2013b; Sareen et al., 2013; Xu et al., 2013). Sense RNA foci have been shown to colocalize with core paraspeckle proteins SFPQ and NONO in C9-ALS/FTD cerebellum (Bajc Česnik et al., 2019). In C9-ALS/FTD brain tissues, sense and antisense RNA foci colocalize with hnRNP A1, hnRNP H/F, SRSF2, and ALYREF (Cooper-Knock et al., 2014; Lee et al., 2013; Sareen et al., 2013). But most of these RNA-binding proteins appear to colocalize with RNA foci at a low frequency; only hnRNP H colocalizes with 70% of all sense foci detected (Lee et al., 2013). Nevertheless, key data to support RNA foci-mediated toxicity are missing (i.e. demonstrating that loss of function of any of these RBPs leads to C9orf72 diseases and upregulation of their functions can rescue phenotypes caused by C9orf72 repeat expansions).

Only a few neuropathological studies have attempted to correlate the abundance and distribution of RNA foci with C9-ALS/FTD clinical features. In a large patient population study conducted at the Mayo Clinic, patients with more antisense RNA foci in middle frontal gyrus

(cortical layers 3–6) neurons showed a later age of onset (Dejesus et al., 2017). However, a contradictory observation was made by Mizielinska et al. who showed that patients with more sense RNA foci had an earlier age of symptom onset in a small number of C9orf72 FTD patients, and antisense RNA foci showed a similar trend (Mizielinska et al., 2013). In agreement with this, antisense RNA foci are associated with nucleoli and mis-localization of TDP-43 (Aladesuyi Arogundade et al., 2019; Ash et al., 2013). Perhaps the most striking evidence supporting the possibility that RNA toxicity underlies neurodegeneration in C9-ALS/FTD is a unique case study in which nervous system was analyzed for pathology before and after death in an individual who had part of the frontal lobe dissected for epilepsy five years before the onset of FTD symptoms. Subsequently, postmortem tissue was analyzed 8 years after the symptoms onset. In this study by Vatsavayai et al., sense and antisense RNA foci (as well as DPR inclusions and neuronal loss) were found to precede both symptoms of FTD and TDP-43 pathology (Vatsavayai et al., 2016).

In summary, expressing GGGGCC repeats in model systems clearly recapitulates both cellular pathology (RNA pathology and DPR aggregates) and neuronal degeneration seen in patients, even though unphysiologically high levels of expression were used. It is also challenging to dissect the relative contributions of RNA foci or DPR proteins to disease pathogenesis since these repeats will produce both RNA foci and DPR proteins, and the relative contributions of sense and antisense repeat–containing RNAs remain unclear.

1.2.5 Synergistic mechanisms

Sense and antisense RNA foci can occur in the same cells and either have been found to co-occur with DPR proteins. However the presence of sense RNA foci does not affect the likelihood of detecting the abundant DPR species, namely poly(GP) and poly(GR) in brain and spinal cord suggesting that formation of RNA foci do not prevent (or enhance) repeat containing RNA transcripts from being transported to the cytoplasm and translated (Aladesuyi Arogundade et al., 2019). In C9-ALS/FTD patients, pathological evidence exists for both loss of C9orf72 function and gain of toxicity. Whether loss of C9orf72 function synergizes with gain of

toxicity to exacerbate ALS/FTD disease is not known. Mice with loss of C9orf72 do not develop ALS/FTD-related behavioral deficits, but additional stressors might be required as second hits to induce neurodegeneration in these mouse models. Shi et al. reported that loss of C9orf72 in human iPS-derived motor neurons impact lysosomal biogenesis and vesicular trafficking, and exacerbate toxicity to poly(GR) and poly(PR) exposure (Shi et al., 2018). Similarly, loss of C9orf72 protein sensitized cells to toxicity induced by expression of 30 and 60 GGGGCC repeats (Maharjan et al., 2017). Shao et al. bred C9orf72 knockout mice with a BAC transgenic mouse expressing the repeat-expanded full-length human C9orf72 gene to determine the synergism (Shao et al., 2019). However, since transgene overexpression would compensate for loss of the mouse C9orf72 endogenous protein, this casts doubt on such a strategy. But surprisingly, the transgenic mouse line does not express full-length C9orf72 proteins from the transgene and C9orf72 haploinsufficiency exacerbate motor behavior deficits in a dose-dependent manner (Shao et al., 2019). More recently, Zhu et al. bred mice expressing a C9orf72 transgene with 450 repeats that did not encode the C9ORF72 protein, and inactivation of one or both endogenous C9orf72 alleles inhibited autophagy and exacerbated cognitive deficits, hippocampal neuron loss, glial activation and accumulation of DRPs (Zhu et al., 2020). It is premature to say that C9orf72 loss of function induces neurodegeneration together with toxic RNA and DPR proteins. Further investigations crossing C9orf72 KO mice with transgenic mice that do not express the full-length C9orf72 proteins or injecting AAV virus expressing GGGGCC repeats into C9orf72 KO mice are needed to address this question. In addition, poly(GA) recruits poly(GR) into inclusions and reduces poly(PR) toxicity when co-expressed in human cells and Drosophila (Yamakawa et al., 2015; Yang et al., 2015b). Whether interaction between individual DPR proteins enhances or suppresses their toxicity is thus a point of interest. Poly(GA) can also induce nuclear RNA foci in cells expressing 80 GGGGCC repeats and in patient fibroblast cells, suggesting a positive feedback loop between RNA foci and DPR proteins (Zhou et al., 2017). Finally, translational frameshifting has been suggested to occur in cells expressing short C9orf72 repeats (Tabet et al., 2018) and other repeat expansions (Wojciechowska et al., 2014), which might produce chimeric

repeat peptides. However, it is unknown whether such a frameshift occurs in C9orf72 mutation carriers, but if it does, the contribution of chimeric repeat peptides to disease pathogenesis remains to be discerned.

1.3 PATHOLOGICAL CONSEQUENCES UNDERLYING C9-ALS/FTD

1.3.1 Nucleocytoplasmic transport deficits

Active transport of proteins and RNAs through nuclear pore complexes, a process called nucleocytoplasmic transport (NCT), is essential for cellular functions (Knockenhauer and Schwartz, 2016). Zhang et al. showed that RanGAP1 binds to GGGGCC repeat RNA in vitro and is sequestered into sense RNA foci. RanGAP1 activates Ran small GTPase, which plays an important role in regulating the interactions between cargo molecules and transport receptors, such as the importin and exportin family of proteins (Knockenhauer and Schwartz, 2016). In both Drosophila overexpressing 30 GGGGCC repeats and C9-ALS iPSC-derived neurons, the nucleocytoplasmic Ran gradient is decreased, and the nuclear import of proteins and nuclear export of RNAs are compromised. In addition, the repeat toxicity can be readily suppressed by increased activity of RanGAP1, suggesting the RNA foci–mediated NCT deficit is a fundamental pathway in C9-ALS/FTD pathogenesis (Zhang et al., 2015). In parallel, unbiased genetic screenings for phenotypic modifiers of Drosophila expressing GGGGCC repeats (Freibaum et al., 2015) or poly(PR) (Boeynaems et al., 2016), yeast (Jovičič et al., 2015) and human cells expressing poly(GR) or poly(PR) (Kramer et al., 2018), identified that proteins involved in NCT mitigate or exacerbate disease phenotypes. Mechanistically, poly(GR) and poly(PR) interact with nucleopore proteins (Nups), including the central channel of the nucleopore, to reduce trafficking (Shi et al., 2017). Poly(GA) also sequesters nucleocytoplasmic transport proteins, such as HR23, and induces an abnormal distribution of RanGAP1 in mice (Zhang et al., 2016). The primary cause for the NCT dysfunction in C9-ALS/FTD is unknown but a number of human studies have

documented that abnormalities in the nuclear envelope are a part of C9-ALS/FTD pathology (Hutten and Dormann, 2019; Vatsavayai et al., 2018; Zhang et al., 2019). NCT defects have also been reported in other neurodegenerative disorders, such as Alzheimer's (Eftekharzadeh et al., 2018) and Huntington's disease (Gasset-rosa et al., 2017; Grima et al., 2017) and have been shown to be a pathological feature in SOD1-ALS (Shang et al., 2017), suggesting that it may play a more global role in neurodegenerative process.

1.3.2 Alteration in stress granules

Eukaryotic cells have evolved sophisticated strategies to combat unexpected cellular stress. Cytoplasmic ribonucleoprotein (RNP) granules, such as P-bodies and stress granules (SGs), assemble quickly under stress to sequester mRNAs, translation initiation factors, 40S ribosomes, and many other RNA-binding proteins. In this way, only essential proteins needed for survival are produced. These granular structures can either dissemble upon release of cellular stress or be degraded by the autophagy pathway. Dysregulated formation or clearance of SGs has been proposed as a key pathogenic mechanism for ALS/FTD (Li et al., 2013). In recent years, groundbreaking work from several groups showed that SG-associated RNA-binding proteins, such as FUS and hnRNP1/2, undergo liquid-liquid phase separation (LLPS) to form droplets in vitro and have the propensity to further fibrilize into irreversible hydrogel or even insoluble amyloid structures (Masato Kato et al., 2012; Molliex et al., 2015; Murakami et al., 2015; Patel et al., 2015). One characteristic of these RBPs is that they all contain prion-like, intrinsically disordered low-complexity domains (LCD). Poly(GR) and poly(PR) interact with these LCD proteins, impair LLPS, and disrupt the dynamics of stress granules (Boeynaems et al., 2017). Consistent with this, primary cortical neurons overexpressing poly(PR) showed a reduction in cytoplasmic P-bodies with larger sizes and an increase in stress granule formation (Wen et al., 2014), and knockdown of several of the LCD proteins modifies the eye degeneration phenotype in Drosophila expressing poly(GR) (Lee et al., 2016). Activation of the stress granule response or exposure to either poly(GR) or poly(PR) was also sufficient to disrupt nucleocytoplasmic

transport by promoting the sequestration of several nuclear pore proteins into SGs (Zhang et al., 2018). Interestingly, poly(GR) and poly(PR) themselves undergo LLPS at high concentrations, and GGGGCC repeat RNA also undergoes gel transition itself (Jain and Vale, 2017) and promotes the phase transition of RNA granule proteins in vitro and in cells (Fay, 2017). While the transient nature of stress granule assembly may preclude their abundance in pathological tissues, a few studies have documented stress granule-like inclusions of TIA-1 and EIF3 that colocalize with TDP-43 inclusions in the spinal cord of ALS or brain of FTLD patients (Liu-Yesucevitz et al., 2010). Similarly, a new mouse model of C9-ALS/FTD with AAV-mediated expression of 149 GGGGCC repeats at birth leads to TIA-1 and EIF3 stress granule-like bodies co-localizing with pathological TDP-43 in neurons (Chew et al., 2019). These mice undergo progressive neurodegeneration coinciding with behavioral defects and invaginations of the nuclear membrane that are similar to those found in humans (Chew et al., 2019; Saberi et al., 2017; Vatsavayai et al., 2018).

1.3.3 Nucleolar dysfunction

The nucleolus is the site of ribosome biogenesis. When overexpressed in cultured cells, astrocytes, primary neurons, iPSC-derived neurons, and Drosophila, poly(GR) and poly(PR) colocalize with nucleoli leading to abnormal nucleolar morphology and impaired ribosomal RNA maturation (Kwon et al., 2014; Wen et al., 2014). However, poly(GR) and poly(PR) do not localize within the nucleolus in C9orf72 patient brains. But sense RNA foci can bind nucleolin, a principle component of the nucleolus. This is supported by the finding of aberrant subcellular localization of nucleolin in C9orf72 iPSC-derived motor neurons and patient motor cortex (Haeusler et al., 2014). Contrary to this, antisense RNA foci have been found to associate more often with nucleoli than sense foci in tissue obtained from autopsy (Aladesuyi Arogundade et al., 2019). Nucleolin mis-localization was also found in C9orf72 BAC transgenic mice without significant changes in ribosomal RNA processing or splicing (O'Rourke et al., 2015). Interestingly, C9orf72 patient brains exhibit bidirectional nucleolar volume changes, with smaller

nucleoli overall but enlarged nucleoli in neurons containing poly(GR) inclusions (Mizielinska et al., 2017).

1.3.4 Translation inhibition and ubiquitin proteasome system

In addition to regulating stress granule dynamics and ribosomal RNA synthesis, overexpression of poly(GR) and (PR) blocked global translation in an in-vitro translation assay and in cell lines (Kanekura et al., 2016). This was attributed to direct binding of poly(GR) and poly(PR) to mRNA, thereby blocking access to the translational machinery. Poly(PR) and poly(GR) also interact with translation initiation and elongation factors and ribosomal subunits in pull down assays (Kanekura et al., 2016). In addition, GGGGCC repeat-containing RNAs sequester ribosomal subunits, trigger stress granule formation, and inhibit translation (Fay, 2017; Green et al., 2017). Interestingly, 26S proteasome complexes, components of the ubiquitin proteasome system (UPS), are sequestered within poly(GA) aggregates in cells as revealed by protein cryo-electron tomography, which allows 3D imaging of the cell interior in close-to-native conditions (Guo et al., 2018). These results provide new insight into the mechanism by which poly(GA) deposition promotes UPS impairment and regulates protein homeostasis.

1.3.5 DNA damage

Nucleolar stress induces DNA damage, and postmitotic neurons are particularly susceptible to DNA damage. An age-dependent increase in DNA damage and oxidative stress was reported in iPSC-derived motor neurons of patients with C9orf72 repeat expansions (Lopez-Gonzalez et al., 2016). DNA damage is also increased in spinal cord neurons of C9orf72 ALS patients (Farg et al., 2017). Such DNA damage is partially caused by poly(GR) since expression of poly(GR) in iPSC-derived control neurons or neuronal cell lines and in mice in vivo is sufficient to induce DNA damage and toxicity (Choi et al., 2019). Mechanistically, poly(GR) binds to Atp5a1 and compromises mitochondrial function, leading to increased oxidative stress and an overactivated Ku80-dependent DNA repair pathway (Choi et al., 2019; Lopez-Gonzalez et

al., 2019). Introducing ectopic Atp5a1 expression or reduction in oxidative stress by treatment with antioxidants partially rescues DNA damage in motor neurons from C9orf72 carriers and in neurons expressing poly(GR). As a result of DNA damage, the levels of phosphorylated ATM and P53 and other downstream proapoptotic proteins, such as PUMA, Bax, and cleaved caspase-3, are significantly increased in C9orf72 patient neurons. Partial loss of Ku80 function in these neurons through CRISPR/Cas9-mediated ablation or small RNA-mediated knockdown suppresses the apoptotic pathway. Thus, poly(GR)-mediated DNA damage contributes to ALS/FTD pathogenesis, and partial inhibition of the overactivated Ku80-dependent DNA repair pathway is a promising therapeutic target.

1.4 THERAPUETIC APPROCHES for C9-ALS/FTD

1.4.1 Transcript targeting

Since the pivotal discovery of repeat expansions in C9orf72 causing ALS and FTD, research has overall favored that gain of function from dipeptide repeat proteins and/or repeat expanded RNA drive toxicity. Thus, a primary route to effective therapeutic treatment is reducing the levels of repeat expanded RNA transcripts, a strategy that would have potential to prevent toxicity from either RNA and/or simultaneously translation of DPRs. The most developed such therapeutic strategies are antisense oligonucleotide therapies (ASOs). These are synthetic oligonucleotides or oligonucleotide analogs that bind to target RNAs. Depending on their chemical modifications, ASOs selectively degrade mRNAs through endonuclease RNase H recruitment or prevent the interaction of RNAs with RBPs, thereby modulating their splicing/processing without degradation (Bennett et al., 2019). In 2016, the ASO Nusinersen (Spinraza) became the first FDA approved treatment for spinal muscular atrophy. Nursinersen functions by modulating the splicing of SMN2 pre-mRNA to increase the expression of survival motor neuron protein (Hua et al., 2007). ASOs are currently in Phase 1 or 2 trials for LRRK2-Parkinson's disease and Tau associated Alzheimer's disease and FTD and in Phase III trials for

Huntington's disease and superoxide dismutase ALS (Miller et al., 2013; Tabrizi et al., 2019).

ASOs have shown promise in preclinical trials at reducing sense RNA foci, rescuing cells from glutamate excitotoxicity and correcting aberrant gene expression profiles in fibroblasts and patient derived IPS motor neurons (Donnelly et al., 2013; Lagier-Tourenne et al., 2013; Sareen et al., 2013). We and others have also demonstrated that ASOs can specifically target transcript variants 1 (NM_145005.6) and 3 (NM_001256054.2) that carry the repeat expansion without reducing variant 2 (NM_018325.5) expression that encodes the functional C9ORF72 protein, thereby targeting gain of function toxicity without exacerbating loss of function. In this study, utilizing transgenic mice expressing 450 repeats, ASOs significantly reduced levels of sense RNA foci and DPRs as well as rescuing the behavioral and cognitive deficits observed in the treated mice (Jiang et al., 2016). Based on these and other encouraging results, a phase I clinical trial of ASOs targeting the sense strand for C9-ALS patients has been initiated by Ionis Pharmaceuticals and its partner Biogen Inc. in September 2018 (NCT03626012).

RNA interference (RNAi) is an alternative therapeutic strategy which involves short interfering RNAs (siRNAs), short hairpin RNAs (shRNAs) or micro RNAs (miRNAs) that also aim to mitigate gain of function toxicity by targeting RNA in the cytoplasm of cells (Castanotto and Rossi, 2009). If successful, this results in the degradation of the RNA transcripts, steric inhibition of RBPs binding the RNA and prevention of RNA foci forming, but their effect on in vivo models has yet to be tested (Hu et al., 2017; Lagier-Tourenne et al., 2013; Martier et al., 2019a, 2019b). Notably, a single administration of an adenoviral-mediated delivery of an RNAi could lead to a long-lasting therapeutic effect. This can be an advantage since ASOs require repeat administration, but in the former instance treatment is not "druggable," i.e. one cannot stop or lower therapy in the event of an adverse effect (Wang et al., 2019).

Additional therapies aim to mitigate toxicity by targeting the secondary structure of repeat-containing sense RNA. For example, the small molecule TMPyP4 binds the G-quadruplex and has been shown to prevent sequestration of RBPs by (GGGGCC)8 RNA (Zamiri et al., 2014), reduce sense RNA foci in Drosophila overexpressing (GGGGCC)30 RNA and rescue

NCT defects and neurodegeneration (Zhang et al., 2015). Additionally, several small molecules designed to specifically target the GGGGCC hairpin have been shown to significantly decrease sense RNA foci and poly(GP) in cells overexpressing (GGGGCC)66 RNA and in iPSC-derived neurons (Su et al., 2014; Wang et al., 2020). It remains to be seen whether these compounds also reduce poly(GR) and poly(PR), the two DPR proteins that have been shown to be most toxic in model systems, and whether they can reduce cellular toxicity both in vitro and in vivo.

Several studies have sought to reduce transcription of repeat-containing RNA using CRISPR/Cas strategies (Heidenreich, 2016). As a proof of concept, genetic correction of C9orf72 repeat expansions in patient iPS cells has been achieved by using CRISPR/Cas9 to cut out the C9orf72 repeat expansions and repair the gene through non-homologous end joining (Choi et al., 2019; Shi et al., 2018). More recently, marked reduction in transcription of repeat-containing sense RNA transcripts was achieved by using CRISPR/Cas9 to remove the promotor region of C9orf72 variants 1 and 3 (Krishnan et al., 2020). In addition, Pinto et al. targeted enzymatically-dead Cas9 to directly bind repeat expanded DNAs, such as CTG expansion in DM1, CTGG expansion in DM2 and GGGGCC expansion in C9-ALS/FTD. Instead of cleaving DNA, dCas9 sterically impeded transcription of repeat-containing RNA, leading to a drastic decrease in the production of DPRs (Pinto, 2017). Apart from targeting DNA, RNA-targeting Cas9 with RNA endonuclease has been used to degrade repeat expanded RNAs, reducing RNA foci and DPRs in a manner similar to ASOs (Batra et al., 2017). The clinical use of CRISPR/Cas technology in C9-ALS/FTD is still in its infancy. Ethical concerns, adequate methods of delivery and cell targeting, off-target and safety measures, and treatment efficacy are the main issues that need to be addressed before applying this method to patients.

Several non-redundant proteins including SUPT4H and PAF1C, have been identified that facilitate RNA polymerase II transcription of C9orf72 through the complex secondary structure formed by the GC repeat expansion (Goodman et al., 2019; Kramer et al., 2016). Depleting SUPT4H and PAF1C has been shown to reduce sense and antisense C9orf72 repeat transcripts, as well as RNA foci and DPR products, and ameliorate neurodegeneration in C9orf72 iPSC-derived

neurons and in Drosophila (Goodman et al., 2019; Kramer et al., 2016). However, an effective therapeutic strategy would require specific action against C9orf72 repeat RNA since depleting SUPT4H results in a global reduction of RNA (Naguib et al., 2019).

1.4.2 DPR reduction using antibody strategies

In addition to preventing toxic DPR production by targeting RNA, another therapeutic approach is utilizing antibodies targeting DPRs to mitigate gain of function toxicity by reducing or possibly eliminating DPRs. Both active and passive immunizations have been explored to combat the prion-like propagation of misfolded proteins such as amyloid- and tau in Alzheimer's disease, and -synuclein in Parkinson's disease (Gallardo and Holtzman, 2017). An immunization approach could also prevent the cell-to-cell transmission of DPRs but a main concern is developing antibodies that are specific to the DPRs since similar short repetitive sequences are present in the human proteome (Chang et al., 2016; Hock and Polymenidou, 2016; Ravits, 2014; Zhou et al., 2017). Nevertheless, antibodies against poly(GA) were recently shown to reduce poly(GA) as well as poly(GP) and poly(GR), improve behavioral deficits, decrease neuroinflammation and neurodegeneration and increase survival in mice (Nguyen et al., 2020). An alternative approach to target DPRs involves therapy utilizing the heat shock protein, HSPB8. Overexpression of HSPB8 has been shown to facilitate autophagy-mediated clearance of misfolded proteins and reduce the levels of insoluble DPRs including poly(GR) and poly(PR) (Cristofani et al., 2018).

1.4.3 Pathway inhibition using small molecule approaches

Even further downstream are therapies aimed at correcting cellular pathways affected by C9orf72 repeat expansion, such as stress granule assembly and nuclear cytoplasmic transport. For example, inhibiting stress granule assembly by using ASOs targeting Ataxin 2 mitigates nucleocytoplasmic transport defects and neurodegeneration in patient derived IPS neurons and mice (Zhang et al., 2018). Reducing Ataxin 2 also extends the lifespan of TDP-43 mice, which is promising for C9-ALS/FTD and additional diseases involving stress granule assembly and

NCT defects (Becker et al., 2017). Furthermore, Zhang et al. demonstrated that reducing nuclear export factors SRSF1 or exportin 1, or using selective inhibitors of nuclear export (SINEs), a drug that blocks exportin 1, ameliorates the toxicity seen in a Drosophila model of C9-ALS/FTD (Zhang et al., 2015). The therapeutic benefit of inhibiting nuclear export is perhaps an effect of reducing levels of repeat containing RNA (Hautbergue et al., 2017), thus lowering levels of DPRs or reversing mislocalization of RBPs such as TDP-43 caused by NCT defects (Zhang et al., 2015). SINE compounds were also shown to be beneficial in rats overexpressing mutant TDP-43, improving primary neuron survival and partially rescuing loss of motor function (Archbold et al., 2018). Currently, Karyopharm Therapeutics and its partner Biogen Inc. are taking one of the SINE compounds, KPT-350, into clinical trials (Fig. 1.3).

1.5 CONCLUSIONS and FUTURE PERSPECTIVES

Since the discovery of C9orf72 repeat expansions, an impressive effort has been developed to investigate disease mechanisms. Many disease models were developed to determine loss of function and/or gain of toxicity and downstream cellular function alterations. Therapeutic approaches and biomarkers have also been explored. Excitingly, antisense oligonucleotide therapy to selectively degrade repeat-containing RNAs has gone into a Phase I clinical trial for C9orf72 ALS patients. Based on the pace of research, promising therapy for the most common form of familial ALS is on the horizon.

1.6 ACKNOWLEDGEMENTS

Chapter 1, in part, has been submitted for publication of the material as it may appear in The Development of Neurotherapeutics in the Era of Translational Medicine, 2020. Aladesuyi Arogundade, Olubankole; Jiang, Jie; Ravits, John, Elsevier, 2020. The dissertation author was the coauthor of this chapter.

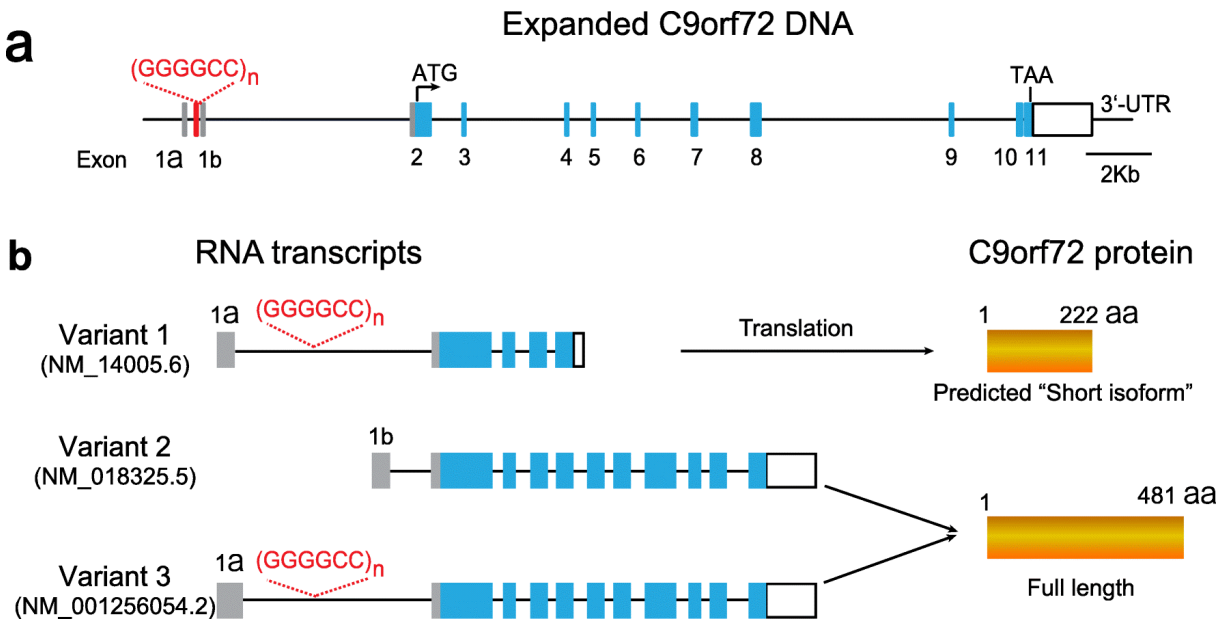

Figure 1.1. C9orf72 gene structure, RNA transcripts, and proteins. (a) Schematic representation of the human C9orf72 gene with expanded GGGGCC hexanucleotide repeats. (b) Three RNA transcripts can be produced from the C9orf72 gene. Variant 1 is predicted to result in a "short isoform" C9ORF72 protein of 222 amino acids, whereas variants 2 and 3 encode a long C9ORF72 protein of 481 amino acids.

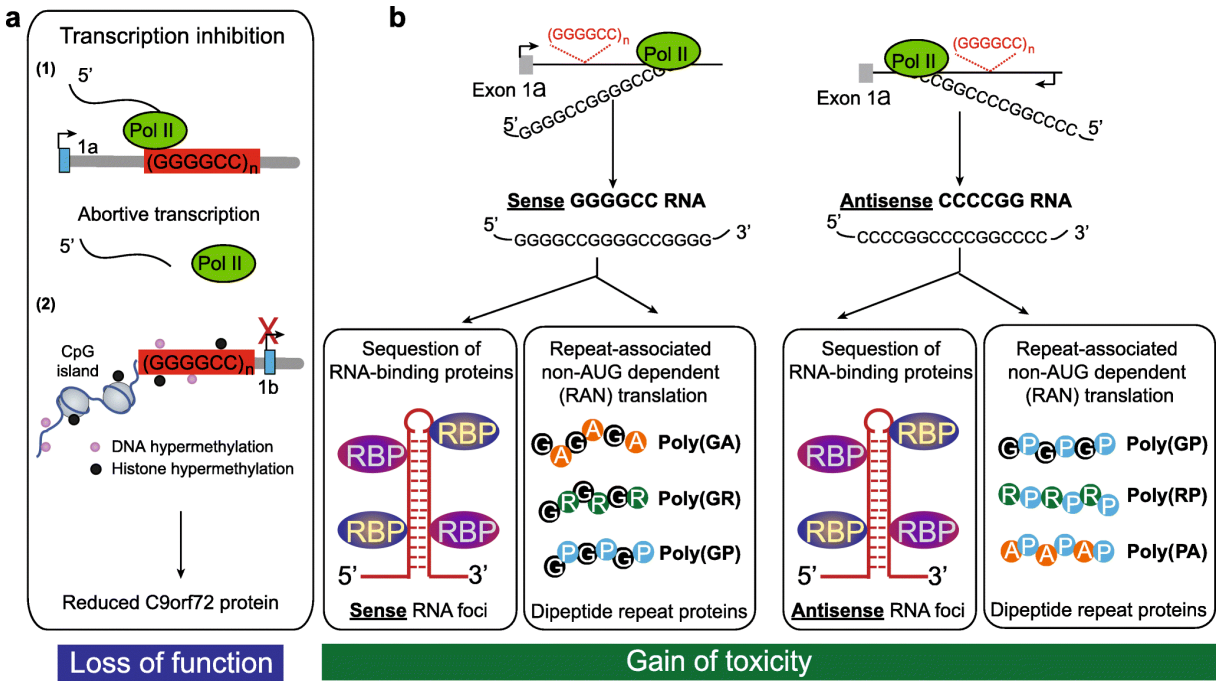

Figure 1.2. Proposed pathogenic mechanisms in C9orf72 ALS/FTD. (a) The presence of expanded GGGGCC repeats potentially causes abortive transcription from exon 1a and hypermethylation of both DNA and histones to reduce C9orf72 RNA transcription, leading to a loss of C9orf72 protein function. (b) Bidirectionally transcribed repeat-containing RNAs cause neuronal toxicity by sequestration of RNA-binding proteins into RNA foci or production of at least 5 aberrant dipeptide repeat proteins [poly(GA), poly(GP), poly(GR), poly(PR), and poly(PA)] through a novel repeat-associated non-AUG-dependent translation mechanism.

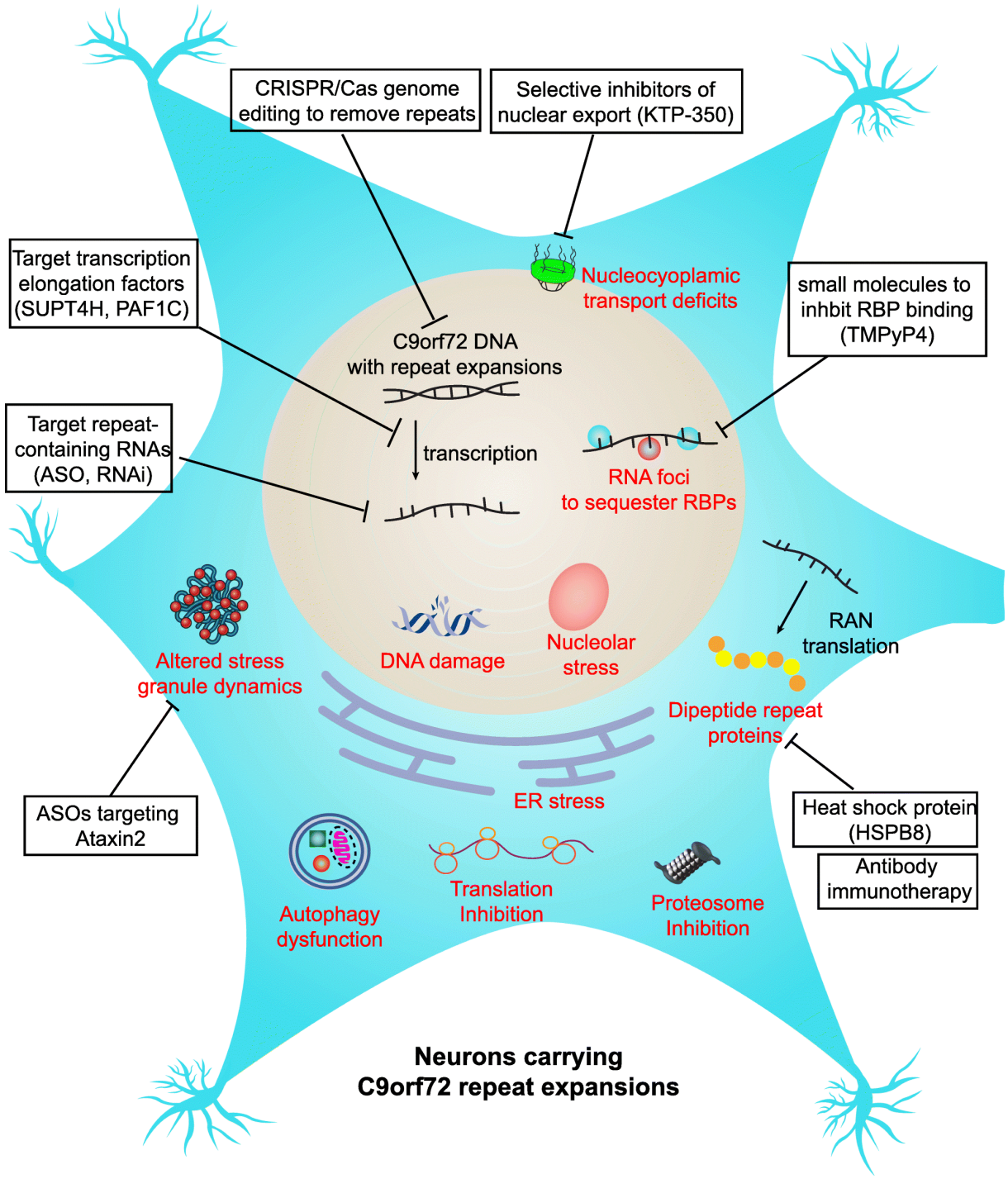

Figure 1.3. Cellular processes impaired by the C9orf72 repeat expansions and potential therapeutic interventions. A wide range of cellular pathways have been implicated in c9ALS/FTD, including DNA damage, nucleolar stress, nucleocytoplasmic transport deficits, ER stress, autophagy dysfunction, translational inhibition, proteasome inhibition, and altered stress granule dynamics. Therapies targeting these deficits, as well as directly targeting repeat expanded C9orf72 DNA/RNA and DPR proteins, are also highlighted.

Chapter 2

Antisense RNA foci are associated with nucleoli and TDP-43 mislocalization in C9orf72-ALS/FTD: A quantitative study

2.1 MAIN TEXT

Three main mechanisms are thought to contribute to neurodegeneration in C9ORF72 amyotrophic lateral sclerosis (ALS) and frontotemporal dementia (FTD) (C9-ALS/FTD): toxicity from transcribed expanded repeat RNAs, toxicity from RAN-translated dipeptide repeat proteins (DPRs), and loss of C9ORF72 protein function (Dejesus-hernandez et al., 2011; Gendron et al., 2013; Mizielinska et al., 2013; Mori et al., 2013; Renton et al., 2011; Zu et al., 2013). Sense and antisense RNA foci have both been consistently observed in C9-ALS/FTD neuropathology (Cooper-Knock et al., 2015; Dejesus et al., 2017; Gendron et al., 2013; Lagier-Tourenne et al., 2013; Mizielinska et al., 2013; Zu et al., 2013) and hypothesized to cause neurodegeneration by sequestering critical RNA binding proteins (Cooper-Knock et al., 2014; Haeusler et al., 2014). Antisense but not sense RNA foci have been shown to correlate with mislocalization of TDP-43, a signature protein of ALS and frontotemporal lobar degeneration (FTLD) (Cooper-Knock et al., 2015). A unique circumferential studding of nucleoli by antisense RNA foci was observed in a case report of two C9-FTLD cases (Vatsavayai et al., 2016) and recently re-discussed with two additional cases (Vatsavayai et al., 2018). Understanding the relative contributions from sense

and antisense strands to pathogenesis is critical, since antisense oligonucleotides (ASOs) are expected to ameliorate toxicity whether stemming from RNAs or DPRs.

We evaluated RNA foci in five C9-ALS cases with and without FTD in our short-postmortem interval ALS repository (Saberi et al., 2017). C9-ALS/FTD was confirmed by repeat-primed PCR and Southern blotting. Consistent with the literature, both sense and antisense RNA foci were widely distributed throughout the nervous systems (Cooper-Knock et al., 2015; Dejesus et al., 2017; Gendron et al., 2013; Mizielinska et al., 2013; Zu et al., 2013). They were not concentrated in the motor or frontal cortex, the anatomical regions of direct relevance to C9-ALS/FTD (Fig. 2.1a and b). Overall, the mean prevalence of sense and antisense RNA foci over multiple CNS regions were 16% and 20% in neurons and 1% and 1% in glia, respectively (Fig. 2.1c). Antisense RNA foci were significantly denser than sense RNA foci within the RNA foci-positive neurons ($p < 0.0001$; Fig. 2.1d). As reported in C9-FTD and one case of C9-ALS, we also observed that in large neurons, RNA foci were frequently localized to nucleoli, identified as a prominent immunofluorescent density within the nucleus, often directly abutting their circumference (Fig. 2.2a). We confirmed nucleolar localization using the nucleolar marker nucleolin (Fig. 2.2b). We quantified the association and overall on average, 27% of antisense RNA foci but only 9% of sense RNA foci were perinucleolar. We saw that perinucleolar antisense RNA foci were more frequent in disease-related areas than non-disease-related areas and were more likely than sense RNA foci to be perinucleolar in disease-related areas but this did not reach significance in disease-unrelated areas: 35% of antisense RNA foci but only 13% of sense foci in disease-related areas were perinucleolar, compared to 17% and 4%, respectively, in disease-unrelated areas (Fig. 2.1e and f). The preponderance of nucleolar antisense RNA foci but not sense RNA foci tended to correlate with the burden of TDP-43 pathology in frontal cortex (Fig. 2.3; Table 2.1).

We evaluated the relationship between RNA foci and TDP-43 mislocalization using co-fluorescent in situ hybridization and immunofluorescence. We did this in neurons in the anterior horn of spinal cord, where identification of motor neurons by location in the anterior

horn is readily done (Fig. 2.2c and d). Nucleolar localization of RNA foci was confirmed by imaging through the z-plane. As previously reported (Cooper-Knock et al., 2015), antisense RNA foci were associated with TDP-43 pathology and sense foci were not: antisense foci were seen in 67% of neurons with cytoplasmic aggregation of TDP-43 and 16% of neurons with preserved nuclear TDP-43 ($p = 0.008$; Fig. 2.4b), compared to sense foci which were seen in 20% of neurons with cytoplasmic aggregation of TDP-43 and 18% of neurons with preserved nuclear TDP-43 ($p = 0.5$, Fig. 2.4a). Importantly, the difference between antisense and sense foci held true for the perinucleolar RNA foci: perinucleolar antisense RNA foci were seen in 67% of neurons with cytoplasmic aggregation of TDP-43 and 20% of neurons with preserved nuclear TDP-43 ($p = 0.008$; Fig. 2.2e), compared to perinucleolar sense RNA foci, which were seen in 9% of neurons with cytoplasmic TDP-43 and 11% of neurons with preserved nuclear TDP-43 ($p = 0.7$; Fig. 2.2f and Table 2.2). Overall, the co-occurrence of TDP-43 abnormalities and perinucleolar antisense RNA foci was significantly greater than expected ($p < 0.001$; Fig. 2.2g), while the co-occurrence of TDP-43 abnormalities and perinucleolar sense RNA foci was as expected ($p = 0.6$; Fig. 2.2g).

The association of antisense RNA foci and nucleoli is important in light of recent discussions about nucleolar stress contributing to the pathogenesis of C9-ALS/FTD (Haeusler et al., 2014; Kwon et al., 2014; Mizielinska et al., 2017; Tao et al., 2015). The nucleolus is the site of many localized functions such as ribosomal biogenesis and disruptions to nucleolar function can dramatically affect many functions such as rates of protein synthesis. Alterations in nucleolar morphology as well as altered rates of protein synthesis have been found in C9-FTLD/ALS frontal cortex (Mizielinska et al., 2017) and cellular model (Haeusler et al., 2014; Tao et al., 2015), although not confirmed by all (Schludi et al., 2015). Thus far, sense RNA foci (Haeusler et al., 2014) and the arginine-containing DPRs, poly-GR and poly-PR (Kwon et al., 2014; Tao et al., 2015) have been implicated to cause or at least to be associated with nucleolar stress in C9-ALS/FTD pathogenesis. While antisense RNA foci were previously found to correlate with mislocalization of TDP-43 in C9-ALS (Cooper-Knock et al., 2015) and antisense RNA

foci studding of nucleoli have been observed in C9-FTLD (Vatsavayai et al., 2016), the co-occurrence of nucleolar antisense RNA foci with TDP-43 neuropathology has not been reported or quantitated. In our study, we found that nucleolar antisense RNA foci are significantly more associated with disease, especially with neuronal TDP-43 cytoplasmic aggregation and our findings bring the different aspects together. It has been suggested that nucleolar antisense RNA foci may form early in disease and precede TDP-43 aggregation (Vatsavayai et al., 2016). In summary, antisense RNA foci have unique neuropathological features compared to sense RNA foci including nucleolar localization, anatomic distribution, and correlation with TDP-43 pathology. This re-enforces that antisense RNA may play an important role in pathogenesis and be an important target for therapy.

2.2 SUPPLEMENTAL MATERIALS and METHODS

2.2.1 CNS tissues

Human tissues were obtained using a short-postmortem interval acquisition protocol that followed HIPAA-compliant informed consent procedures and were approved by Institutional Review Board (Benaroya Research Institute, Seattle, WA IRB #10058 and University of California San Diego, San Diego, CA IRB #120056). The ALS nervous systems were from patients who presented with ALS as the clinical phenotype, with or without FTD, and all had progressed and died from their motor impairment. For this study, we evaluated five C9 ALS cases (confirmation by repeat-primed PCR and Southern blotting; previously published in Saberi et al. 2018).

2.2.2 CNS region, cell types, and relationships to disease

In brain, we studied the following regions: frontal lobe, motor cortex, parietal cortex, occipital cortex. In spinal cord, we examined anterior and posterior horns at cervical, thoracic, and lumbosacral levels. We examined layer 5 of brain with special attention to layer 5 of the motor cortex and its Betz cells, and all regions of the spinal cord with special attention to Rexed

lamina IX of the anterior horn and its spinal motor neurons. 15 – 129 cells were analyzed for each region. Cell classification to neuron or glia was based on morphology. To classify a cell as neuronal, at least three of the following four criteria were met: cytoplasm was large, there was lipofuscin, nuclear diameter was greater than 10 m, and there was a single prominent nucleolus. To classify a cell as glial, nuclei were small, cytoplasm was small and compact, there was no lipofuscin, and no prominent nucleolus. In our analysis, we regarded the following regions as clinically-related: motor cortex, frontal cortex and anterior horn of spinal cord; the following regions as being clinically-unrelated: parietal cortex, occipital cortex and posterior horn of spinal cord.

2.2.3 Fluorescence *in situ* hybridization (FISH)

For all images, we used formalin-fixed paraffin-embedded (FFPE) human spinal cords and brain sections with 6 m thickness. Custom LNA oligonucleotides (Exiqon Inc., Woburn, MA) were designed against the sense and antisense hexanucleotide repeat-containing RNAs. The probe sequence for detection of sense RNA foci was: TYE563- CCCCGGCCCCGGCCCC. The probe sequence for detection of antisense RNA foci was: TYE563- GGGGCCGGGGCCGGGG. Hybridization was carried out under RNase-free conditions. Briefly, 6 m paraffin sections were deparaffinized in Xylene and were then rehydrated through an ethanol series of 100%, 90%, 70% and 50% EtOH for 5 minutes each. Sections were permeabilized in 0.2% Triton-X in 1X PBS for 10 minutes, washed twice in 1X PBS for 5 minutes each, and dehydrated through an ethanol series of 70% EtOH, 95% EtOH, and 100% EtOH for 1 minute each. Sections were dried and blocked for 20 minutes at 66^{o}C in hybridization buffer. Hybridization buffer for sense RNA foci consisted of 50% formamide, 2X SSC, 50 mM sodium phosphate (pH 7), 10% dextran sulfate, and 2 mM ribonucleoside vanadryl complex. Hybridization buffer for antisense RNA foci consisted of 50% formamide, 2X SSC with sodium replaced by lithium ions, 50 mM sodium phosphate (pH 7), 10% dextran sulfate, and 2 mM ribonucleoside vanadryl complex. Sections were incubated with denatured LNA probe (final concentration 200 nM) overnight at 66^{o}C. The

following day, slides were washed in 0.1% Tween-20/2X SSC/1X PBS at room temperature for 5 minutes and were then put into three stringency washes of 0.2X SSC/1X PBS at 60^{o}C for ten minutes each. Cell nuclei were stained in DAPI (final concentration 1 g/mL) for 10 minutes. Autofluorescence was quenched by immersion in 0.1% Sudan Black in 70% EtOH for 15 seconds. Slides were mounted with ProLong Gold Antifade Mountant with DAPI (Fisher # P36931).

2.2.4 Co-FISH and immunofluorescence (IF) (Co-FISH-IF)

For co-FISH-IF, we created a protocol that blended FISH and IF by stepping down temperatures from highest to lowest. On the first day, sections were deparaffinized with Citrisolv (FISHER brand #04-355-121) and hydrated through a serial dilution of ethanol. Antigen retrieval was performed in a high pH solution (Vector #H-3301) in a pressure cooker for 40 minutes at a temperature of 90C. Next, we performed prehybridization and hybridization with FISH probes as described above and incubated the slides overnight at 66^{o}C. On day two, the slides were washed with SSC as described above and were incubated with primary antibody overnight. Primary antibodies were diluted in 2% FBS in 1X PBS. For TDP-43, we used rabbit anti-TDP-43 (Proteintech, #12892-1-AP, 1/300). For nucleolin, we used polyclonal rabbit anti-nucleolin (Abcam, ab22758, 1/400). On the third day, slides were incubated with secondary antibodies (mixed donkey anti-rabbit (Jackson Immuno Research #26601, Alexa 488, 1/500) for 60 minutes at room temperature. Secondary antibodies were diluted in 2% FBS in 1X PBS. After 20 minutes staining with 0.1% DAPI (Lifetech, #D21490) we quenched CNS auto-fluorescence with 0.1% Sudan Black in 70% EtOH for 10- 30 seconds. Slides were cover slipped using ProLong Gold Antifade Mountant with DAPI.

2.2.5 Visualization and quantification

RNA foci were visualized using an inverted Olympus FV1000 laser scanning confocal microscope, under 60X and 100X oil magnifications. If the nucleus of a neuron was not present

in the imaged plane the neuron was not quantified.For each patient, five to ten images were acquired from every layer in each region. Single slices were acquired except in cases where RNA foci were observed at varying depths. In those cases, z-stacks were acquired to capture all RNA foci. Maximum projections of z-stacks were compiled using Fiji. For each CNS region, the following features were quantitated: number of glial cells and neurons for each layer, the number and type of cells with RNA foci, and the number of RNA foci. Nuclei and RNA foci were counted by a single observer in a blinded manner. To quantify RNA foci, two metrics were used: prevalence, defined as percentage of cells that had at least one RNA foci, and density, defined as number of RNA foci found in each foci-positive cell.

2.2.6 Statistics

Variables were compared using two-tailed Mann-Whitney tests. Multiple comparisons were followed by Holm-Sidak post hoc test. Error bars are presented as standard error of mean. Fisher's exact tests were used to compare interaction between RNA foci and TDP-43 pathology and expected values were calculated as: Expected value = (Observed value for RNA foci +) / (Total) * (Observed value for cytoplasmic TDP-43). P-values below 0.05 were considered significant. All data analysis and graphing was performed using GraphPad Prism version 7.03 for Windows (GraphPad Software, La Jolla, CA) and MATLAB 2014a (Mathworks, Natick, MA).

2.3 ACKNOWLEDGEMENTS

This research was supported by grants from ALS Association (5356S3), Target ALS (20134792), National Institute of Neurological Diseases and Stroke (NIH R01NS088578 and NS047101), and Pam Golden. OAA is supported by National Science Foundation Graduate Research Fellowship (DGE-1650112). TO is supported by NINDS CReATe Consortium (U54NS092091). Len Petrucelli provided extra sense probe for FISH. We thank the patients and their families for their generous contribution to this research.

Chapter 2, in full, is a reformatted reprint of the material as it appears in Aladesuyi Aro-

gundade, Olubankole; Stauffer, Jennifer; Saberi, Shahram; Diaz Garcia, Sandra; Malik, Sahana; Basilim, Hani; Rodriguez, Maria; Ohkubo, Takuya; Ravits, John. Acta Neuropathologica, 2019. The dissertation author was the coauthor of this paper.

Table 2.1. Cytoplasmic aggregation of TDP-43 and nucleolar RNA foci in motor neurons within the anterior horn of spinal cord by co-FISH-IF

		Nucleolar RNA foci				
		Cytoplasmic TDP-43		Nuclear TDP-43		
		Observed	Expected	Observed	Expected	p-value
Antisense	Foci-positive	43	34	32	41	<0.001
	Foci-negative	2	11	21	12	
Sense	Foci-positive	8	9	24	23	0.6
	Foci-negative	9	8	19	20	

Table 2.2. TDP-43 pathology and nucleolar RNA foci in frontal cortex (-: none, +: slight, ++: moderate, +++: numerous; NCI: neuronal cytoplasmic inclusion, DN: dystrophic neurites)

Case No.	TDP-43		Nucleolar RNA foci	Nucleolar associated RNA foci
	NCI	DN	Antisense	Sense
14	-	+	11	0
81	+	+	14	67
90	++	++	67	0
91	+	+	25	0
98	++	+++	50	0

Figure 2.1. Regional prevalence of sense and antisense RNA foci. (a) Sense and antisense RNA foci are widespread throughout the brain and spinal cord. (b) The percentage of neurons with sense and antisense RNA foci were not significantly different in disease related or disease un-related areas of the CNS. (c) Sense and antisense RNA foci are more common in neurons than glial cells (disease related tissues, n = 25; $p < 0.0001$ for both). (d) The density of antisense RNA foci is significantly greater than that of sense RNA foci in overall areas of the brain and spinal cord shown in (a) (n = 146, 152, respectively; $p < 0.0001$). (e) Sense and antisense RNA foci localize to the nucleolus throughout the brain and spinal cord (perinucleolar foci / total foci). (f) Antisense RNA foci have greater nucleolar localization than sense RNA foci in disease related areas of the CNS ($p = 0.03$), but not in disease un-related areas of the CNS ($p = 0.4$). Antisense RNA foci localized in nucleoli correlate to disease-related areas of the CNS ($p = 0.02$), and sense RNA foci do not ($p = 0.4$, Wilcoxon test). Frontal cortex (FCx), motor cortex (MCx), anterior horn (AH), parietal cortex (PCx), occipital cortex (OCx), posterior horn (PH). The line inside the box and whisker plot is the median, the ends of the box are upper and lower quartiles, and the whiskers mark the highest and lowest values.

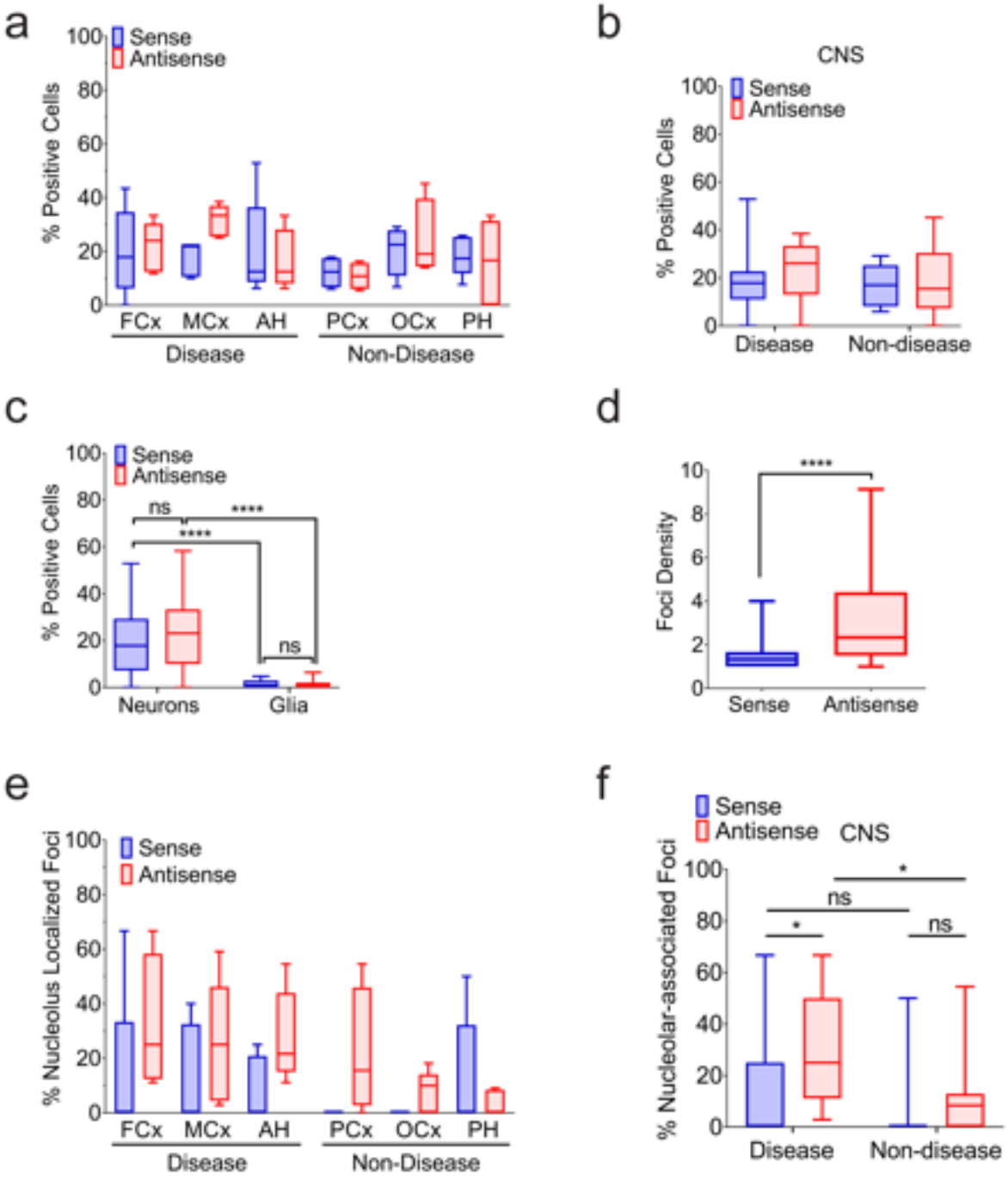
a
Sense
Antisense
% Positive Cells
100
80
60
40
20
0
FCx
MCx
AH
PCx
OCx
PH
Disease
Non-Disease
b
CNS
Sense
Antisense
% Positive Cells
Disease
Non-disease
c
Sense
Antisense
% Positive Cells
ns
****
****
ns
Neurons
Glia
d
****
Foci Density
10
8
6
4
2
0
Sense
Antisense
e
Sense
Antisense
% Nucleolus Localized Foci
FCx
MCx
AH
PCx
OCx
PH
Disease
Non-Disease
f
Sense
Antisense
CNS
% Nucleolar-associated Foci
*
ns
*
ns
Disease
Non-disease

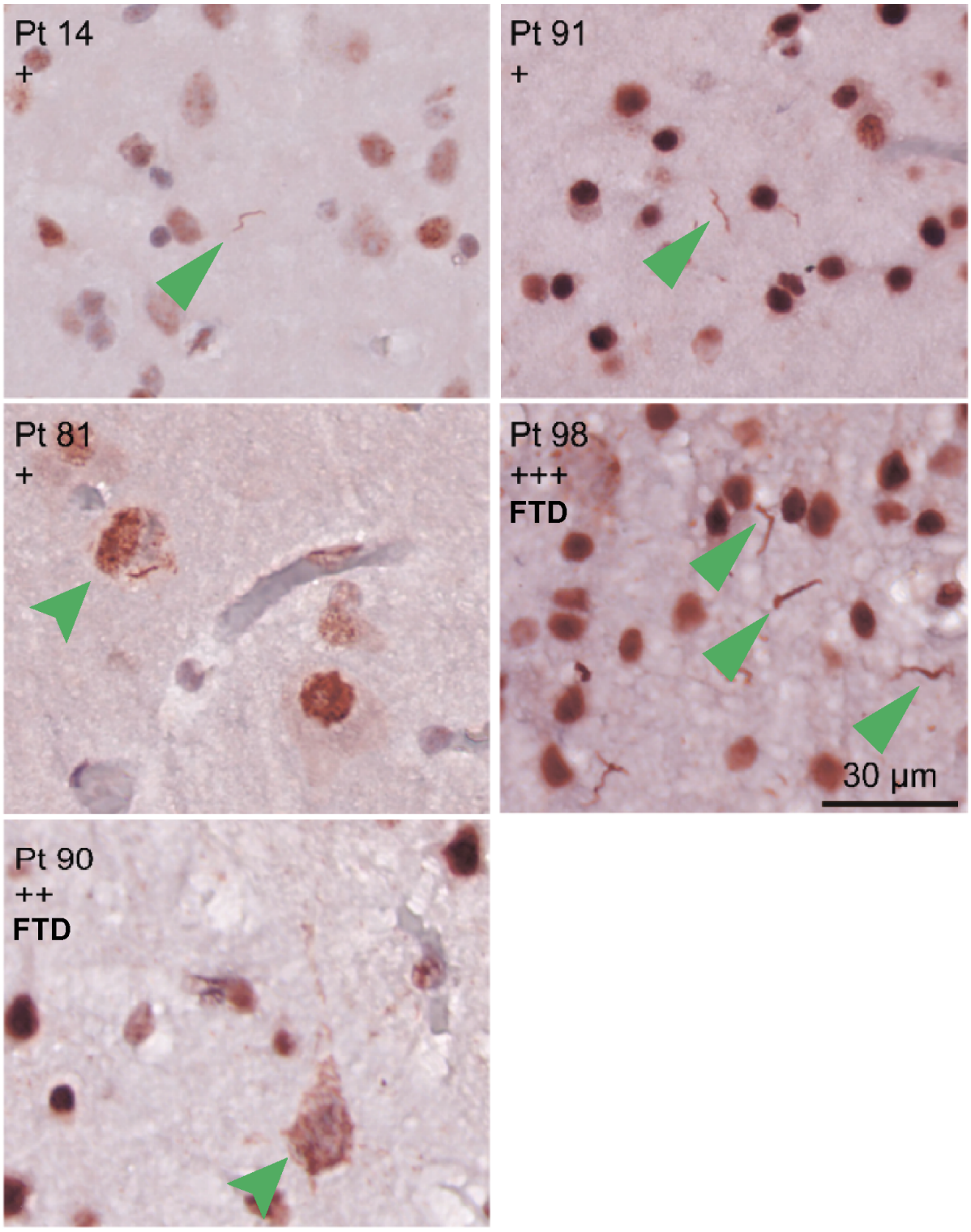

Figure 2.2. TDP-43 pathology is increased in C9-ALS/FTD frontal cortex. Immunohistochemistry reveals the prevalence of TDP-43 mislocalization in C9-ALS (pt.14, 81 and 91) and C9-ALS/FTD (pt.90 and 98) frontal cortex. TDP-43 pathology (+: slight, ++: moderate, +++: numerous) identified by dystrophic neurites (arrows) or neuronal cytoplasmic inclusions (beveled arrowheads).

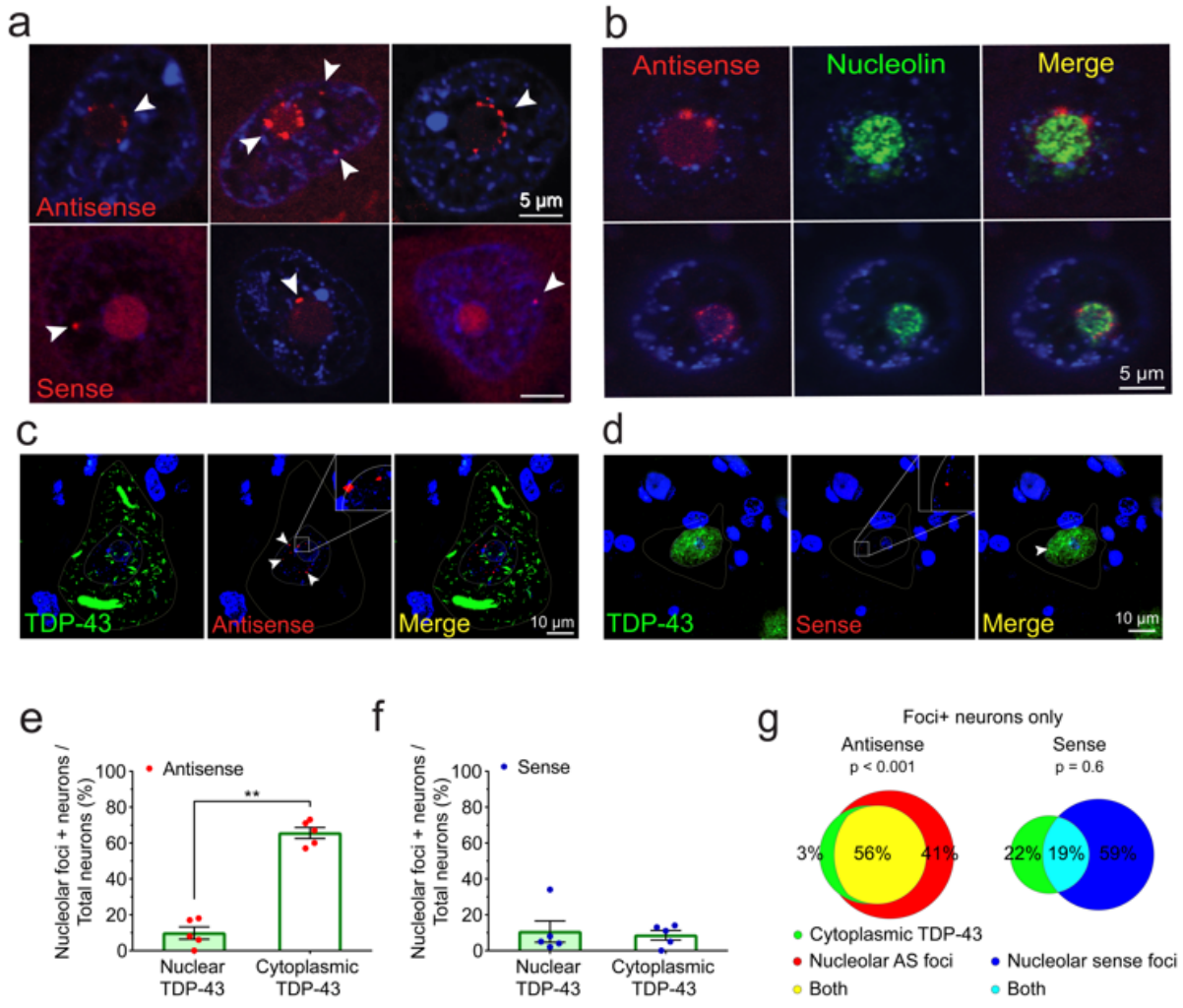

Figure 2.3. Antisense RNA foci have unique neuropathological features compared to sense RNA foci. (a) Sense and antisense RNA foci (arrowheads) are observed in the nucleoplasm or on the periphery of nucleoli of neurons (outer, middle and innermost dashed lines mark the cytoplasm, nucleoplasm and nucleolus, respectively). (b) Nucleolar localization is confirmed by nucleolar marker nucleolin. (c and d) Neurons containing antisense RNA foci often have cytoplasmic aggregation of TDP-43 and neurons with sense RNA foci often have preserved nuclear TDP-43 (inset scale, 500 nm). (e) The percentage of neurons with nucleolar antisense RNA foci was significantly increased in neurons with cytoplasmic aggregation of TDP-43 compared to preserved nuclear TDP-43 ($p = 0.008$). (f) The percentage of neurons with nucleolar sense RNA foci was not significantly different in neurons with cytoplasmic aggregation of TDP-43 compared to preserved nuclear TDP-43 ($p = 0.7$, Mann-Whitney test). (g) The co-occurrence of nucleolar antisense RNA foci and cytoplasmic aggregation of TDP-43 is significantly greater than expected while the co-occurrence of nucleolar sense RNA foci and cytoplasmic aggregation of TDP-43 is not. Area proportional Venn-diagrams represent Fisher's exact test.

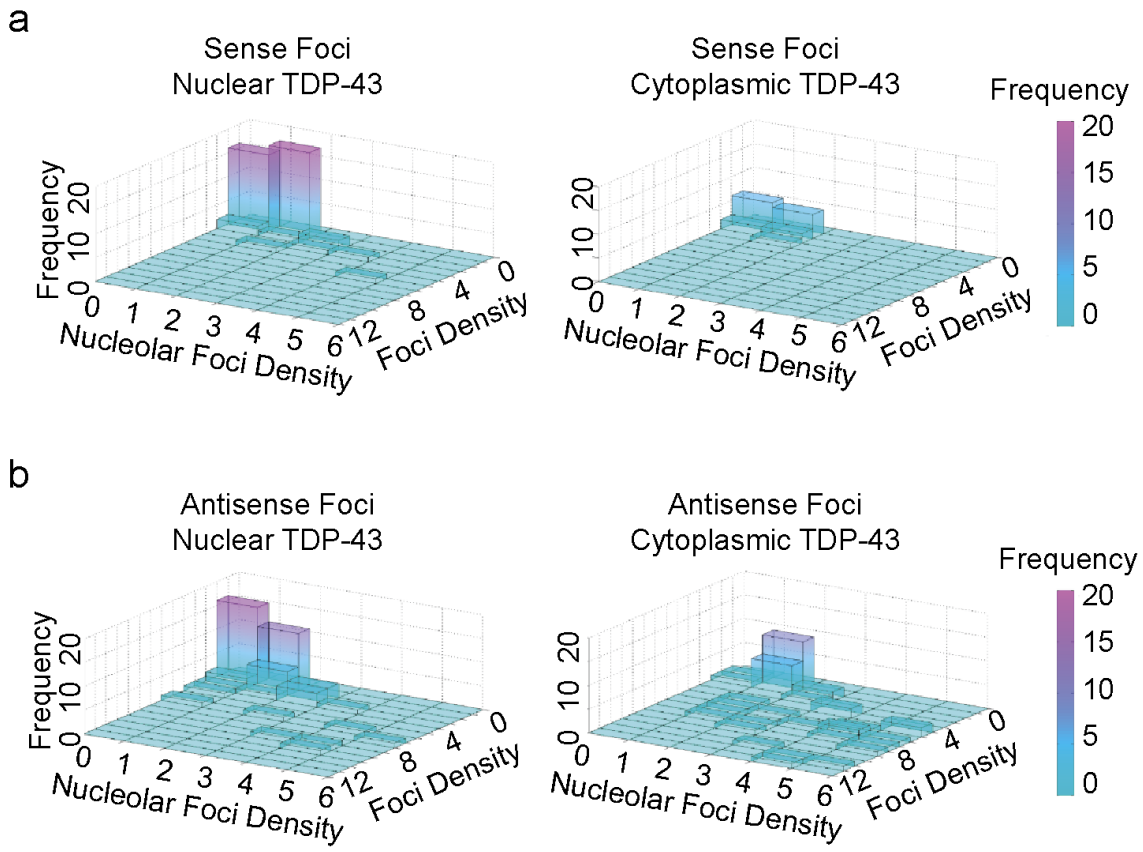

Figure 2.4. Nucleolar antisense but not sense RNA foci are increased in spinal motor neurons with TDP-43 mislocalization. 3D histograms reveal the distribution of sense (a) or antisense (b) RNA foci and nucleolar RNA foci in spinal motor neurons. The data shown here represent neurons with RNA foci and nuclear TDP-43 (left) or RNA foci and cytoplasmic TDP-43 (right).

Chapter 3

Biphasic nucleolar stress in C9orf72 and sporadic ALS spinal motor neurons correlates with TDP-43 mislocalization

3.1 ABSTRACT

Nucleolar stress has been implicated in pathology and disease pathogenesis of amyotrophic lateral sclerosis (ALS) and frontotemporal dementia (FTD) both from repeat expansion of GGGGCC in C9orf72 (C9-ALS/FTD) and sporadic ALS. Previously we reported that antisense RNA transcripts are unique in C9-ALS because of their nucleolar localization in spinal motor neurons and correlation with TDP-43 mislocalization, the hallmark of proteinopathy of ALS and FTD. Here we further studied postmortem spinal cord tissue in 11 control, 11 C9-ALS and 11 SALS nervous systems to determine if there is other evidence of nucleolar stress. We found nucleolar shrinkage in both C9-ALS and SALS spinal motor neurons. We found this in neurons both with and without TDP-43 mislocalization or nucleolar antisense RNA foci. Surprisingly, nucleolar shrinkage was greatest in neurons without these hallmarks, findings consonant with other reports. Thus, nucleolar stress in both C9-ALS and SALS spinal motor neurons appears to be biphasic – shrinkage is greatest before the other main pathological hallmarks appear.

3.2 INTRODUCTION

Nucleolar stress has been implicated in C9orf72 amyotrophic lateral sclerosis (ALS) and frontotemporal dementia (FTD) (Haeusler et al., 2014; Kwon et al., 2014; Mizielinska et al., 2017; O'Rourke et al., 2015; Wen et al., 2014). Normally, humans express 2-20 copies of the C9orf72 intronic repeat of GGGGCC, but the repeat can be expanded to thousands of copies. Toxicity is produced from repeat expansion-containing RNA transcripts that sequester RNA binding proteins and are exported to the cytoplasm, producing repeat-associated non-ATG translated dipeptide repeat proteins (DPRs) (Dejesus-hernandez et al., 2011; Renton et al., 2011). The repeat expansion is bidirectionally transcribed to produce sense and antisense RNA transcripts. DPRs containing the arginine residue, sense-encoded poly(GR) and antisense-encoded poly(PR), have repeatedly been found to be most toxic when overexpressed in cells and animal models (Boeynaems et al., 2016; Choi et al., 2019; Freibaum et al., 2015; Jovičič et al., 2015; Kanekura et al., 2016; Lee et al., 2016; May et al., 2014; Mizielinska et al., 2014; Ohki et al., 2017; Schludi et al., 2015; Swaminathan et al., 2018; Swinnen et al., 2018; Tao et al., 2015; Wen et al., 2014; White et al., 2019; Yamakawa et al., 2015; Yang et al., 2015; Yong-Jie Zhang et al., 2017; Zhang et al., 2018, 2015; Zu et al., 2011). In cellular models, poly(GR) and poly(PR) co-localize to nucleoli and cause nucleolar stress characterized by alterations of nucleolar size and impaired ribosomal biogenesis (Kanekura et al., 2016; Kwon et al., 2014; Wen et al., 2014). However, poly(GR) and poly(PR) were not found to co-localize to nucleoli in patient tissue (Schludi et al., 2015).

Overexpression of sense RNA transcripts causes sequestration of nucleolin and disruption of ribosomal genesis (Haeusler et al., 2014; Marta M. Fay et al., 2017). Both sense and antisense RNA transcripts form perinucleolar RNA foci in patient cells (Aladesuyi Arogundade et al., 2019; Cooper-Knock et al., 2015). Compared to sense RNA foci, antisense RNA foci localize to the nucleolus with increased prevalence in brain and spinal cord regions that undergo neurodegeneration (Aladesuyi Arogundade et al., 2019). Nucleolar antisense RNA foci are

increased in frontal cortical neurons of C9-ALS patients diagnosed with FTD and correlate with elevated TDP-43 pathology, the hallmark proteinopathy of ALS (Aladesuyi Arogundade et al., 2019). In spinal motor neurons, antisense RNA foci and the presence of nucleolar antisense RNA foci correlate with TDP-43 mislocalization, suggesting that nucleolar antisense RNA foci are relevant to disease pathogenesis (Aladesuyi Arogundade et al., 2019; Cooper-Knock et al., 2015).

Nucleolar stress has been reported in C9 frontotemporal lobar degeneration (FTLD) pathology. Overall, C9-FTLD frontal cortical neurons had smaller nucleoli when compared to controls. However, neurons with sense RNA foci, poly-GR or poly-GA had larger nucleoli than neurons without these pathological features. It remains unknown what accounts for the smaller nucleolar size and it is possible that TDP-43 mislocaliztion, antisense RNA foci or other pathological markers correlate with decreased nucleolar size. Nucleolar size alterations have also been observed in C9-ALS patient lymphocytes, fibroblasts, lymphocytes and patient derived iPS neurons (Haeusler et al., 2014). In these cellular models, nucleoli were found to be larger when compared to controls and this phenotype was recapitulated by overexpressing 21 repeats of GGGGCC in HEK293T cells (Haeusler et al., 2014). Nucleolin staining was dispersed from C9 lymphocytes and fibroblast nucleoli and scattered in the nucleus (Haeusler et al., 2014). Interestingly, overexpression of poly-GR in HeLa cells competitively sequesters ribosomal RNA and nucleophosmin and cause the dispersion of the nucleolus (White et al., 2019). These cellular phenotypes were specific to C9-ALS compared to controls, non-ALS or non-C9-ALS. RNA profiling of C9-ALS iPS cells revealed that ribosome biogenesis is a main pathway downregulated (Ho et al., 2020 PREPRINT). Similarly, laser capture microdissection data from SALS spinal motor neurons revealed dysregulation of RNA encoding ribosomal proteins and decreases in ribosomal maturation have been reported in C9-ALS lymphoblasts and motor cortex (Haeusler et al., 2014; Krach et al., 2018). Alterations to nucleolar size in ALS indicate nucleolar stress is an important node in C9-ALS disease pathogenesis (Haeusler et al., 2014; Kwon et al., 2014; Mizielinska et al., 2017; Tao et al., 2015; Wen et al., 2014; White et al.,

2019).

The nucleolus is a membraneless organelle composed of RNA, DNA and proteins. The dynamic structure of the nucleolus is intrinsically linked to its multiple roles in cellular physiology. By convention the primary function of the nucleolus is ribosome biogenesis but beyond this, the nucleolus facilitates multiple processes including cellular stress response, genome maintenance and repair, cell cycle progression, development and aging (Boisvert et al., 2007; Lo et al., 2006; Nalabothula et al., 2010; Qin et al., 2014). In this study, we sought to determine if nucleolar stress occurs in C9-ALS and to determine if alterations correlated with key pathological markers, and, in addition, compare them to SALS spinal motor neurons and TDP-43 pathological markers. We found significant abnormalities in nucleoli of C9-ALS nervous systems and also similar abnormalities in SALS. In both, the nucleolar shrinkage was greatest in neurons with normal TDP-43 and no pathological biomarkers, and the nucleolar size increased as pathological markers expressed and TDP-43 mislocalized. This suggests that nucleolar stress is upstream in pathogenesis and early changes occur before RNA and protein aggregations appear.

3.3 MATERIALS and METHODS

3.3.1 CNS Tissues

Human tissues were obtained using a short-postmortem interval acquisition protocol that followed HIPAA-compliant informed consent procedures and were approved by Institutional Review Boards and came from two sources, the University of California, San Diego (UCSD) ALS biorepository (Benaroya Research Institute, Seattle, WA IRB #10058 and UCSD IRB #120056) and the Target ALS biorepository (by material transfer agreement). The ALS nervous systems were from patients who presented with ALS as the clinical phenotype, with or without FTD, and all had progressed and died from their motor impairment. For this study, we evaluated 11 C9 ALS cases (confirmation by repeat-primed PCR and Southern blotting) and 11 sporadic ALS cases.

3.3.2 CNS region and cell types

In spinal cord, we examined the alpha and gamma motor neurons in Rexed lamina IX of anterior horn lumbosacral sections. Alpha motor neurons were classified by their large multipolar cytoplasm, presence of lipofuscin, and a single prominent nucleolus. ESRRG immunostaining was used to classify gamma motor neurons.

3.3.3 Immunohistochemistry (IHC)

On day 1, sections were deparaffinized with Citrisolv (Fisher Scientific #04-355-121) and hydrated with different dilutions of alcohol. Endogenous peroxidase activity was quenched with 0.06% H2O2 for 15 min. Antigen retrieval was performed in a high pH solution (Vector #H-3301) in a pressure cooker for 20 min at a temperature of 120^{o}C. Following antigen retrieval, sections were permeabilized with 1% FBS (Atlanta Biologicals #511150) and 0.2% Triton X-100 (Sigma #65H2616) in PBS for 15 min and then blocked with 1% FBS in PBS for 25 min. The sections were incubated overnight with the primary antibody, rabbit polyclonal anti-ESRRG (1:500, ProteinTech, Cat# 14017-1-AP). On the second day, after 60-min incubation with the secondary antibody (Immpress reagent kit, anti-Rabbit, Vector) in room temperature, signals were detected using Immpact DAB (Vector #sk-4105) for 1–5 min. Counterstaining was performed with 0.1% Cresyl Ecth Violet. For IHC visualization, slides were scanned with Hamamatsu Nanozoomer 2.0HT Slide Scanner at 40X magnification.

3.3.4 Immunofluorescnece (IF)

On day one, sections were deparaffinized with Citrisolv (FISHER brand #04-355-121) and hydrated through a serial dilution of ethanol. Sections were permeabilized with 1% FBS (Atlanta Biologicals #511150) and 0.2% Triton X-100 (Sigma #65H2616). Following permeabilization, antigen retrieval was performed in a high pH solution (Vector # H- 3301) in a pressure cooker for 20 minutes at a temperature of 120^{o}C. Next, sections were blocked with 2% FBS in 1x PBS for 60 min. and were incubated with primary antibody overnight. Primary antibodies were diluted in

2% FBS in 1X PBS. For TDP-43, we used mouse monoclonal anti-TDP-43 (NovusBiologicals, #H00023435-M01, 1/500) and for ESRRG we used rabbit polyclonal anti-ESRRG (1:500, ProteinTech, Cat# 14017-1-AP). On day two, slides were incubated with secondary antibodies (goat anti-mouse Abcam #1150116, Alexa594, 1/500 and donkey anti-rabbit Jackson Immuno Research #715545, Alexa 488, 1/500) for 60 min. at room temperature. Secondary antibodies were diluted in 2% FBS in 1X PBS. We quenched CNS auto-fluorescence with 0.1% Sudan Black in 70% EtOH for 15 seconds. Slides were cover slipped using ProLong Gold Antifade Mountant with DAPI.

3.3.5 Co-fluorescence *in situ* hybridization (co-FISH-IF)

On day one, sections were deparaffinized with Citrisolv (FISHER brand #04-355-121) and hydrated through a serial dilution of ethanol. Sections were permeabilized with 1% FBS (Atlanta Biologicals #511150) and 0.2% Triton X-100 (Sigma #65H2616). Following permeabilization, antigen retrieval was performed in a high pH solution (Vector # H- 3301) in a pressure cooker for 20 minutes at a temperature of 120^{o}C. Next, we performed prehybridization and hybridization with FISH probes (GGGGCC3-Cy3, 80nM, ISIS, #693839) as described in (Aladesuyi Arogundade et al., 2019) and incubated the slides overnight at 66^{o}C. On day two, slides were washed three times with 2x SSC for 20 min at 55^{o}C and then washed twice in 0.2x SSC for 20 min at 55^{o}C. Next, sections were blocked with 2% FBS in 1x PBS for 60 min. and were incubated with primary antibody overnight. Primary antibodies were diluted in 2% FBS in 1X PBS. For TDP-43, we used rabbit polyclonal anti-TDP-43 (Proteintech, #12892-1- AP, 1/1000). For fibrillarin, we used mouse monoclonal anti-fibrillarin (SC-166001, 1/100). On day three, slides were incubated with secondary antibodies (donkey anti-mouse Jackson Immuno Research #715545, Alexa 488, 1/500 and goat anti-rabbit Abcam #31634, Alexa 647, 1/500) for 60 min. at room temperature. Secondary antibodies were diluted in 2% FBS in 1X PBS. We quenched CNS auto-fluorescence with 0.1% Sudan Black in 70% EtOH for 15 seconds. Slides were cover slipped using ProLong Gold Antifade Mountant with DAPI.

3.3.6 Confocal microscopy

For IF and co-FISH-IF, neurons were visualized using the fast mode for Zeiss 800 laser scanning microscope with airyscan, under 40X water magnification. If the nucleus of a neuron was not present in the imaged plane the neuron was not quantified. Maximum projections of z-stacks were compiled using Zen Black. Nucleolar, nuclear and cytoplasmic area were calculated using Fiji. The number and intracellular localization of antisense RNA foci and the presence of TDP-43 in the nucleus or mislocalizad to the cytoplasm were observed. Quantifications were made by a single observer in a blinded manner.

3.3.7 Statistics

We analyzed data in two different ways. We compared variables between the different groups (control, C9 and SALS) using two-tailed Mann-Whitney tests and represented the findings in bar graphs. Error bars are presented as standard error of mean. In addition, we compared variables using Kolmogorov-Smirnov tests and represented the findings in cumulative distribution curves. Using these two methods allowed statistics to make both population and individual comparisons. P-values below 0.05 were considered significant. All data analysis and graphing were performed using GraphPad Prism version 8.2.1 for Windows (GraphPad Software, La Jolla, CA).

3.4 RESULTS

3.4.1 Nucleolar size is reduced in C9-ALS and SALS spinal motor neurons

We determined nucleolar, nuclear and cystoplasmic areas using fibrillarin immunofluoresense, DAPI immunofluorescence and background fluorescence respectively in lumbosacral spinal motor neurons (SMNs) from 11 control, C9-ALS and SALS nervous systems each (Table 3.1; Fig. Fig. 3.1A; 3.7A). All three compartments were smaller in C9-ALS and SALS than

controls either when combined within groups or averaged within each nervous system (Fig. 3.1B-G). In order to determine whether the smallness was more specific to one compartment or another, we compared ratios of nucleolar to nuclear area, nucleolar to cytoplasmic area, and nuclear to cytoplasmic area. Compared to controls, the ratio of nucleolar to nuclear area was significantly decreased in both C9-ALS and SALS SMNs (Fig. 3.6A and B), indicating greater shrinkage of nucleoli compared to nuclei. Since the ratio of nuclear to cytoplasmic area was increased in both C9-ALS and SALS SMNs compared to controls, (Fig. 3.6E and F), indicating greater shrinkage of cytoplasm compared to nuclei, the ratio of nucleolar to cytoplasmic area was not an analogous comparison. Indeed, the ratios of nucleolar to cytoplasmic areas were slightly increased in C9-ALS or similar in SALS SMNs compared to controls (Fig. 3.6C and D). In these determinations, there are differences in the number of surviving neurons from each ALS nervous system, ranging between 9 and 45 SMNs. In order to verify that our results were not skewed by variation in numbers of surviving neurons, we re-analyzed our data by random sampling of neurons from each case, re-sampling and analyzing between 2 and 13 neurons 1000 times (Fig. 3.7A). As the sample size of randomly selected neurons increased from 2 to 13, the observed statistical significance stabilized at counting 6 neurons (Fig. 3.7B-G), verifying our results. Thus, we observe overall size reduction in C9-ALS and SALS especially affecting the nucleolar subcellular compartment.

3.4.2 ESRRG expression is specific to gamma motor neurons

Since cytoplasmic area was decreased in both C9-ALS and SALS SMNs, we also wondered if our analysis was specific for alpha motor neurons or skewed by a heterogeneous neuronal population including gamma motor neurons and whether or not there was a size bias because of overall shrinkage in ALS. Gamma motor neurons are small neurons that reside in Rexed lamina IX in the anterior part of anterior horns along with alpha motor neurons. In mice, expression of estrogen related receptor gamma (ESRRG), also known as ERR3, has been used to identify gamma motor neurons: gamma motor neurons have nuclear expression of ESRRG and

alpha motor neurons do not (Friese et al., 2009). We used ESRRG expression to identify gamma and alpha motor neurons in a subset of control (n=8), C9-ALS (n=6) and SALS (n=7) nervous systems. Nuclear ESSRG was found in putative gamma motor neurons and was absent in all putative alpha motor neurons (Fig. 3.2A). As expected, gamma motor neurons were smaller than alpha motor neurons in control, C9-ALS and SALS cases (Fig. 3.2B-D; Fig. 3.8A). On average, gamma motor neurons were 630 $\pm 370 \mu m^2$ in controls, 450 $\pm 250 \mu m^2$ in C9-ALS and 590 $\pm 420 \mu m^2$ in SALS, with a maximum size of 1930, 1140 and 1920 μm^2, in control, C9-ALS and SALS cases respectively (Fig. 3.2H). In order to exclude potential gamma motor neurons from the analysis, we used a lower threshold of 2000 m2 cytoplasmic size (Fig. 3.8B and C). We also used an upper threshold of 3000 m2 cytoplasmic size to exclude larger alpha neurons so we could compare samples with similar cytoplasmic size distributions (Fig. 3.2E).

In this subsample of similarly sized alpha motor neurons, we evaluated shrinkage of nucleoli (Fig. 3.2F-G; Supplemental Fig. 3.2E and F). Nucleolar area was significantly decreased in C9-ALS (p=0.009) and trended toward significance in SALS SMNs (p=0.1) (Fig. 3.2F). Likewise, the ratios of nucleolar to nuclear area and nucleolar to cytoplasmic area were also decreased in C9-ALS (p=0.01, p=0.02) and trended toward significance in SALS SMNs (p=0.06, p=0.1) (Fig. 3.2G; Fig. 3.8F). Conversely, nuclear area and the ratio of nuclear to cytoplasmic area were similar to controls in both C9-ALS (p=0.7, p=0.9) and SALS SMNs (p=0.8, p>0.9) (Fig. 3.8D-E). This shows that the decrease in the nucleolar size especially affects the alpha motor neurons, the main targets of the disease, significantly in C9-ALS and likely also in SALS.

An important but not well-studied aspect of ALS pathology is the involvement of gamma motor neurons in TDP-43 proteinopathy. TDP-43 proteinopathy has been observed in non-alpha motor neuron cell types including oligodendrocytes and large neurons in Clarke's column (Brettschneider et al., 2014). Since we were able to define gamma motor neurons with ESRRG immunostaining (Fig. 3.2A), we used this to examine if TDP-43 mislocalization also occurred in gamma motor neurons. Similar to alpha motor neurons lacking ESRRG expression, C9-ALS gamma motor neurons expressing nuclear ESRRG also had mislocalized nuclear TDP-43 that

formed cytoplasmic inclusions (Fig. 3.2I).

3.4.3 Sex specific SMN size differences are disrupted in C9-ALS and SALS

We also wondered if differences in patient sex, age of disease onset or duration of disease correlated with changes in SMN nucleolar size. Sex differences have been reported in human spinal cord; axons in the lateral corticospinal tract were found to be larger in males compared to females (Zhou et al., 2000). In animals, Mierzejewska-Krzyzowska et al. reported that male rats had larger alpha motorneurons compared to females but Dukkipati et al. found alpha motorneuron size to be similar in wild-type mice (Dukkipati et al., 2018; Mierzejewska-Krzyzowska et al., 2014). Interestingly, Dukkipati et al. reported that male G93A mice had larger soma size compared to wildtype mice, but female G93A mice had smaller alpha motorneurons compared to wild-types. Sexually dimorphic vulnerability in ALS has been suggested to occur in humans and animal models of disease with males having earlier disease onset, higher incidence and higher prevalence (Dukkipati et al., 2018; McCombe and Henderson, 2010; Suzuki et al., 2007). In our study, the majority of C9-ALS and SALS cases were male and were age and sex matched to controls (Table 3.1). We found that in controls, cytoplasmic and nuclear area were significantly larger in males compared to females (p=0.04, p=0.04) but nucleolar area was not significantly different when stratified by sex (p=0.1) (Fig. 3.3A, D and G). Sex differences were not present in C9-ALS SMNs when we compared cytoplasmic, nuclear or nucleolar area ($p<0.9$; p=0.5; p=0.9, respectively) (Fig. 3.3B, E and H) or in SALS SMNs (p=0.2; p=0.5; p=0.4, respectively) (Fig. 3.3C, F and I). There was no correlation between disease onset or disease course and SMN size indices (Fig. 3.9A-F).

3.4.4 Biphasic nucleolar size reduction correlates with TDP-43 mislocalization

Mizilenska et al., found that decreased nucleolar volume in C9-FTLD frontal cortical neurons was most prominent in neurons lacking sense RNA foci, poly(GA) or poly(GR)

(Mizielinska et al., 2017). Since we found that nucleolar area was decreased not only in C9-ALS SMNs but also in SALS SMNs, we wondered if other pathological markers such as TDP-43 mislocalization correlated to a greater reduction in nucleolar size. We re-analyzed our data, stratifying neurons by normal nuclear TDP-43 localization or mislocalized nuclear TDP-43 that formed cytoplasmic aggregates. Using an antibody specific to the C-terminus of TDP-43, we observed that all C9-ALS and SALS SMNs lacking nuclear TDP-43 had cytoplasmic TDP-43 inclusions (Fig. 3.4A). But, interestingly, nucleolar area was reduced in C9-ALS SMNs with either nuclear TDP-43 or mislocalized TDP-43 (Fig. 3.4B and C). Similarly, nuclear area was reduced in SALS SMNs with either nuclear TDP-43 or mislocalized TDP-43 (Fig. 3.4B and C). Indeed, reductions in nuclear size and cytoplasmic size was greatest in neurons without TDP-43 mislocalilzation in C9-ALS (Fig. 3.4D-G). This suggests that the nucleolar shrinkage may be one of the earliest neuronal changes and then increases as neuronal degeneration proceeds, that is, it occurs and then reverses suggesting the process of nucleolar stress is biphasic.

3.4.5 Biphasic nucleolar size reduction correlates with antisense RNA foci

We wanted to see how the presence of antisense RNA foci and TDP-43 mislocalization correlated with reduced nucleolar size in ALS SMNs. Cooper-Knock et al. have previously shown that antisense RNA foci correlate with TDP-43 pathology in SMNs (Cooper-Knock et al., 2015). We further expanded on this finding by showing that the nucleolar localization of antisense RNA foci in cells accounted for 97% of the co-occurrence of antisense RNA foci and TDP-43 mislocalization (Aladesuyi Arogundade et al., 2019). In light of these previous observations, we analyzed our current data, stratifying neurons by the presence of antisense RNA foci, nucleolar antisense RNA foci and TDP-43 mislocalization (Fig. 3.10). Nucleolar size was decreased in neurons with or without nucleolar antisense RNA foci and shrinkage was greatest in neurons without nucleolar antisense RNA foci (Fig. 3.5A and B). Similarly, nuclear and cytoplasmic area were decreased in neurons with or without nucleolar antisense RNA foci

(Fig. 3.5C-F). We also found that decrease in nucleolar, nuclear and cytoplasmic area occurred in neurons regardless of the nucleolar localization of antisense RNA foci (Fig. 3.11A-F). Thus, surprisingly, it seems nucleolar shrinkage occurs in two phases.

Lastly, we stratified neurons by the presence of either TDP-43 mislocalization or nucleolar antisense RNA foci or both and compared the correlation of nucleolar, nuclear and cytoplasmic area between these groups. SMNs from controls had the largest nucleoli, nuclei and cytoplasms (Fig. 3.5G-I). SMNs from SALS cases had smaller nucleoli, nuclei and cytoplasms than controls and this difference was greatest in neurons that had normal nuclear TDP-43 (Fig. 3.5G-I). SMNs from C9-ALS cases had smaller nucleoli, nuclei and cytoplasms than both controls and SALS and this difference was greatest in neurons with normal nuclear TDP-43 and no nucleolar antisense RNA foci. C9-ALS SMNs with TDP-43 mislocalization and no nucleolar antisense RNA foci had smaller nucleoli, nuclei and cytoplasms than neurons with nucleolar antisense RNA foci with or without TDP-43 mislocalization (Fig. 3.5G-I). This is consistent with nucleolar stress having two phases, nucleolar shrinkage early in disease, and then reversal with the occurrence of pathology, either TDP-43 mislocalization and/or antisense RNA foci.

3.5 DISCUSSION

In this study, we extend previous findings identifying nucleolar stress in C9-ALS and extend them to SMNs in SALS. Overall, SMNs in ALS cases, either C9-ALS or sporadic, have smaller nucleoli compared to controls, yet, surprisingly, neurons with pathological markers, TDP-43 mislocalization or antisense RNA foci, have larger nucleoli when compared to neurons lacking such pathology. Similarly, Mizielinska et al. also found nucleolar shrinkage in C9-FTLD frontal cortical neurons to be greatest in neurons without sense RNA foci or DPRs (Mizielinska et al., 2017). It would seem logical that nucleolar shrinkage progresses as a part of the pathological changes within degenerating neurons but there appear to be consistent findings that in ALS, nucleolar shrinkage is found in the absence of pathological markers such as TDP-43

mislocalization/aggregation, RNA foci or DPRs. This suggests that nucleolar stress marked by shrinkage may occur as one of the earliest mechanisms. Disease pathways including nuclear cytoplasmic transport defects, dysfunctional stress granule assembly and aberrant immune responses have been shown to contribute to neurodegeneration and could correlate with nucleolar shrinkage in the absence of TDP-43 mislocalization, RNA foci or DPRs (Boeynaems et al., 2017; Burberry A, Suzuki N, Wang JY, Moccia R, Mordes DA, 2016; Burberry et al., 2020; Chew et al., 2019; Farg et al., 2014; Freibaum et al., 2015; Hartmann et al., 2018; Hutten and Dormann, 2019; Jain and Vale, 2017; Jovičič et al., 2015; Kramer et al., 2018; Lee et al., 2016; Li et al., 2013; Liu-Yesucevitz et al., 2010; Marta M. Fay et al., 2017; Sellier et al., 2016; Shao et al., 2019; Shi et al., 2017, 2018; Ugolino et al., 2016; Vatsavayai et al., 2018; Zhang et al., 2015, 2016; Zhu et al., 2020).

TDP-43 mislocalization, RNA foci and DPRs may drive nucleolar stress, and our methods may not be sensitive enough to detect their presence in every cell. For example, repeat-containing RNA transcripts could be toxic before forming RNA foci that are detectable by our hybridization methods. Similarly, DPRs could be toxic before forming large aggregates detected by confocal microscopy. Notably, White et al. have demonstrated that soluble arginine-rich DPRs competitively sequester nucleophosmin and ribosomal RNA in vitro, resulting in disruption of the nucleolar structure (White et al., 2019). Poly(GR)-induced dispersion of nucleoli is consistent with Mizielinska et al. reporting that poly(GR) correlates with enlarged nucleoli in C9-FTLD frontal cortical neurons (Mizielinska et al., 2017; White et al., 2019). The findings could be explained by high concentrations of soluble poly(GR) inducing nucleolar shrinkage and low concentrations of soluble poly(GR) inducing nucleolar enlargement. Overall, a shift from high to low concentration of DPRs that are soluble and undetectable by immunostaining, to insoluble aggregates that are detectable by immunostaining, could underlie the biphasic nature of nucleolar stress observed in pathology. Additionally, altered function of TDP-43 could induce nucleolar dysfunction before large cytoplasmic aggregates and complete nuclear clearing are detected. Previously, we have shown that TDP-43 mislocalization is intrinsically linked to nucleolar antisense

RNA foci (Aladesuyi Arogundade et al., 2019). In rare cases of C9-ALS, it has been shown that TDP-43 pathology occurs later in disease while sense and antisense RNA foci can precede TDP-43 pathology (Vatsavayai et al., 2016). In the spinal cord, DPRs are rare and increased presence of nucleolar antisense but not sense RNA foci correlate with TDP-43 mislocalization (Aladesuyi Arogundade et al., 2019; Schludi et al., 2017). Thus, it remains possible that antisense RNA transcripts and DPRs first induce toxicity by way of the nucleolus and then cause TDP-43 mislocalization concurring with enlarged nucleolar size.

Decreased ribosomal biogenesis from RNA profiling of three SALS and one C9-ALS patients as well as from C9-ALS lymphoblasts and motor cortex is in line with nucleolar stress marked by a reduction in nucleolar volume (Haeusler et al., 2014; Krach et al., 2018). Ribosomal biogenesis is an energy-demanding task and can be inhibited as a cellular response to stress (Boisvert et al., 2007; Mizielinska et al., 2017). Alternatively, gain of function mechanisms underlying C9-ALS and SALS can directly impair ribosomal biogenesis. Reduced ribosomal biogenesis and protein translation as well as altered nucleolar size have been shown to occur in cellular models of C9-ALS supporting that C9-ALS gain of toxicity mechanisms disrupt nucleolar function (Haeusler et al., 2014; Kwon et al., 2014; Mizielinska et al., 2017; Tao et al., 2015; Wen et al., 2014; White et al., 2019).

It is also unknown if reduced nucleolar size occurs in additional cell-types vulnerable to neurodegeneration such as Von Economo neurons, and if reduced nucleolar size is also a feature of sporadic ALS (SALS) and SALS-FTD. The anterior cingulate cortex and frontoinsular are the primary regions to degenerate at the onset of FTD. Von Economo neurons found in layer V of the anterior cingulate cortex and frontoinsular are suggested to support social behavior and emotionality and selectively degenerate in FTD (Nana et al., 2019; Santillo et al., 2013). Nuclear clearing and cytoplasmic inclusions of TDP-43 were found to correlate with dystrophy of neurites in frontoinsular Von Economo neurons but it remains to be seen if nucleolar stress is also a neuropathological feature of Von Economo neurons (Nana et al., 2019).

With the increasing knowledge on how various genetic and environmental factors affect

the risk and progression of ALS, it is important to factor in categorization based on sex. Sexual dimorphisms have been found in human, mouse and rat spinal cord, with males exhibiting larger axons in the lateral corticospinal tract, larger cell size and increased density of alpha and gamma motorneurons (Mierzejewska-Krzyzowska et al., 2014; Suzuki et al., 2007; Zhou et al., 2000). Our study was inadvertently skewed to include more males than females yet in controls, alpha motor neurons were larger in males than in females. Interestingly, C9-ALS and SALS males and females had similar alpha motor neuron size, however, compared to controls, decrease in neuron size was greater in males than in females. A larger study is needed to investigate the extent to which sexual dimorphism might affect neurodegeneration in ALS, but thus far, several studies in humans and rodents have indicated that males have increased vulnerability in ALS (McCombe and Henderson, 2010; Suzuki et al., 2007; Zhou et al., 2000). Integrating sex-specific guidelines and strategies in treatments may prove useful in improving the design and outcomes of clinical trials as well as patient responses to treatments.

In summary, we have demonstrated that nucleolar stress occurs in C9-ALS and SALS spinal motor neurons is biphasic. Compared to controls, nucleoli are smaller in C9-ALS and SALS spinal motor neurons and this shrinkage is greatest in cells lacking TDP-43 mislocalization or nucleolar antisense RNA foci. Thus, biphasic nucleolar stress may occur in ALS pathology, where nucleolar shrinkage first occurs in the absence of pathological markers followed by nucleolar enlargement coinciding with TDP-43 mislocalization or nucleolar antisense RNA foci. This supports previous findings from neuropathology and cellular models and has important implications for the pathobiology of nucleolar stress in ALS.

3.6 ACKNOWLEDGEMENTS

This research was supported by grants from ALS Association (5356S3), Target ALS (20134792), National Institute of Neurological Diseases and Stroke (NIH R01NS088578 and NS047101), UCSD Microscopy Core (NINDS NS047101) and Pam Golden. OAA is supported

by National Science Foundation Graduate Research Fellowship (DGE-1650112). We thank the patients and their families for their generous contribution to this research.

Chapter 3, in part is currently being prepared for submission for publication of the material. Aladesuyi Arogundade, Olubankole; Nguyen, Sandra; Leung, Ringo; Wainio, Danielle; Rodriguez, Maria; Ravits, John. The dissertation author was the primary author of this material.

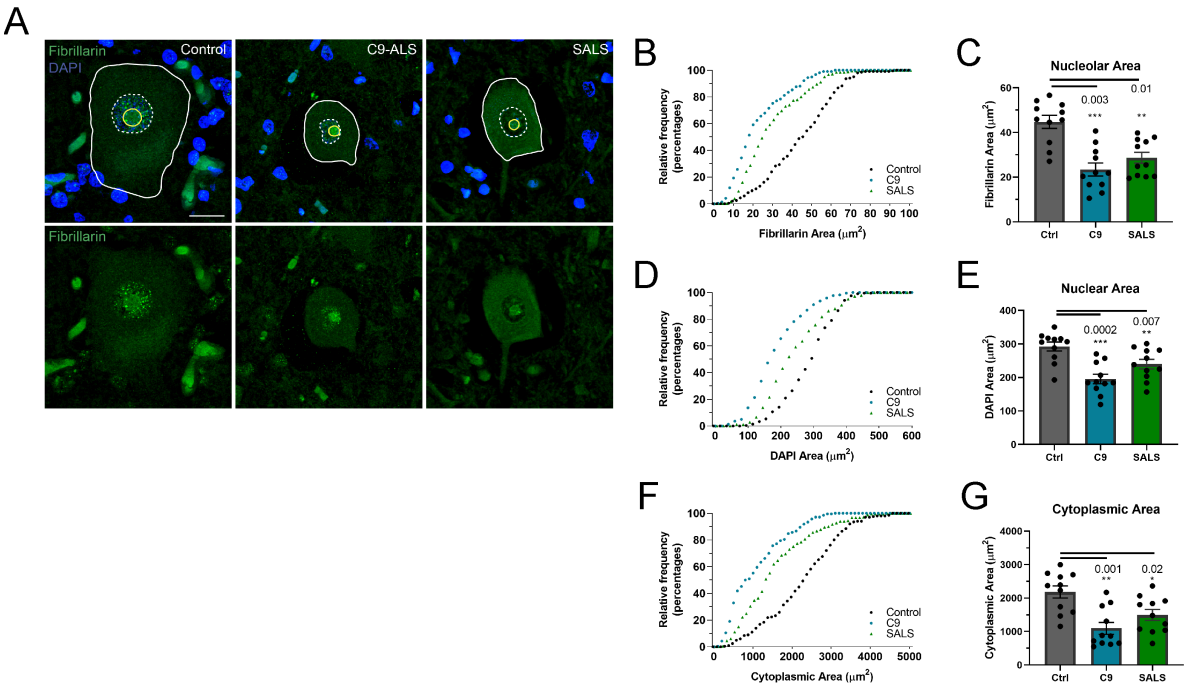

Figure 3.1. Nucleolar shrinkage occurs in C9-ALS and SALS spinal motor neurons. (A) Nucleolar area is identified by fibrillarin staining (green), nuclear area is identified by DAPI and cytoplasmic area is identified by autofluorescnce in control, C9-ALS and SALS spinal motor neurons. Nucleolar (B-C), nuclear (D-E) and cytoplasmic (F-G) area are decreased in C9-ALS and SALS neurons compared to controls.

Table 3.1. Patient demographics (DC: Disease Course; DO: Disease Onset; A: Axial, CI: Cognitive Impairment; LL: Lower Limb; S: Swallowing)

Group	Case ID	Age (yrs)	Gender	DC (yrs)	DO (yrs)	Site of Onset
Control	4	75	M	NA	NA	NA
Control	7	61	M	NA	NA	NA
Control	10	78	M	NA	NA	NA
Control	39	77	M	NA	NA	NA
Control	42	61	M	NA	NA	NA
Control	65	82	M	NA	NA	NA
Control	67	77	M	NA	NA	NA
Control	76	68	M	NA	NA	NA
Control	78	58	F	NA	NA	NA
Control	103	92	F	N/A	N/A	N/A
Control	115	94	M	N/A	N/A	N/A
C9-ALS	14	73	F	1.5	71.5	Bulbar
C9-ALS	81	58	M	1.5	56.5	Bulbar
C9-ALS	91	61	M	3.5	57.5	Bulbar
C9-ALS	120	64	M	7.5	56.5	Bulbar
C9-ALS	126	70	M	1.8	68.25	Arm
C9-ALS	119-JHU	61	F	2.6	58	LL
C9-ALS/FTD	86-JHU	74	M	7.3	67	Bulbar,S, LL, CI
C9-ALS/FTD	88-JHU	59	M	1.7	57	Bulbar, Speech, CI
C9-ALS	MN2	55	F	2.3	52	Bulbar, Speech
C9-ALS	PCJ	58	M	3.6	54	A, Respiratory, Trunk
C9-ALS	PYF	59	M	0.4	58	LL
SALS	29	77	F	3	74	LL
SALS	32	71	M	1.5	69.5	Respiratory, Trunk
SALS	43	74	M	1.8	72.25	Respiratory, Trunk
SALS	46	51	F	2.5	48.5	Arm
SALS	60	58	F	3	55	Bulbar
SALS	94	62	M	7	55	Bulbar
SALS	109	49	M	1.5	47.5	Leg
SALS	110	53	M	Unknown	N/A	Body twitches
SALS	111	59	F	3.5	55.5	Leg
SALS	123	57	M	4	53	Body twitches
SALS	125	67	M	1.5	65.5	Arm

Figure 3.2. Gamma motor neurons are identified by ESRRG immunofluorescence. (A) Immunohistochemistry of ESRRG in control, C9-ALS and SALS lumbar spinal cord. Alpha motors (third column) lack nuclear ESRRG immunofluorescence. Gamma motor neurons (fourth column) have nuclear ESRRG immunofluorescence. (B-D) Distribution of cytoplasmic area for gamma neurons (dashed lines) and alpha motor neurons (solid lines) in control, C9-ALS and SALS lumbar spinal cord (red dashed line, threshold for alpha motor neurons). (E) Comparison of similar distribution of cytoplasmic area in sub-sample of control, C9-ALS and SALS alpha motor neurons (dashed lines, cytoplasmic area thresholds: 2000 and 32000 μm). (F) Nucleolar area and (G) nulceolar to nuclear area ratio are decreased in sub-samples of C9-ALS and SALS neurons compared to control neurons with similar cytoplasmic size. (H) Distribution of cytoplasmic area is non-significantly reduced in C9-ALS and SALS gamma motor neurons compared to controls. (I) TDP-43 mislocalization occurs in alpha motor neurons (white dashed outline) and in gamma neurons (yellow dashed outline) identified by nuclear ESRRG immunofluorescence (arrowheads).

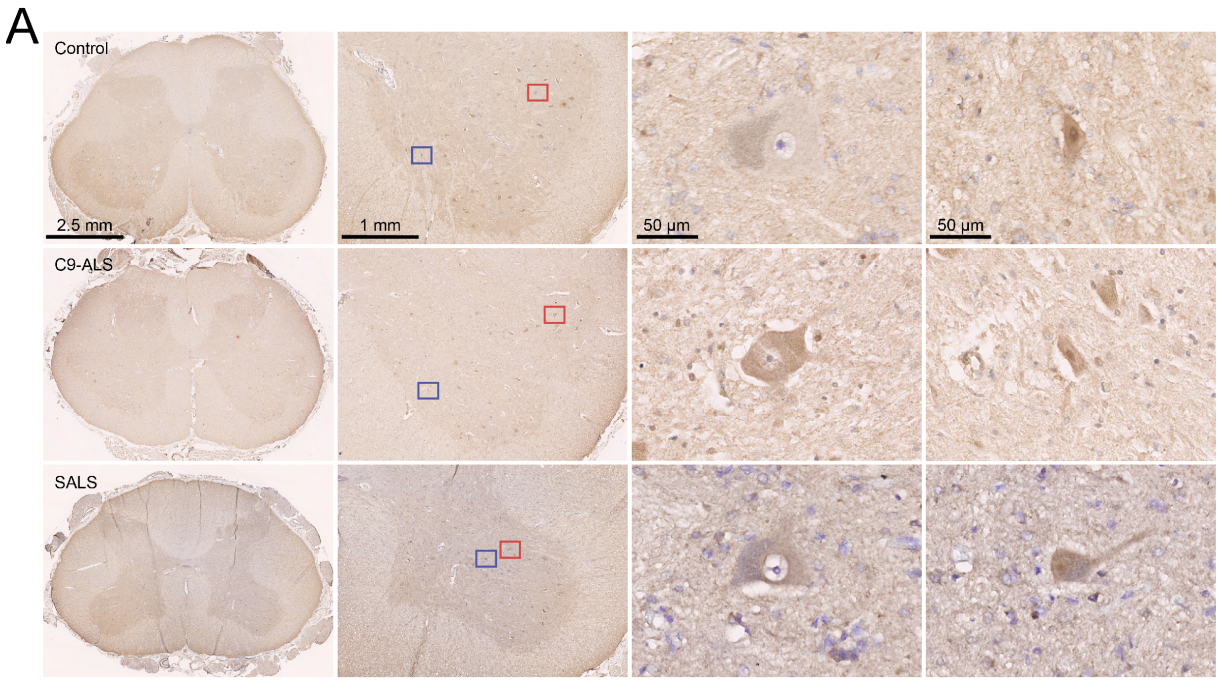
A
Control
C9-ALS
SALS
2.5 mm
1 mm
50 µm
50 µm

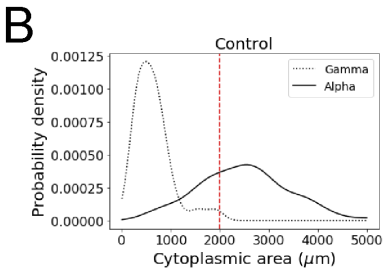
B
Control
Gamma
Alpha
Probability density
Cytoplasmic area (µm)

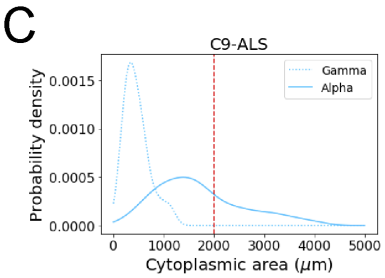
C
C9-ALS
Gamma
Alpha
Probability density
Cytoplasmic area (µm)

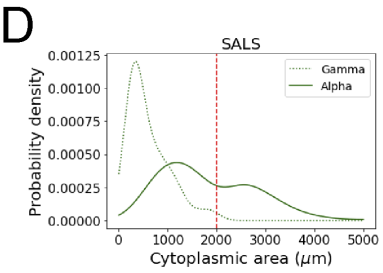
D
SALS
Gamma
Alpha
Probability density
Cytoplasmic area (µm)

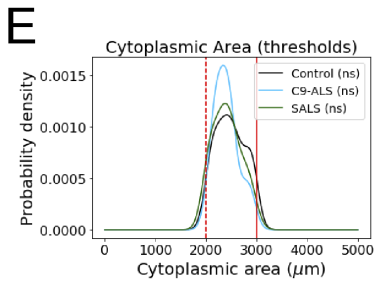
E
Cytoplasmic Area (thresholds)
Control (ns)
C9-ALS (ns)
SALS (ns)
Probability density
Cytoplasmic area (µm)

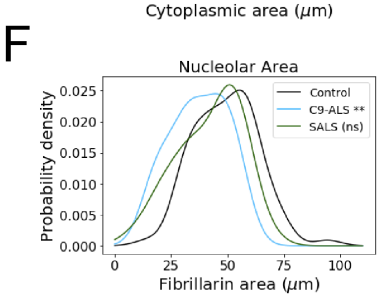
F
Nucleolar Area
Control
C9-ALS **
SALS (ns)
Probability density
Fibrillarin area (µm)

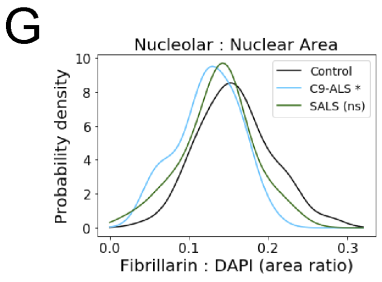
G
Nucleolar : Nuclear Area
Control
C9-ALS *
SALS (ns)
Probability density
Fibrillarin : DAPI (area ratio)

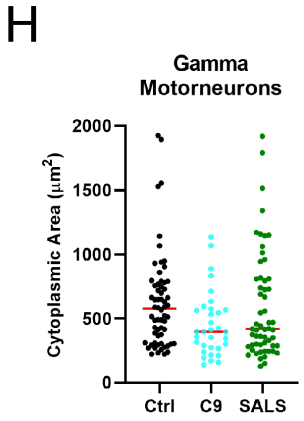
H
Gamma Motorneurons
Cytoplasmic Area (µm²)
Ctrl
C9
SALS

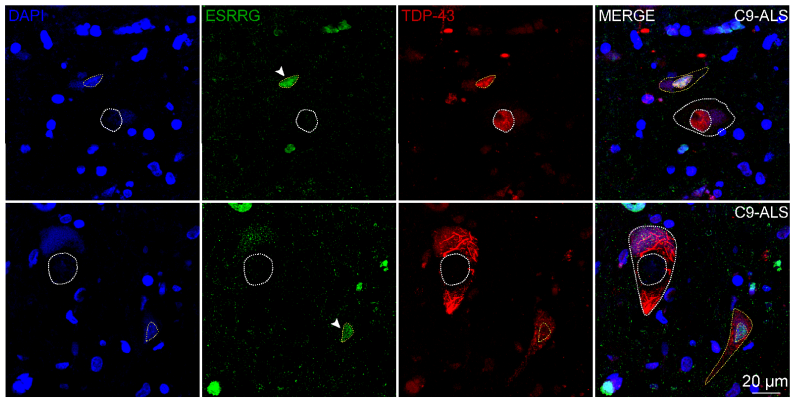
I
DAPI
ESRRG
TDP-43
MERGE
C9-ALS
C9-ALS
20 µm

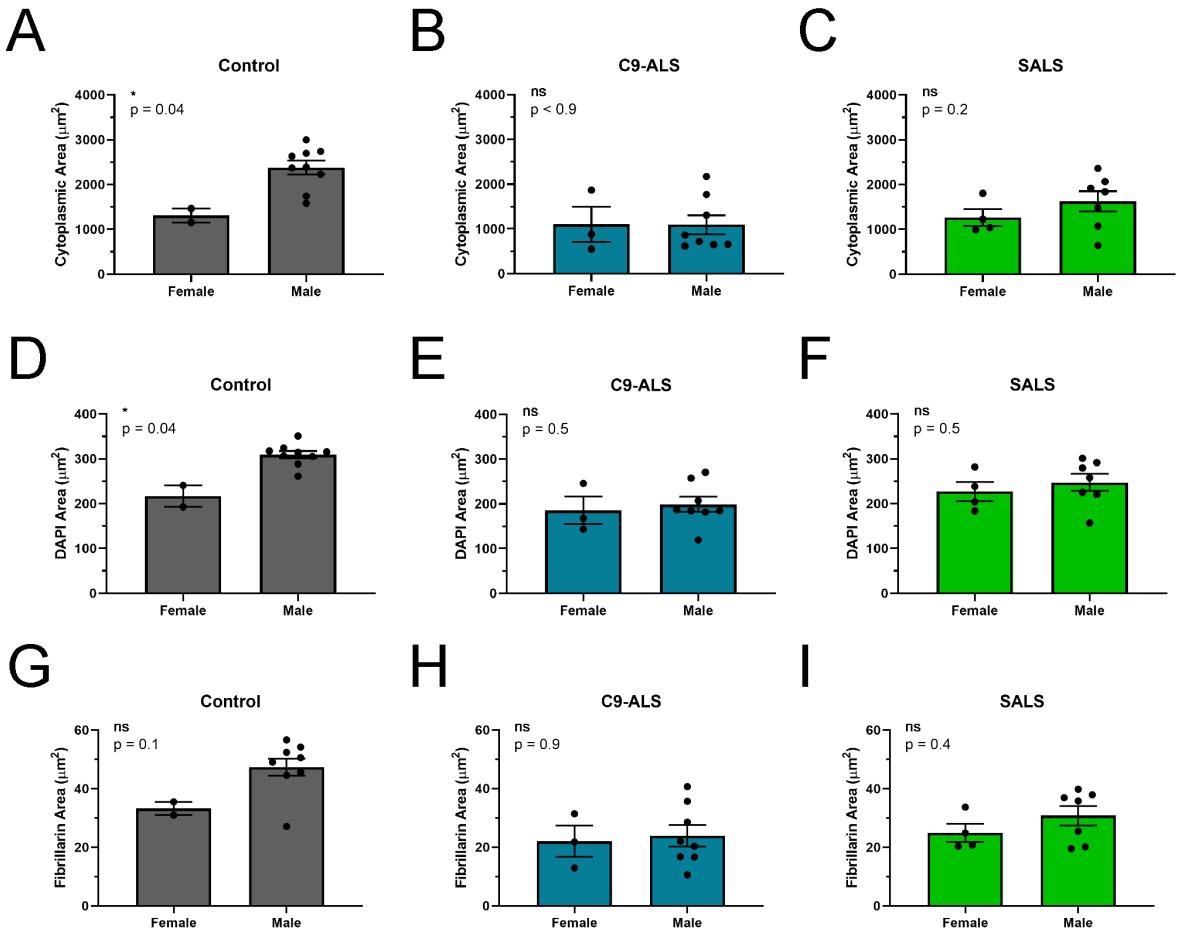

Figure 3.3. Sexual dimorphism in spinal motor neuron cytoplasmic and nuclear area is abolished in C9-ALS and SALS. (A) Cytoplasmic and (D) nuclear area are significantly larger in male control cases compared to females but are similar in (B and E) C9-ALS and (C and F) SALS cases. Nucleolar area is not significantly different between male and female in (G) control, (H) C9-ALS or (I) SALS cases.

Figure 3.4. Biphasic nucleolar stress in C9-ALS and SALS spinal motor neurons is dependent on TDP-43 mislocalization. (A) Nucleolar area is identified by fibrillarin staining (green), nuclear area is identified by DAPI and cytoplasmic area is identified by autofluorescnce in control, C9-ALS and SALS spinal motor neurons. C-terminal TDP-43 immunofluorescence (cyan) was always nuclear in control neurons and was either nuclear or mislocalized to the cytoplasm in ALS neurons. (B-C) Nucleolar area, (D-E) nuclear area, and (F-G) cytoplasmic area are decreased in C9-ALS and SALS neurons with or without TDP-43 mislocalization compared to controls.

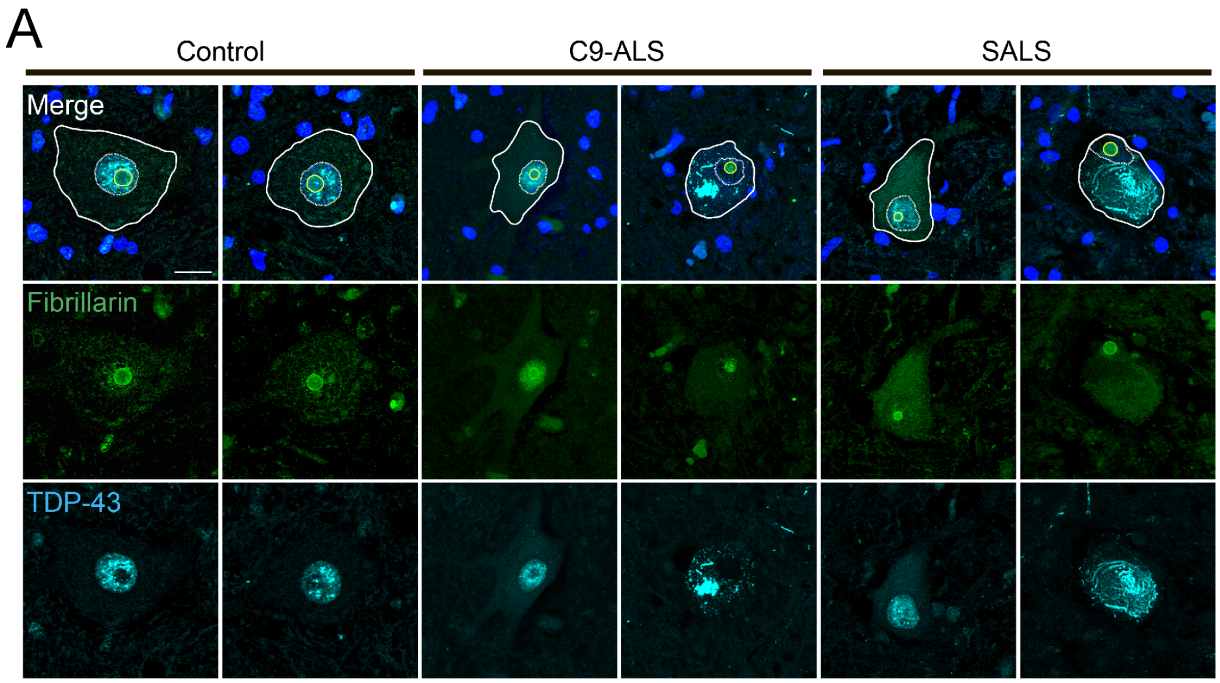
A
Control
C9-ALS
SALS
Merge
Fibrillarin
TDP-43

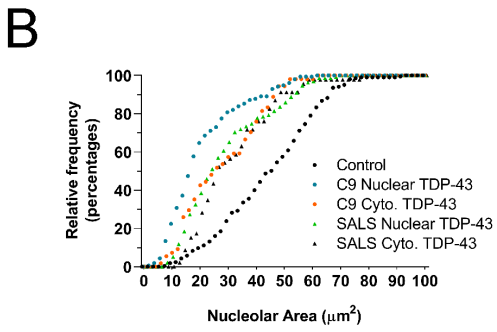
B
Relative frequency (percentages)
Nucleolar Area (μm²)
Control
C9 Nuclear TDP-43
C9 Cyto. TDP-43
SALS Nuclear TDP-43
SALS Cyto. TDP-43

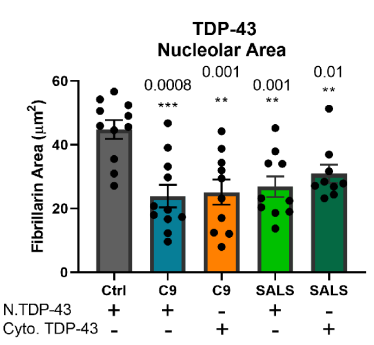
C
TDP-43
Nucleolar Area
Fibrillarin Area (μm²)
0.0008
0.001
0.001
0.01
Ctrl
C9
C9
SALS
SALS
N.TDP-43
Cyto. TDP-43

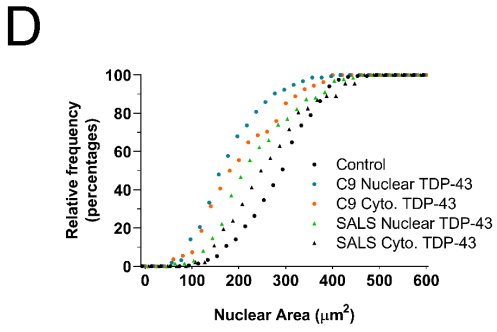
D
Relative frequency (percentages)
Nuclear Area (μm²)
Control
C9 Nuclear TDP-43
C9 Cyto. TDP-43
SALS Nuclear TDP-43
SALS Cyto. TDP-43

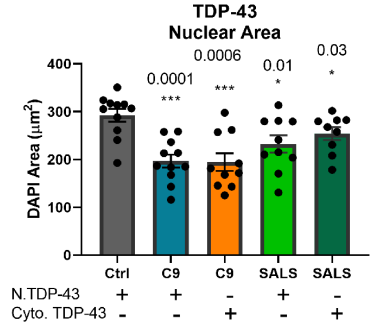
E
TDP-43
Nuclear Area
DAPI Area (μm²)
0.0001
0.0006
0.01
0.03
Ctrl
C9
C9
SALS
SALS
N.TDP-43
Cyto. TDP-43

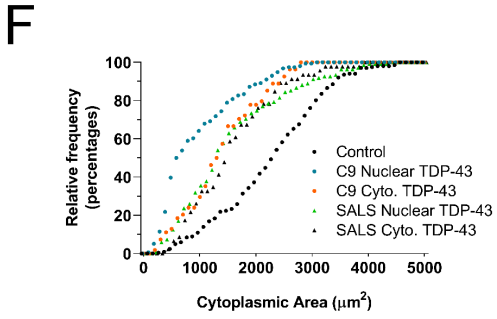
F
Relative frequency (percentages)
Cytoplasmic Area (μm²)
Control
C9 Nuclear TDP-43
C9 Cyto. TDP-43
SALS Nuclear TDP-43
SALS Cyto. TDP-43

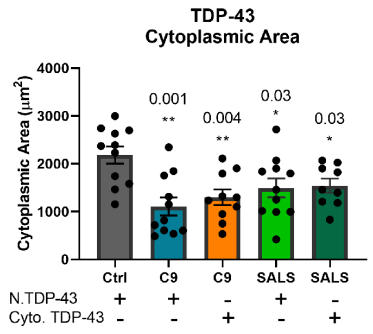
G
TDP-43
Cytoplasmic Area
Cytoplasmic Area (μm²)
0.001
0.004
0.03
0.03
Ctrl
C9
C9
SALS
SALS
N.TDP-43
Cyto. TDP-43

Figure 3.5. Biphasic nucleolar stress in C9-ALS spinal motor neurons is dependent on nucleolar antisense RAN foci. (A-B) Nucleolar area, (C-D) nuclear area, and (E-F) cytoplasmic area are decreased in C9-ALS with or without nucleolar antisense RNA foci and in SALS neurons compared to controls. Scatterplots of group average (top) and individual neurons (bottom) comparing (G) nucleolar and nuclear area, (H) nucleolar and cytoplasmic area, and (I) nuclear and cytoplasmic area (lines indicate linear regression).

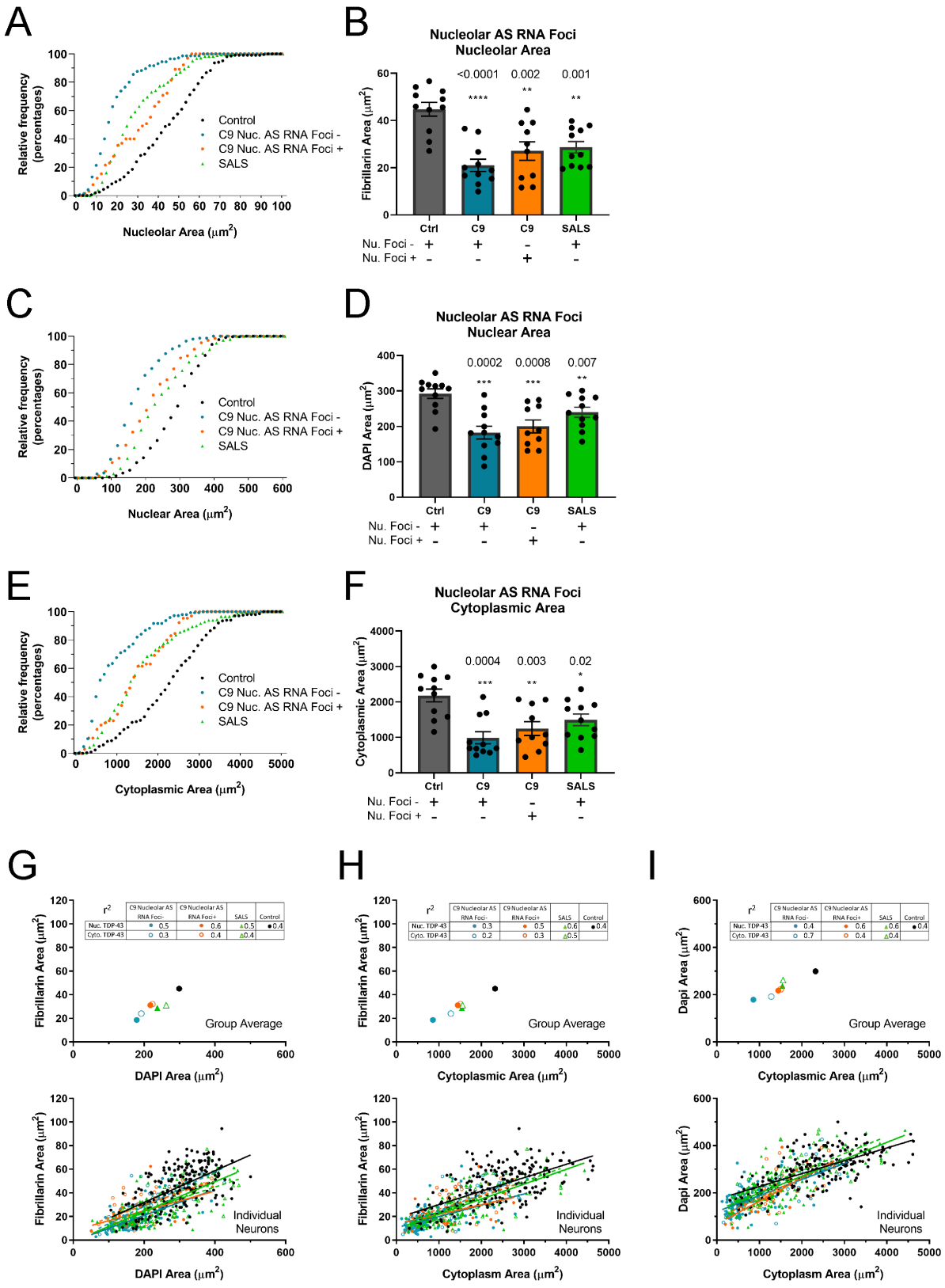
A
Relative frequency (percentages)
Nucleolar Area (μm²)
Control
C9 Nuc. AS RNA Foci -
C9 Nuc. AS RNA Foci +
SALS
B
Nucleolar AS RNA Foci
Nucleolar Area
Fibrillarin Area (μm²)
<0.0001
0.002
0.001
Ctrl
C9
C9
SALS
Nu. Foci -
Nu. Foci +
C
Nuclear Area (μm²)
D
Nucleolar AS RNA Foci
Nuclear Area
DAPI Area (μm²)
0.0002
0.0008
0.007
E
Cytoplasmic Area (μm²)
F
Nucleolar AS RNA Foci
Cytoplasmic Area
0.0004
0.003
0.02
G
DAPI Area (μm²)
Group Average
Individual Neurons
H
Cytoplasmic Area (μm²)
Cytoplasm Area (μm²)
I
Dapi Area (μm²)

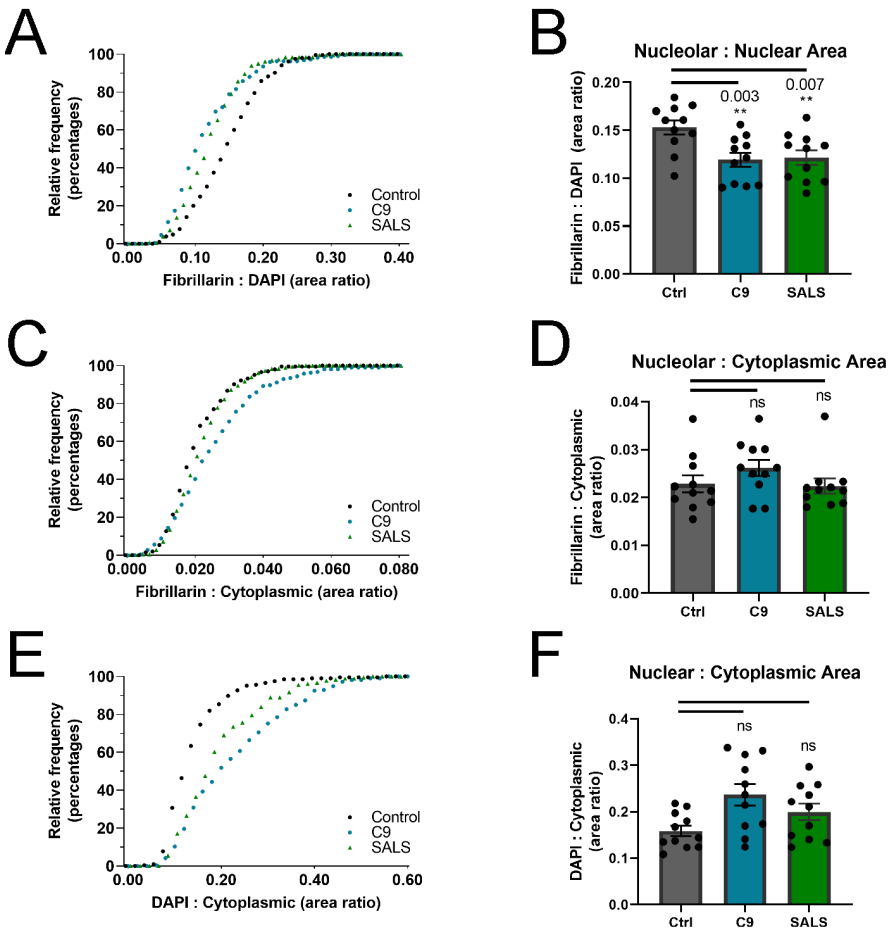

Figure 3.6. Nucleolar to cytoplasmic and nuclear to cytoplasmic area ratios in control, C9-ALS and SALS SMNs. (A-B) Nucleolar to cytoplasmic area ratio is not significantly different in C9-ALS or SALS SMNs compared to controls. Nucleolar to cytoplasmic (C-D) and nuclear to cytoplasmic (E-F) area ratios are non-significantly increased in C9-ALS and SALS SMNs compared to controls.

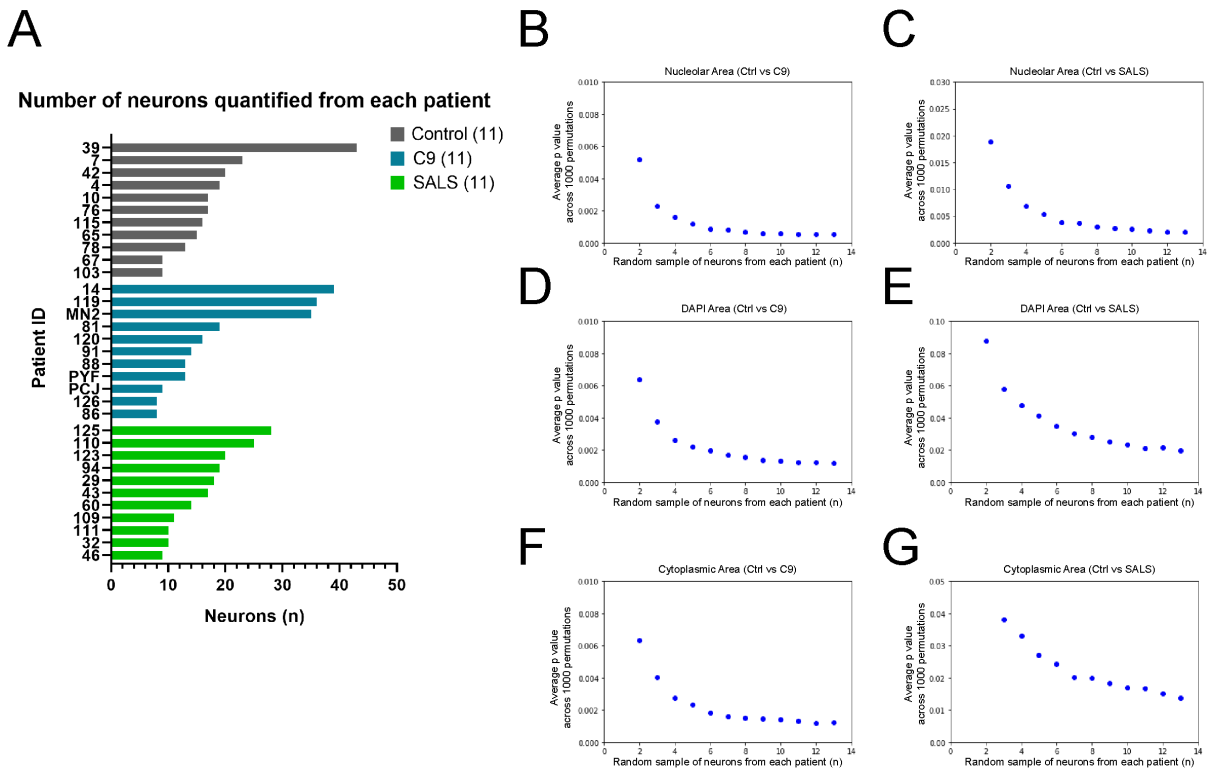

Figure 3.7. Random sampling of spinal motor neurons for statistical analysis. (A) Number of spinal motor neurons quantified from each patient. Random sampling of neurons for analyzing difference in (B) nucleolar area, (D) nuclear area and (F) cytoplasmic area between C9-ALS and control neurons. Random sampling of neurons for analyzing difference in (C) nucleolar area, (E) nuclear area and (G) cytoplasmic area between SALS and control neurons.

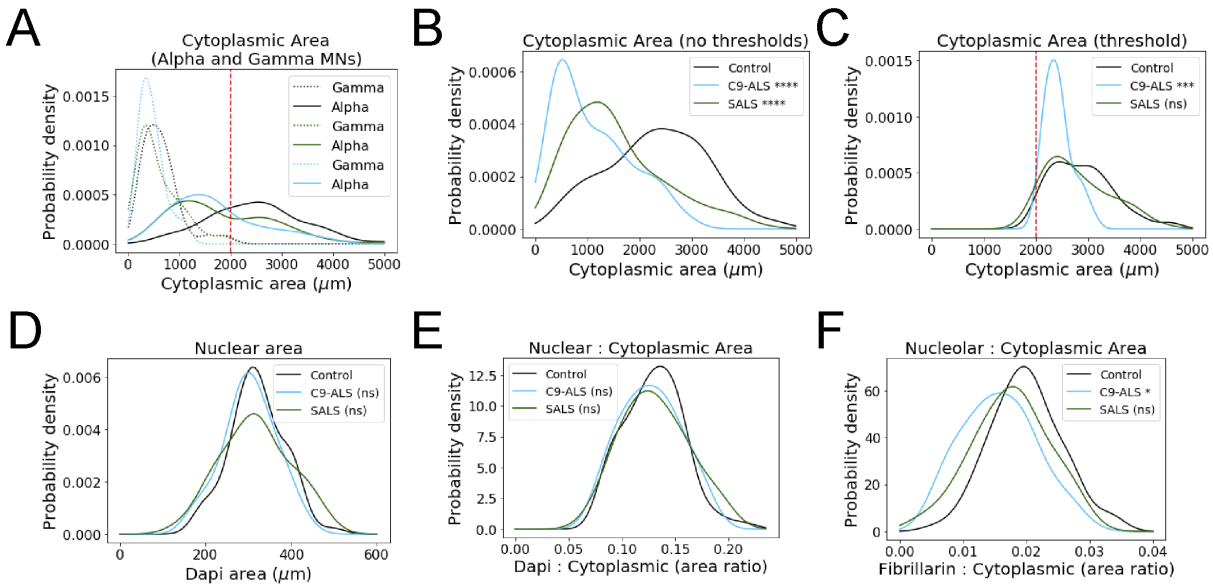

Figure 3.8. Analysis of nuclear and nucleolar abnormalities in a sub-sample of spinal motor neurons. (A) Distribution of cytoplasmic area for gamma (dashed lines, ESRRG positive) and alpha motor neurons (solid lines, ESRRG negative; dashed red line, threshold for alpha motor neurons). (D) Nuclear area and (E) nuclear to cytoplasmic area ratio are not significantly different in a sub-sample of similarly sized C9-ALS or SALS neurons compared to controls. (F) Nucleolar to cytoplasmic area ratio is significantly decreased in a sub-sample of similarly sized C9-ALS but not SALS neurons compared to controls.

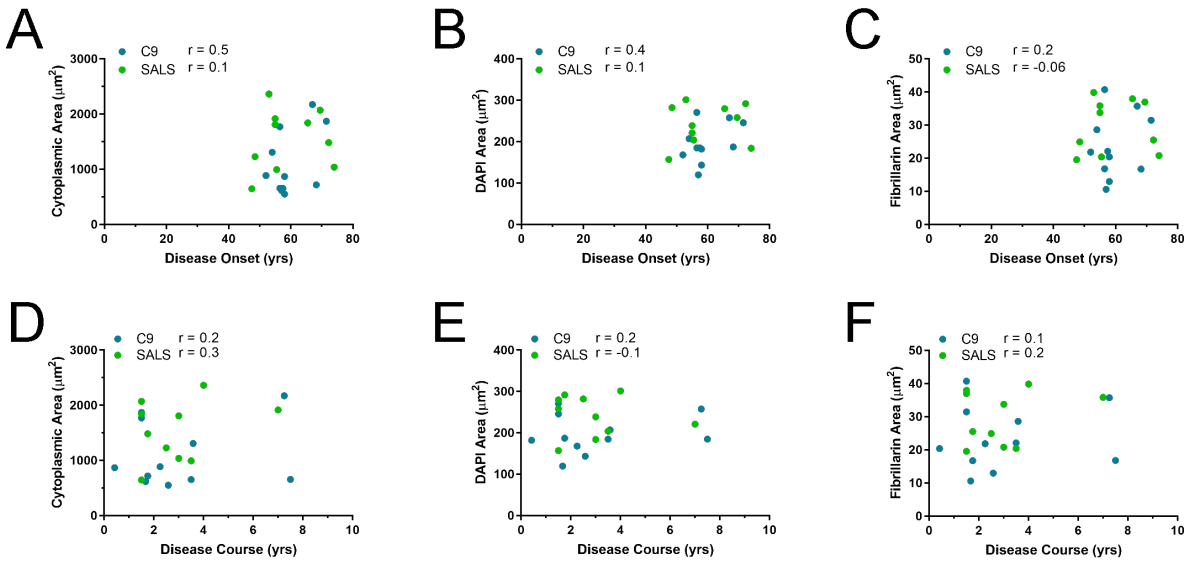

Figure 3.9. Nucleolar, nuclear and cytoplasmic area do not correlate with age at disease onset or disease duration in C9-ALS and SALS spinal motor neurons. Correlation between (A and D) nucleolar (B and E) nuclear or (C and F) cytoplasmic area and age at disease onset or disease course, respectively.

Figure 3.10. Co-FISH-IF in control, C9-ALS and SALS spinal motor neurons. Nucleolar area (yellow dash) is identified by fibrillarin (green), nuclear area (inner white dash) is identified by DAPI (blue) and cytoplasmic area (outer white dash) is identified by autofluorescence. C-terminal TDP-43 immunofluorescence (cyan) was found to be nuclear in control neurons and either nuclear or mislocalized to the cytoplasm in C9-ALS and SALS neurons. Anitsense RNA foci (arrowheads) were nuclear in C9-ALS neurons and often localized to nucleoli.

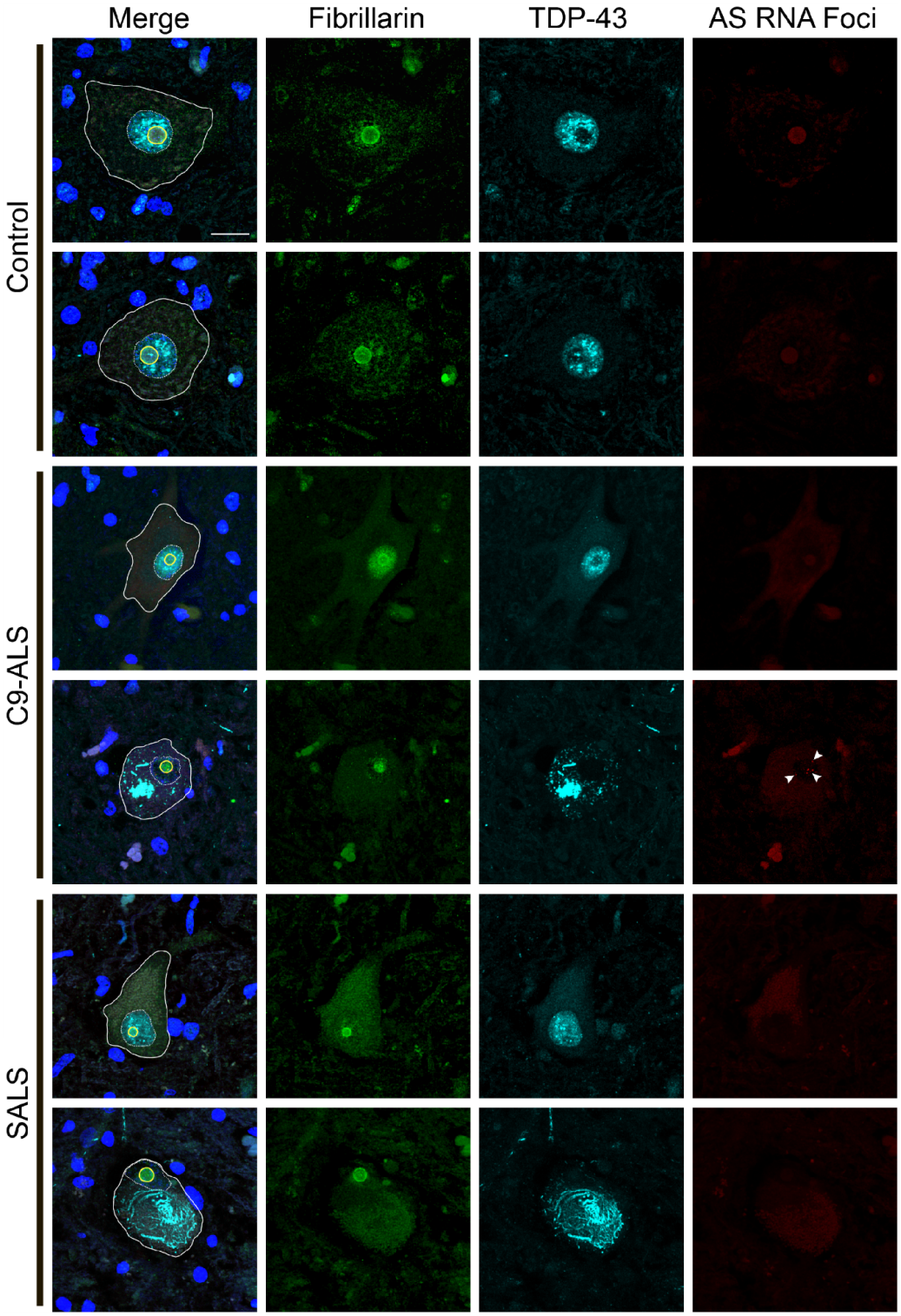
Merge
Fibrillarin
TDP-43
AS RNA Foci
Control
C9-ALS
SALS

Figure 3.11. Biphasic nucleolar stress in C9-ALS and SALS spinal motor neurons is dependent on TDP-43 antisense RNA foci. (A-B) Nucleolar area, (C-D) nuclear area, and (E-F) cytoplasmic area are decreased in C9-ALS and SALS neurons with or without antisense RNA foci compared to controls.

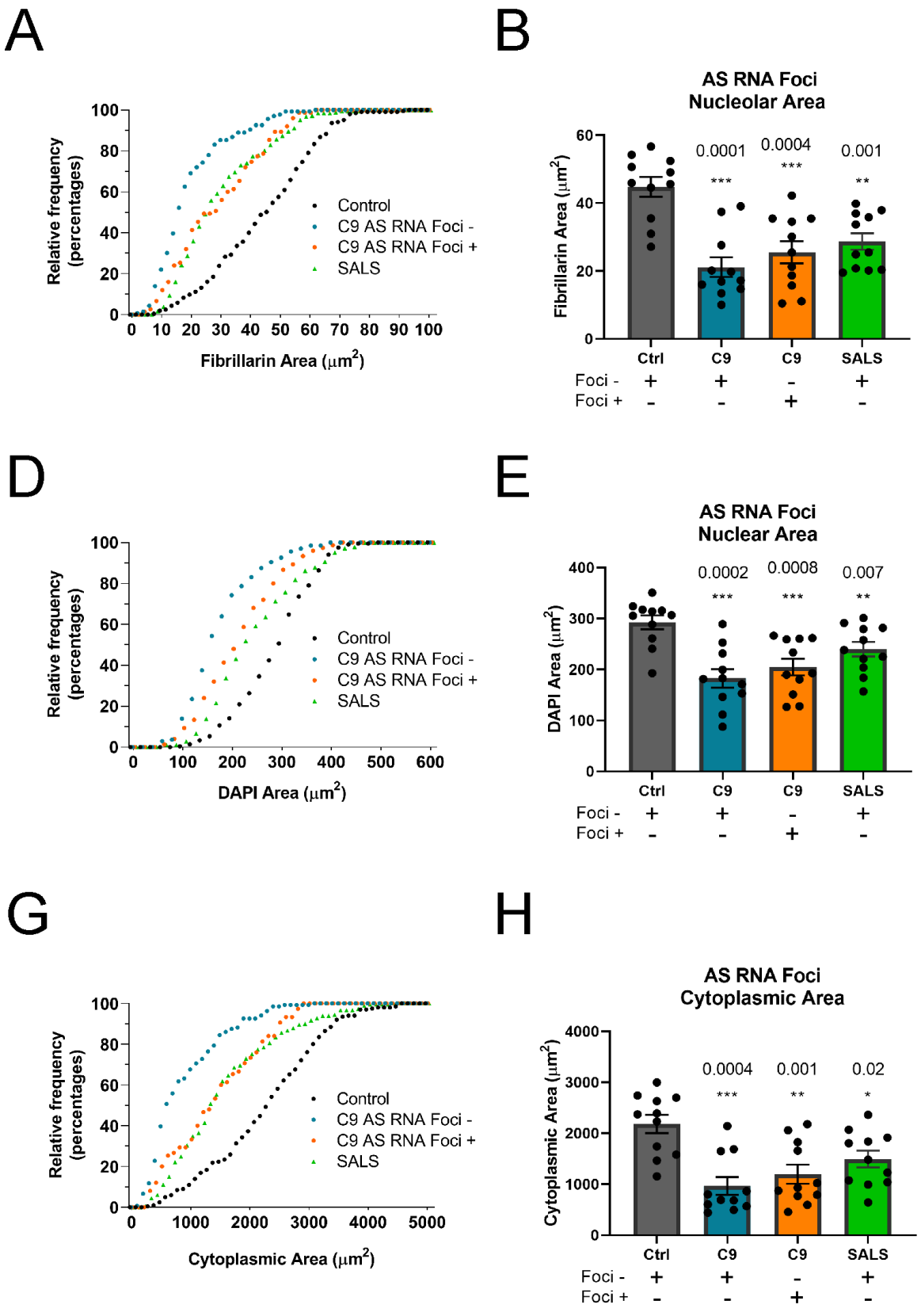
A
Relative frequency (percentages)
Fibrillarin Area (μm²)
Control
C9 AS RNA Foci -
C9 AS RNA Foci +
SALS
B
AS RNA Foci Nucleolar Area
Fibrillarin Area (μm²)
0.0001
0.0004
0.001
Ctrl
C9
C9
SALS
Foci -
Foci +
D
DAPI Area (μm²)
E
AS RNA Foci Nuclear Area
DAPI Area (μm²)
0.0002
0.0008
0.007
G
Cytoplasmic Area (μm²)
H
AS RNA Foci Cytoplasmic Area
Cytoplasmic Area (μm²)
0.0004
0.001
0.02

Chapter 4

Therapeutic approaches targeting gain of function toxicity in C9ORF72 patient fibroblasts

Our lab and others have established that nucleolar stress is associated with C9orf72 gain of function toxicity (Fay, 2017; Haeusler et al., 2014; Kanekura et al., 2016; Kwon et al., 2014; Lee et al., 2016; Mizielinska et al., 2017; Tao et al., 2015; Wen et al., 2014; White et al., 2019; O'Rourke et al. 2015). Both repeat-containing RNA transcripts and arginine containing-dipeptide repeat proteins have been shown to sequester ribosomal RNA and nucleolar proteins, including and nucleolphosmin and ribosomal proteins (Fay, 2017; Haeusler et al., 2014; Kanekura et al., 2016; White et al., 2019). Yet, two key questions remain: 1) is nucleolar stress the cause or consequence of neurodegeneration in C9-ALS/FTD? 2) Will reducing C9orf72 repeat-containing sense and/or antisense RNA transcripts prove to be an effective therapy for C9-ALS/FTD? In order to gain insight to these questions, we have used human fibroblasts from healthy control or C9-ALS patients to model the disease in vitro. The patient fibroblasts contain the endogenous, full length repeat expansion, often exceeding 800 repeats in length. This offers the advantage to better recapitulate potential toxicity of the repeat-containing RNA transcripts occurring in human tissue compared to models that rely on short synthesized repeats often less than 100 repeats in length.

Using correlative light and electron microscopy, we revealed the structure of endogenous

peri-nucleolar antisense RNA foci at high resolution in C9-ALS fibroblasts (Fig. 4.1). The peri-nucleolar antisense RNA foci forms a complex structure comprising and outer shell that directly abuts the nucleolus and an inner core. The occurrence of peri-nucleolar antisense RAN foci in C9-ALS fibroblasts is significant as our previous work highlights the nucleolus as an important organelle where toxicity from antisense RNA may initiate. We also wondered whether nucleolar stress is a phenotypic feature of C9-ALS fibroblasts, and if so, could be used as a measure to test contributions of antisense RNA to toxicity in a cellular model. Haeusler et al. previously identified defects in nucleolin in C9-ALS patient fibroblasts as a characteristic of nucleolar stress that could be replicated by overexpressing $(G4C2)_{21}$ (Haeusler et al., 2014). To characterize a nucleolar stress phenotype in our C9-ALS fibroblasts, we stained nucleoli in control and C9-ALS fibroblasts using an antibody against nucleolin and stained nuclei with DAPI (Fig. 4.2A). We then compared the intensity of nucleolin immunofluorescence between groups to see if there were alterations in nucleolin immunofluorescence and also compared the nucleolin to DAPI area ratio to see if there were differences in nucleolar size. We also stressed fibroblasts with 1 hour of heatshock (42°C) to see if there were differences between the group's responses to stress. Without stress, a portion of C9-ALS fibroblasts had nucleolin intensity exceeding the intensity present in control fibroblasts (Fig. 4.2B-D). There was also a greater variability in nucleolin to DAPI area ratio (Fig. 4.2B-D). C9-ALS fibroblasts also had an altered response to stress. 1 hour of heatshock produced a stereotyped decrease in the nucleolin to DAPI area ratio in control fibroblasts, but this change was bidirectional in C9-ALS fibroblasts and following heatshock, a portion of C9-ALS fibroblasts had nucleolin intensity exceeding the intensity observed in controls (Fig. 4.2B-D). These results demonstrate that C9-ALS fibroblasts recapitulate important hallmarks of C9-ALS pathology including nucleolar antisense RNA foci and nucleolar stress.

Next we aimed generate approaches to test whether reducing repeat-containing antisense RNA transcripts would mitigate the nucleolar stress phenotype in C9-ALS fibroblasts. Currently, antisense oligonucleotides (ASOs) are furthest along the clinical path. ASOs are short syntheti-

cally modified oligonucleotides that catalyze the degradation of target RNA. Already, clinical trials using ASOs targeting C9orf72 sense RNA transcripts are underway but in order for ASOs to be effective, they must target the correct strand. Since there is evidence that both sense and antisense RNA transcripts contribute to toxicity (Aladesuyi Arogundade et al., 2019; Cooper-Knock et al., 2015; Lagier-Tourenne et al., 2013) an effective therapy utilizing ASOs would need may need to target the antisense strand. Previously, our lab has shown that sense strand targeting ASOs can reduce sense RNA transcripts in fibroblasts but do not reduce antisense RNA transcripts (Lagier-Tourenne et al., 2013). In order to determine whether antisense strand-targeting ASOs effectively target repeat-containing antisense RNA transcripts, compared the efficiencies of ASOs targeting the C9orf72 sense or antisense strands. We tested 1 ASO targeting a region 5' or 3' of the sense repeat expansion and 2 ASOs targeting regions 5' or 3' of the antisense repeat expansion (Fig. 4.3A). We used reduction in the number of fibroblasts containing RNA foci to determine the effectiveness of ASOs (Fig. 4.3B). An ASO targeting the (C2G4) repeat expansion is also a candidate, however, since it is complimentary to the fluorescence-in-situ-hybridization (FISH) probes used to detect antisense RNA foci, FISH cannot be used to measure the efficiency of this ASO (Fig. 4.3A). Following two weeks of transfection with ASOs, ASOs targeting 5' or 3' of repeat-containing sense RNA transcripts effectively reduced the number of cells with sense RNA foci (Fig. 4.3C-D). However, ASOs targeting repeat-containing antisense RNA transcripts did not reduce the number of cells with antisense RNA foci (Fig. 4.3E-F). Thus, although ASOs can be used to effectively reduce the sense repeat expansion, they are ineffective at reducing the antisense repeat expansion. Therefore, in order to dissect contributions of C9orf72 sense and antisense RNA gain-of-function mechanisms to nucleolar stress, an alternative approach at reducing antisense RNA transcripts must be used. More so, if the antisense RNA is an important target for therapy, then an alternative to ASOs may be necessary.

Recently, Pinto et al. demonstrated that C9orf72 transcription can be inhibited by using CRISPR interference (CRISPRi). This approach used single-guide RNAs (sgRNAs) targeting the sense repeat expansion to recruit catalytically deactivated Cas9 (dCas9) tagged

to the repressor protein, Krüppel Associated Box (KRAB) to the repeat expansion and inhibit elongation of C9orf72 transcripts through the expansion (Pinto et al., 2017). This approach could be further enhanced by the addition of methyl CpG binding protein 2 (MeCP2) to the dCas9-KRAB fusion protein (Larson et al., 2013; Yeo et al., 2018) and guiding this complex near the transcriptional start site of the C9orf72 sense or antisense transcripts. As a proof of concept, we have synthesized 2 sgRNAs targeting the sense or antisense repeat expansion and 12 sgRNAs targeting the transcriptional start sites of C9orf72 identified by PCR and capped-end analysis of gene expression sequencing (Rizzu et al., 2016; Zu et al., 2013) (Fig. 4.4A). We aim to compare the efficacy of various sgRNAs with dCAS9-KRAB-MeCP2 to mediate CRISPRi in C9-ALS fibroblasts (Fig. 4.4B). Thus we aim to answer the remaining question, will reducing C9orf72 gain of function toxicity mitigate nucleolar stress?

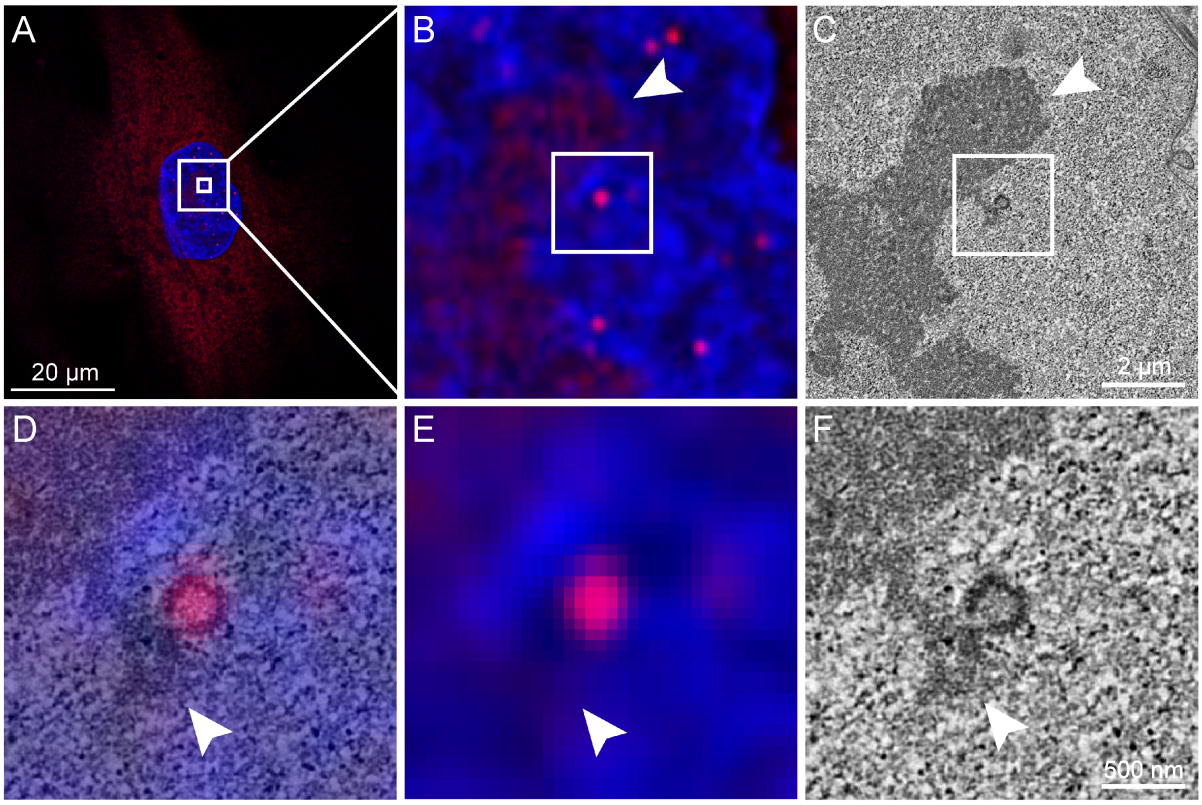

Figure 4.1. C9orf72 antisense RNA transcripts form perinucleolar RNA foci visible by light and electron microscopy. (A) Fluorescence in situ hybridization of antisense RNA foci in C9-ALS fibroblasts. (B and E) Magnifications of nucleolar antisense RNA foci (arrowheads, nucleoli). (C and F) Electron micrographs of nucleolus (arrowheads) and antisense RNA foci. (D) Overlay of light and electron micrographs.

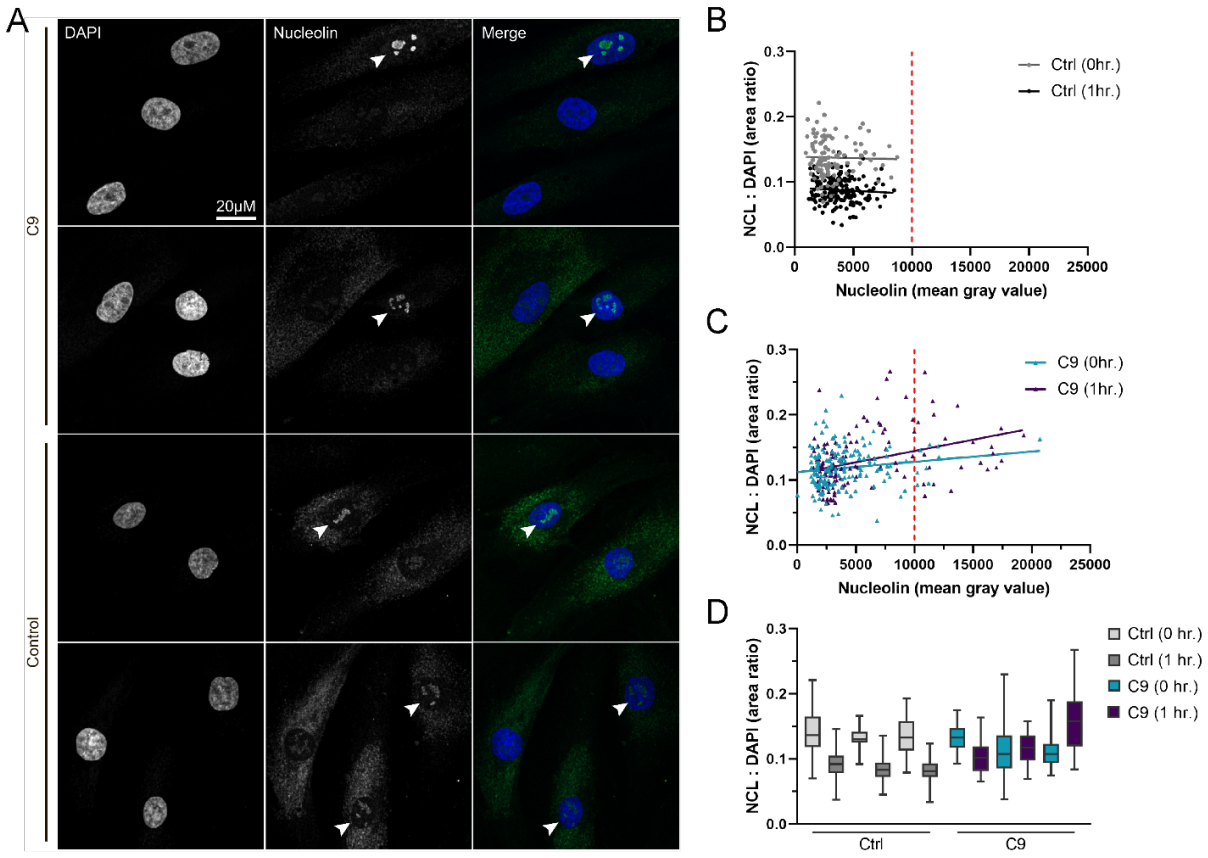

Figure 4.2. Nucleolar stress characterizes the phenotype in C9-ALS fibroblasts. (A) Dapi (blue) and nucleolin (green) staining in control and C9-ALS fibroblasts. Scatterplots of nucleolin to DAPI area ratio are compared to nucleolin immunofluorescence intensity in (B) control and (C) C9-ALS fibrolasts with or without 1 hr of heat shock (42° C). (D) Bar graphs of nucleolin to DAPI area ratio in control and C9-ALS fibroblasts with or without 1 hr of heatshock (42° C).

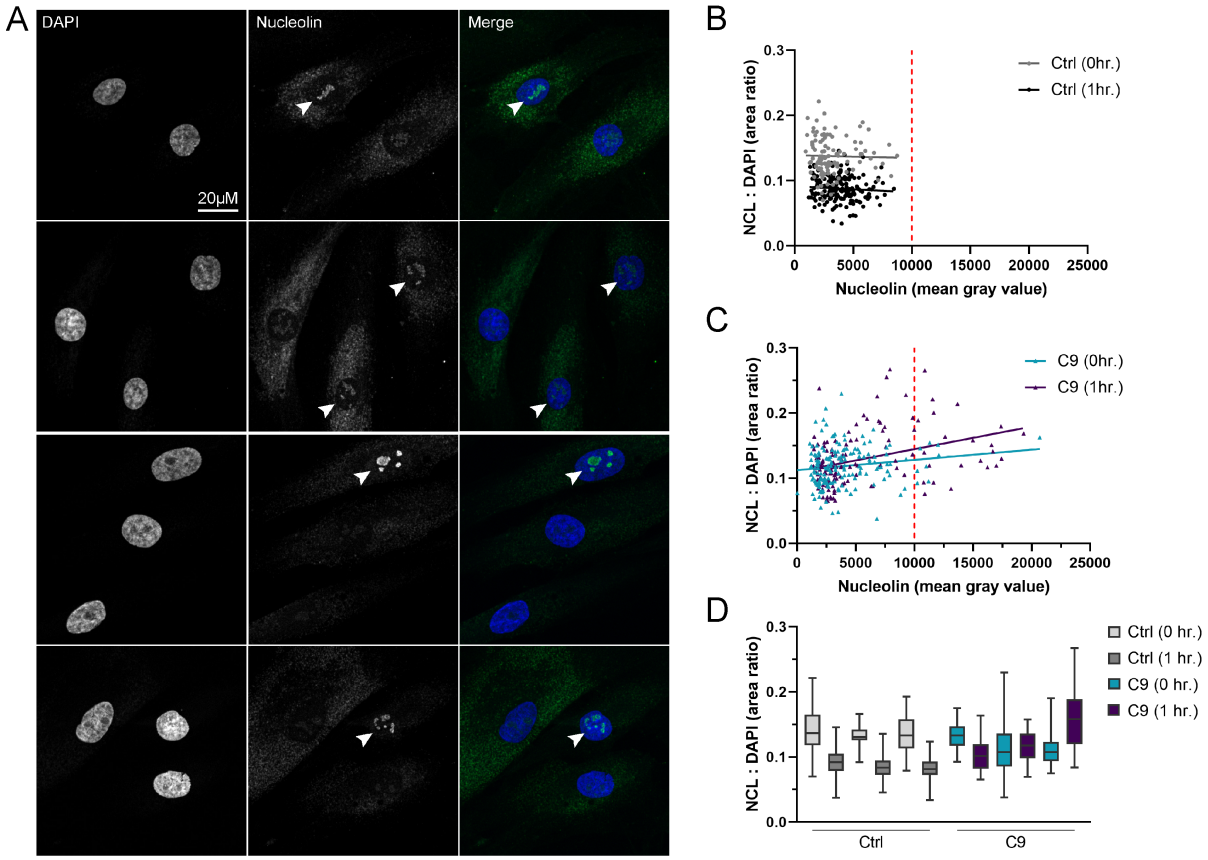

Figure 4.3. Antisense oligonucleotides reduce sense but not antisense RNA foci in C9-ALS fibroblasts. (A) Schematic of C9orf72 repeat expansion DNA and RNA, and antisense oligonucleotide (ASO) target sites. (B) Fluorescence in situ hybridization in C9-ALS fibroblasts of sense (top) or antisense (bottom) RNA foci. (C-D) Effect of ASOs on percentage of cells containing sense RNA foci. (E-F) Effect of ASOs on percentage of cells containing antisense RNA foci.

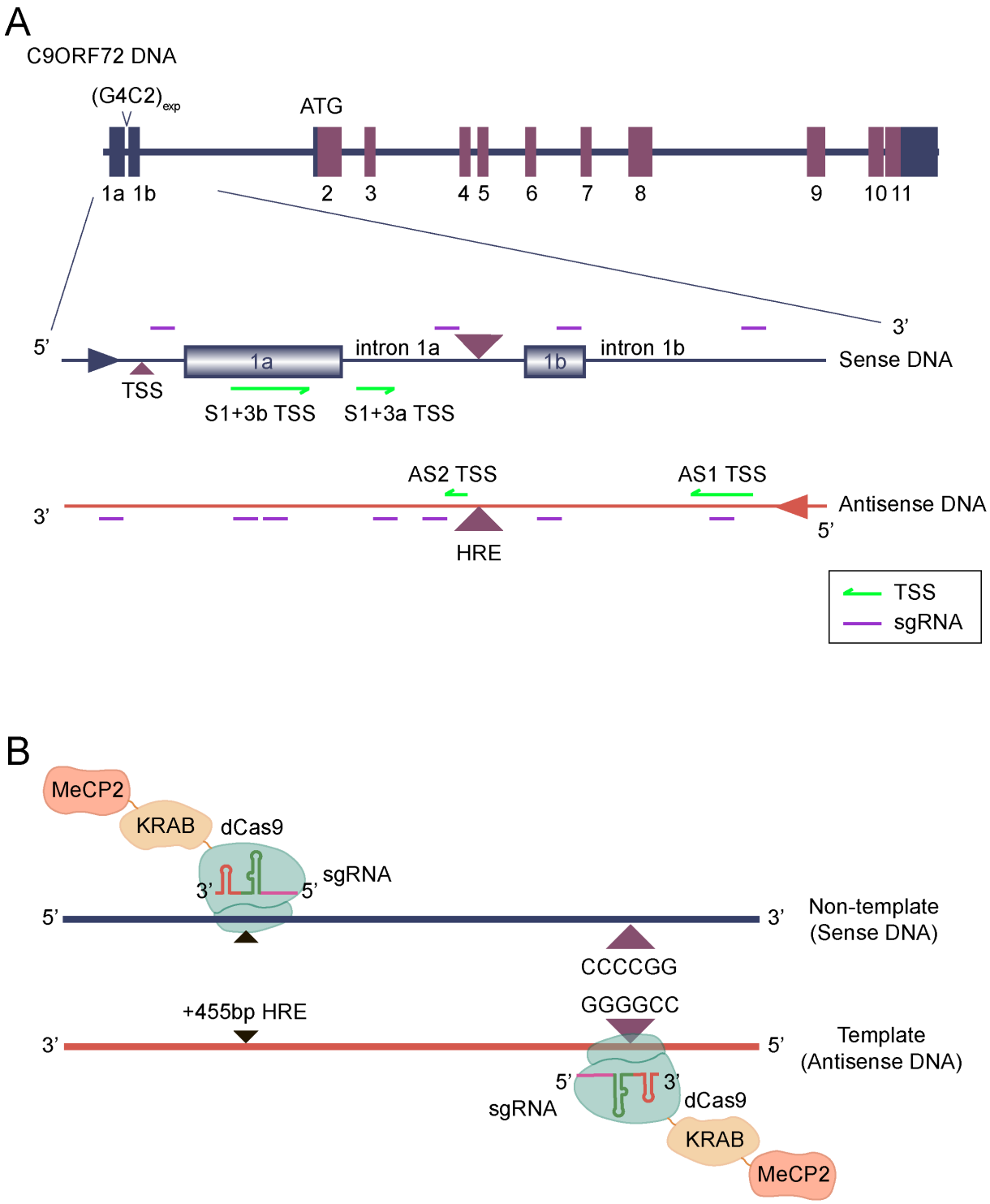

Figure 4.4. CRISPR interference is an alternative approach to reducing C9orf72 sense and antisense RNA transcripts. (A) Schematic illustrating transcriptional start sites (TSS) for C9orf72 repeat expansion sense and antisense transcripts and depicting target sites for sgRNA. (B) Schematic illustrating approach for transcriptional repression of C9orf72 repeat expanded DNA using dCAS9-KRAB-MeCP2.

Chapter 5

Conclusion

Repeat expansion has been shown to produce toxicity through loss of function and gain of function mechanisms involving RNA toxicity or dipeptide repeat proteins (DPRs). Evidence supports that loss of function of C9ORF72 protein, which supports autophagy and immune response, exacerbates gain of function toxicity (Amick et al., 2016; Belzil et al., 2013; Burberry et al., 2020; Dejesus-hernandez et al., 2011; Farg et al., 2014; Gijselinck et al., 2016; Jung et al., 2017; Sellier et al., 2016; Shao et al., 2019; Shi et al., 2018; Sullivan et al., 2016; Ugolino et al., 2016; Webster et al., 2016; Yang et al., 2016; Zhu et al., 2020). While much is known of how toxicity occurs from sense RNA transcripts and arginine-containing DPRs, contributions from the antisense strand to disease are less well understood. However, if the antisense RNA are key contributors of disease, then an effective therapy must target the antisense strand. The work presented in this thesis, extends previous findings highlighting the relevance of C9orf72 antisense RNA to pathology. Vatsavayai et al. previously showed that sense and antisense RNA foci occur early in disease and precede TDP-43 mislocalizaion (Vatsavayai et al., 2016). Cooper-Knock et al. showed that antisense but not sense RNA foci correlate with TDP-43 mislocalization in C9-ALs spinal motor neurons (Cooper-Knock et al., 2015). We have found that the nucleolar localization of antisense RNA foci is an important aspect of how they correlate with disease. peri-nucleolar antisense but not sense RNA foci are increased in brain and spinal cord regions vulnerable to neurodegeneration and the prevalence of peri-nucleolar antisense but not sense

RNA foci in frontal cortical neurons in frontal cortical neurons is increased in patients with FTD. (Aladesuyi Arogundade et al., 2019). peri-nucleolar antisense but not sense RNA foci also correlate with TDP-43 mislocalization in spinal motor neurons and we found that 97% of neurons with antisense RNA foci and TDP-43 mislocalization had at least one antisense RNA foci localized to the nucleolus (Aladesuyi Arogundade et al., 2019).

Since nucleolar stress has been implicated in neurodegenerative disease including C9-ALS/FTD and the nucleolar localization of antisense RNA foci is an important property of their relation to pathology, we sought to gain insight into how peri-nucleolar antisense RNA foci might correlate with nucleolar stress (Aladesuyi Arogundade et al., 2019; Fay, 2017; Haeusler et al., 2014; Kanekura et al., 2016; Kwon et al., 2014; Lee et al., 2016; Mizielinska et al., 2017; O'Rourke et al., 2015; Tao et al., 2015; Wen et al., 2014; White et al., 2019). Mizielinska et al. showed that nucleolar stress occurs in C9-FTLD frontal cortical neurons (Mizielinska et al., 2017). Nucleoli are smaller compared to controls but within C9-FTLD neurons, sense RNA foci, poly-GR and poly-GA inclusions correlate to larger nucleoli compared to neurons without these pathological features. We have further shown that nucleolar stress occurs in both C9-ALS and sporadic ALS spinal motor neurons. Nucleoli are smaller compared to controls but within ALS neurons, pathological features including peri-nucleolar antisense RNA foci and TDP-43 mislocalization correlate with larger nucleoli. This supports the previous finding that nucleolar stress is bi-directional in ALS (Mizielinska et al., 2017). Additionally, these findings stir an interesting question: how does nucleolar stress occur in the absence of pathology? The answer to this question is beyond the scope of our study of neuropathology in postmortem human tissues, therefore we are utilizing in vitro cellular models of C9-ALS/FTD to further elucidate how peri-nucleolar antisense RNA transcripts and nucleolar stress are related.

Perhaps most relevant to our work are cellular models that have identified nucleolar stress as a pathway involved in disease pathobiology as well as models that have discovered RNA binding proteins that can be sequestered by antisense RNA transcripts (Fay, 2017; Haeusler et al., 2016, 2014; Kanekura et al., 2016; Lee et al., 2016; White et al., 2019). For example, Haeusler

et al. showed that enlargement of nucleoli is a phenotypic feature of C9-ALS cells and can be induced in normal cells by expressing repeat expansion RNA (Haeusler et al., 2014). Additionally, defects in ribosomal synthesis and protein translation have been found in C9-ALS and SALS patient spinal motor neurons and C9-ALS iPSCs (Ho et al., 2020 PREPRINT; Krach et al., 2018). These results are in line with our finding that nucleolar stress occurs in C9-ALS/FTD and SALS pathology. We have established that nucleoli are enlarged C9-ALS and SALS spinal motor neurons with pathology compared to proximal neurons without pathology and that nucleolar abnormalities are a property of C9-ALS fibroblasts. Moving forward, we aim to leverage the relevance of the nucleolar stress phenotype in C9-ALS fibroblasts as well as the expression of the endogenous full-length C9orf72 repeat expansion to determine whether reducing RNA toxicity will rescue the disease phenotype. We have established that although antisense oliguncleotides (ASOs) are able to effectively the sense RNA transcript, ASOs are unable to effect antisense RNA transcripts. Thus, an alternative approach such as CRISPR interference may succeed in reducing levels of sense and/or antisense RNA transcripts. Interestingly, since ASOs can be used to selectively reduce the sense strand, and CRISPR interference may specifically affect either the sense or the antisense strand, a comparison of these two approaches will enable a study of how the two strands contribute to disease (Lagier-Tourenne et al., 2013).

However, in addition to disruption of nucleolar homeostasis there are multiple cellular processes that are affected in C9-ALS/FTD including, defects in nuclear cytoplasmic transport and stress granule assembly (Boeynaems et al., 2017, 2016; Chew et al., 2019; Fay, 2017; Freibaum et al., 2015; Hutten and Dormann, 2019; Jain and Vale, 2017; Jovičič et al., 2015; Kramer et al., 2018; Lee et al., 2016; Li et al., 2013; Liu-Yesucevitz et al., 2010; Shi et al., 2017; Vatsavayai et al., 2018; Zhang et al., 2015, 2019). It is difficult to unravel what mechanisms primarily precipitate neurodegeneration and it is possible that multiple pathways intersect to produce pathology. Likewise, identifying RNA binding partners of repeat-expanded sense and antisense RNA transcripts have yet to lead to a plausible route for therapeutic intervention. Although much progress has been made in elucidating the mechanisms underlying RNA toxicity

in C9-ALS/FTD, much of this work has neglected contributions of the antisense RNA strand. Moreover, many of the approaches used to discovery RNA binding partners of repeat expanded C9orf72 transcripts relied on short synthesis RNA transcripts that may fail to recapitulate the interactions RNA binding proteins and the endogenous full-length repeat expansion. Therefore, it is possible that critical RNA binding proteins sequester by sense and/or antisense RNA transcripts have yet to be discovered. In addition to highlighting the importance of peri-nucleolar antisense RNA foci and nucleolar stress to C9-ALS/FTD, our work using C9-ALS fibroblasts as a cellular models aims to motivate the field to incorporate the advantage of studying the endogenous full-length repeat expansion into future research.

At the apex of our research is the goal to translate our discoveries into an effective therapy for patients living with this swiftly fatal neurodegenerative disease. Perhaps the biggest advantage the field has are the seminal discoveries that repeat expansion of C90rf72 are causes of ALS and FTD (Dejesus-hernandez et al., 2011; Renton et al., 2011). Thus much effort has been made to mitigate gain-of-function toxicity (Batra et al., 2017; Bennett et al., 2019; Donnelly et al., 2013; Goodman et al., 2019; Hu et al., 2017; Jiang et al., 2016; Krishnan et al., 2020; Lagier-Tourenne et al., 2013; Martier et al., 2019a, 2019b; Naguib et al., 2019; Pinto et al., 2017; Su et al., 2014; Wang et al., 2020; Zamiri et al., 2014). Our work underscores the need for effective therapies to not only target toxicity from sense RNA transcripts and DPRs but also to effect C9orf72 antisense RNA transcripts. Excitingly, novel research has focuses on repurposing the CRISPR-Cas9 and CRISPR-Cas13 to target specific regions of DNA or RNA. Cas13 systems aim to reduce repeat expansion-containing RNAs similar to how ASOs lead to the degradation of target RNAs (Batra et al., 2017). Success has been made in deleting the repeat expansion in vitro as well as preventing transcription by selectively deleting C9orf72 promotor elements (Krishnan et al., 2020 PREPRINT; Pribadi et al., 2016). Proof of concept has shown that CRISPR interference can also reduce expression of C9orf72 RNA (Pinto et al., 2017). In the future, studies will need to include pre-clinical in vivo analysis of the effectiveness of these strategies in order to support their efficacy in human clinical trials. However, a limitation

to this goal is a lack of an in vivo model that replicates cis-repeat expansion of C9orf72. For example, although mouse models recapitulate many aspects of C9-ALS such as progressive neurodegeneration, motor and cognitive deficits and pathological hallmarks of the disease, these models rely on over expressing the repeat expansion suing bacterial artificial chromosomes or AAV-delivery (Chew et al., 2019, 2015; Jiang et al., 2016a; Liu et al., 2016; O'Rourke et al., 2015; Peters et al., 2015; Zhu et al., 2020). Therefore, the repeat expansion needs to be present within the mouse C9orf72 gene locus in order for CRISPR strategies targeting C9orf72 DNA to be translatable to human clinical trials. Thus, the field could benefit from a mouse models in which repeat expansion of C9orf72, in a similar size as to what is seen in patients, is incorporated into the mouse genome via CRISPR gene editing. Yet, previous efforts to create such a model have proven challenging; Ryan et al. found that while insertion of the long C9orf72 repeat expansion feasible using CRISPR/Cas9, the insertion was not stable across multiple generations (Ryan et al., 2019).

In summary, we have provided insight to how peri-peri-nucleolar antisense RNA foci correlate to regions of neurodegeneration, clinical phenotype of frontotemporal dementia and TDP-43 mislocalization. We have further characterized nucleolar stress in C9-ALS and SALS spinal motor neurons and have presented evidence that biphasic nucleolar stress correlates with TDP-43 mislocalization and peri-peri-nucleolar antisense RNA foci. While the mechanisms underlying neurodegeneration in C9-ALS/FTD are yet to be completely understood the C9orf72 antisense strand remains an important candidate target for therapeutic approaches.

Bibliography

Aladesuyi Arogundade, O., Stauffer, J. E., Saberi, S., Diaz Garcia, S., Malik, S., Basilim, H., Rodriguez, M. J., Ohkubo, T., and Ravits, J. (2019). Antisense rna foci are associated with nucleoli and tdp-43 mislocalization in c9orf72-als/ftd: A quantitative study. *Acta Neuropathologica*, 137(3):527–530.

Almeida, S., Gascon, E., Tran, H., Jung, H., Tania, C., Degroot, S., Tapper, A. R., Sellier, C., Charlet, N., Anna, B., Seeley, W. W., Boxer, A. L., Petrucelli, L., Miller, B. L., and Biao, F. (2013). Modeling key pathological features of frontotemporal dementia with c9orf72 repeat expansion in ipsc-derived human neurons. *Acta Neuropathologica*, 126(3):385–399.

Amick, J., Roczniak-Ferguson, A., and Ferguson, S. M. (2016). C9orf72 binds smcr8, localizes to lysosomes, and regulates mtorc1 signaling. *Molecular Biology of the Cell*, 27(20):3040–3051.

Aoki, Y., Manzano, R., Lee, Y., Dafinca, R., Aoki, M., Douglas, A. G., Varela, M. A., Sathyaprakash, C., Scaber, J., Barbagallo, P., Vader, P., Mäger, I., Ezzat, K., Turner, M. R., Ito, N., Gasco, S., Ohbayashi, N., El Andaloussi, S., Takeda, S., Fukuda, M., Talbot, K., and Wood, M. J. (2017). C9orf72 and rab7l1 regulate vesicle trafficking in amyotrophic lateral sclerosis and frontotemporal dementia. *Brain*, 140(4):887–897.

Archbold, H. C., Jackson, K. L., Arora, A., Weskamp, K., Tank, E. M., Li, X., Miguez, R., Dayton, R. D., Tamir, S., Klein, R. L., and Barmada, S. J. (2018). Tdp43 nuclear export and neurodegeneration in models of amyotrophic lateral sclerosis and frontotemporal dementia. *Scientific Reports*, 8(1):1–18.

Ash, P. E. A., Bieniek, K. F., Gendron, T. F., Caulfield, T., Lin, W.-l., Dejesus-hernandez, M., Blitterswijk, M. M. V., Jansen-west, K., Iii, J. W. P., Rademakers, R., Boylan, K. B., Dickson, D. W., and Petrucelli, L. (2013). Unconventional translation of c9orf72 ggggcc expansion generates insoluble polypeptides specific to c9ftd/als. *Neuron*, 77(4):639–646.

Atanasio, A., Decman, V., White, D., Ramos, M., Ikiz, B., Lee, H. C., Siao, C. J., Brydges, S., Larosa, E., and Bai, Y. a. (2016). C9orf72 ablation causes immune dysregulation characterized by leukocyte expansion, autoantibody production, and glomerulonephropathy in mice. *Scientific Reports*, 6(March):1–14.

Bajc Česnik, A., Darovic, S., Mihevc, S. P., Štalekar, M., Malnar, M., Motaln, H., Lee, Y.-B., Mazej, J., Pohleven, J., Grosch, M., Modic, M., Fonovič, M., Turk, B., Drukker, M., Shaw, C. E., and Rogelj, B. (2019). Nuclear rna foci from c9orf72 expansion mutation form paraspeckle-like bodies. *Journal of Cell Science*, 132(5).

Batra, R., Nelles, D. A., Pirie, E., Blue, S. M., Ryan, J., Wang, H., Chaim, I. A., Thomas, J. D., Zhang, N., Aigner, S., Markmiller, S., Xia, G., and Kevin, D. (2017). Elimination of toxic microsatellite repeat expansion rna by rna-targeting cas9. *Cell*, 170(5):899–912.

Beck, J., Poulter, M., Hensman, D., Rohrer, J. D., Mahoney, C. J., Adamson, G., Campbell, T., Uphill, J., Borg, A., Fratta, P., Orrell, R. W., Malaspina, A., Rowe, J., Brown, J., Hodges, J., Sidle, K., Polke, J. M., Houlden, H., Schott, J. M., Fox, N. C., Rossor, M. N., Tabrizi, S. J., Isaacs, A. M., Hardy, J., Warren, J. D., Collinge, J., and Mead, S. (2013). Large c9orf72 hexanucleotide repeat expansions are seen in multiple neurodegenerative syndromes and are more frequent than expected in the uk population. *American Journal of Human Genetics*, 92(3):345–353.

Becker, L. A., Huang, B., Bieri, G., Ma, R., Knowles, D. A., Jafar-nejad, P., Messing, J., Kim, H. J., Soriano, A., Pulst, S. M., Taylor, J. P., Rigo, F., and Gitler, A. D. (2017). Therapeutic reduction of ataxin 2 extends lifespan and reduces pathology in tdp-43 mice. *Nature*, 544(7650):367–371.

Belzil, V. V., Bauer, P. O., Prudencio, M., Gendron, T. F., Stetler, C. T., Yan, I. K., Pregent, L., Daughrity, L., Baker, M. C., Rademakers, R., Boylan, K., Patel, T. C., Dickson, D. W., and Petrucelli, L. (2013). Reduced c9orf72 gene expression in c9ftd/als is caused by histone trimethylation, an epigenetic event detectable in blood. *Acta Neuropathologica*, 126(6):895–905.

Bennett, C. F., Krainer, A. R., and Cleveland, D. W. (2019). Antisense oligonucleotide therapies for neurodegenerative diseases. *Annual Review of Neuroscience*, 42(1):385–406.

Benussi, L., Rossi, G., Glionna, M., Tonoli, E., Piccoli, E., Fostinelli, S., Paterlini, A., Flocco, R., Albani, D., Pantieri, R., Cereda, C., Forloni, G., Tagliavini, F., Binetti, G., and Ghidoni, R. (2014). C9orf72 hexanucleotide repeat number in frontotemporal lobar degeneration: A genotype-phenotype correlation study. *Journal of Alzheimer's Disease*, 38(4):799–808.

Blitterswijk, M. V., Dejesus-hernandez, M., Niemantsverdriet, E., Baker, M. C., Finch, N. A., Bauer, P. O., Serrano, G., Beach, T. G., Josephs, K. A., Knopman, D. S., Petersen, R. C., Boeve, B. F., Graff-radford, N. R., Boylan, K. B., Dickson, D. W., and Rademakers, R. (2013). Associations of repeat sizes with clinical and pathological characteristics in c9orf72 expansion carriers (xpansize-72): a cross-sectional cohort study. *Lancet Neurology*, 12(10):1–18.

Boeynaems, S., Bogaert, E., Kovacs, D., Konijnenberg, A., Timmerman, E., Volkov, A., Guharoy, M., De Decker, M., Jaspers, T., Ryan, V. H., Janke, A. M., Baatsen, P., Vercruysse, T., Kolaitis,

R. M., Daelemans, D., Taylor, J. P., Kedersha, N., Anderson, P., Impens, F., Sobott, F., Schymkowitz, J., Rousseau, F., Fawzi, N. L., Robberecht, W., Van Damme, P., Tompa, P., and Van Den Bosch, L. (2017). Phase separation of c9orf72 dipeptide repeats perturbs stress granule dynamics. *Molecular Cell*, 65(6):1044–1055.e5.

Boeynaems, S., Bogaert, E., Michiels, E., Gijselinck, I., Sieben, A., Jovičić, A., De Baets, G., Scheveneels, W., Steyaert, J., Cuijt, I., Verstrepen, K. J., Callaerts, P., Rousseau, F., Schymkowitz, J., Cruts, M., Van Broeckhoven, C., Van Damme, P., Gitler, A. D., Robberecht, W., and Van Den Bosch, L. (2016). Drosophila screen connects nuclear transport genes to dpr pathology in c9als/ftd. *Scientific Reports*, 6(August 2015):7–14.

Buchman, V. L., Cooper-Knock, J., Connor-Robson, N., Higginbottom, A., Kirby, J., Razinskaya, O. D., Ninkina, N., and Shaw, P. J. (2013). Simultaneous and independent detection of c9orf72 alleles with low and high number of ggggcc repeats using an optimised protocol of southern blot hybridisation. *Molecular Neurodegeneration*, 8(1):1–6.

Burberry, A., Suzuki1, N., Wang, J.-Y., Moccia, R., Mordes, D. A., Stewart, M., Suzuki-Uematsu, S., Ghosh, S., Singh, A., Merkle, F. T., Koszka, K., Li, Q.-Z., Zon, L., Rossi, D. J., Trowbridge, J. J., Notarangelo, L. D., and Eggan, K. (2016). Loss-of-function mutations in the c9orf72 mouse ortholog cause fatal autoimmune disease. *Sci Transl Med.*, 8(347):347ra93.

Burberry, A., Wells, M. F., Limone, F., Couto, A., Smith, K. S., Keaney, J., Gillet, G., van Gastel, N., Wang, J. Y., Pietilainen, O., Qian, M., Eggan, P., Cantrell, C., Mok, J., Kadiu, I., Scadden, D. T., and Eggan, K. (2020). C9orf72 suppresses systemic and neural inflammation induced by gut bacteria. *Nature*, (May 2019).

Castanotto, D. and Rossi, J. J. (2009). The promises and pitfalls of rna-interference-based therapeutics. *Nature*, 457(7228):426–433.

Celona, B., Von Dollen, J., Vatsavayai, S. C., Kashima, R., Johnson, J. R., Tang, A. A., Hata, A., Miller, B. L., Huang, E. J., Krogan, N. J., Seeley, W. W., and Black, B. L. (2017). Suppression of c9orf72 rna repeat-induced neurotoxicity by the als-associated rna-binding protein zfp106. *eLife*, 6:1–17.

Chang, Y. J., Jeng, U. S., Chiang, Y. L., Hwang, I. S., and Chen, Y. R. (2016). The glycine-alanine dipeptide repeat from c9orf72 hexanucleotide expansions forms toxic amyloids possessing cell-to-cell transmission properties. *Journal of Biological Chemistry*, 291(10):4903–4911.

Chew, J., Cook, C., Gendron, T. F., Jansen-West, K., Del Rosso, G., Daughrity, L. M., Castanedes-Casey, M., Kurti, A., Stankowski, J. N., Disney, M. D., Rothstein, J. D., Dickson, D. W., Fryer, J. D., Zhang, Y. J., and Petrucelli, L. (2019). Aberrant deposition of stress granule-resident proteins linked to c9orf72-associated tdp-43 proteinopathy. *Molecular Neurodegeneration*, 14(1):1–15.

Chew, J., Gendron, T. F., Prudencio, M., Sasaguri, H., Castanedes-casey, M., Lee, C. W., Jansen-west, K., Kurti, A., Murray, M. E., Bieniek, K. F., Bauer, P. O., Whitelaw, E. C., Rousseau, L., Stankowski, J. N., Stetler, C., Daughrity, L. M., Perkerson, E. A., Desaro, P., Johnston, A., Overstreet, K., Edbauer, D., Rademakers, R., Boylan, K. B., Dickson, D. W., Fryer, J. D., and Petrucelli, L. (2015). C9orf72 repeat expansions in mice cause tdp-43 pathology, neuronal loss, and behavioral deficits. 348(6239):1151–1154.

Choi, S. Y., Lopez-Gonzalez, R., Krishnan, G., Phillips, H. L., Li, A. N., Seeley, W. W., Yao, W. D., Almeida, S., and Gao, F. B. (2019). C9orf72-als/ftd-associated poly(gr) binds atp5a1 and compromises mitochondrial function in vivo. *Nature Neuroscience*, 22(6):851–862.

Ciura, S., Lattante, S., Le Ber, I., Latouche, M., Tostivint, H., Brice, A., and Kabashi, E. (2013). Loss of function of c9orf72 causes motor deficits in a zebrafish model of amyotrophic lateral sclerosis. *Annals of Neurology*, 74(2):180–187.

Coffee, B., Zhang, F., Warren, S. T., and Reines, D. (1999). Acetylated histones are associated with fmr1 in normal but not fragile x-syndrome cells. *Nature Genetics*, 22(2):98–101.

Conlon, E. G., Lu, L., Sharma, A., Yamazaki, T., Tang, T., Shneider, N. A., and Manley, J. L. (2016). The c9orf72 ggggcc expansion forms rna g-quadruplex inclusions and sequesters hnrnp h to disrupt splicing in als brains. *eLife*, 5(September2016):1–28.

Cooper-Knock, J., Higginbottom, A., Stopford, M. J., Highley, J. R., Ince, P. G., Wharton, S. B., Pickering, S., Kirby, J., Hautbergue, G. M., and Shaw, P. J. (2015). Antisense rna foci in the motor neurons of c9orf72-als patients are associated with tdp-43 proteinopathy. *Acta Neuropathologica*, 130(1):63–75.

Cooper-Knock, J., Walsh, M. J., Higginbottom, A., Highley, J. R., Dickman, M. J., Edbauer, D., Ince, P. G., Wharton, S. B., Wilson, S. A., Kirby, J., Hautbergue, G. M., and Shaw, P. J. (2014). Sequestration of multiple rna recognition motif-containing proteins by c9orf72 repeat expansions. *Brain: a journal of neurology*, 137(Pt 7):2040–2051.

Cristofani, R., Crippa, V., Vezzoli, G., Rusmini, P., Galbiati, M., Cicardi, M. E., Meroni, M., Ferrari, V., Tedesco, B., Piccolella, M., Messi, E., Carra, S., and Poletti, A. (2018). The small heat shock protein b8 (hspb8) efficiently removes aggregating species of dipeptides produced in c9orf72-related neurodegenerative diseases. *Cell Stress and Chaperones*, 23(1):1–12.

Davidson, Y. S., Barker, H., Robinson, A. C., Thompson, J. C., Harris, J., Troakes, C., Smith, B., Al-Saraj, S., Shaw, C., Rollinson, S., Masuda-Suzukake, M., Hasegawa, M., Pickering-Brown, S., Snowden, J. S., and Mann, D. M. (2014). Brain distribution of dipeptide repeat proteins in frontotemporal lobar degeneration and motor neurone disease associated with expansions in c9orf72. *Acta Neuropathologica Communications*, 2(1):1–13.

Dejesus, M., Nicole, H., Xue, A. F., Tania, W., Kevin, F. G., Heckman, M. G., Vasilevich, A.,

Murray, M. E., Rousseau, L., Weesner, R., Lucido, A., Parsons, M., Chew, J., Josephs, K. A., Parisi, J. E., Knopman, D. S., Petersen, R. C., Boeve, B. F., Graff, N. R., Jan, R., Yan, D. B., Petrucelli, L., Boylan, K. B., Dickson, D. W., Blitterswijk, M. V., and Rademakers, R. (2017). In-depth clinico-pathological examination of rna foci in a large cohort of c9orf72 expansion carriers. *Acta Neuropathologica*, 134(2):255–269.

Dejesus-hernandez, M., Mackenzie, I. R., Boeve, B. F., Boxer, A. L., Baker, M., Rutherford, N. J., Nicholson, A. M., Finch, N. A., Flynn, H., Adamson, J., Kouri, N., Wojtas, A., Sengdy, P., Hsiung, G.-y. R., Karydas, A., Seeley, W. W., Josephs, K. A., Coppola, G., Geschwind, D. H., Wszolek, Z. K., Feldman, H., Knopman, D. S., Petersen, R. C., Miller, B. L., Dickson, D. W., Boylan, K. B., and Graff-radford, N. R. (2011). Expanded ggggcc hexanucleotide repeat in noncoding region of c9orf72 causes chromosome 9p-linked ftd and als. *Neuron*, 72(2):245–256.

Dobson-Stone, C., Hallupp, M., Loy, C. T., Thompson, E. M., Haan, E., Sue, C. M., Panegyres, P. K., Razquin, C., Seijo-Martínez, M., Rene, R., Gascon, J., Campdelacreu, J., Schmoll, B., Volk, A. E., Brooks, W. S., Schofield, P. R., Pastor, P., and Kwok, J. B. (2013). C9orf72 repeat expansion in australian and spanish frontotemporal dementia patients. *PLoS ONE*, 8(2).

Dols-Icardo, O., García-Redondo, A., Rojas-García, R., Sánchez-Valle, R., Noguera, A., Gó mez Tortosa, E., Pastor, P., Hernández, I., Esteban-Pérez, J., Suárez-Calvet, M., Antó n Aguirre, S., Amer, G., Ortega-Cubero, S., Blesa, R., Fortea, J., Alcolea, D., Capdevila, A., Antonell, A., Lladó, A., Munoz-Blanco, J. L., Mora, J. S., vila, L.-D., De Rivera, F. J. R., Lleó, A., and Clarimón, J. (2014). Characterization of the repeat expansion size in c9orf72 in amyotrophic lateral sclerosis and frontotemporal dementia. *Human Molecular Genetics*, 23(3):749–754.

Donnelly, C. J., Zhang, P. W., Pham, J. T., Heusler, A. R., Mistry, N. A., Vidensky, S., Daley, E. L., Poth, E. M., Hoover, B., Fines, D. M., Capdevila, A., Antonell, A., Lladó, A., Munoz-Blanco, J. L., Mora, J. S., vila, L.-D., De Rivera, F. J. R., Lleó, A., and Clarimón, J. (2013). Rna toxicity from the als/ftd c9orf72 expansion is mitigated by antisense intervention. *Neuron*, 80(2):415–428.

Dukkipati, S. S., Garrett, T. L., and Elbasiouny, S. M. (2018). The vulnerability of spinal motoneurons and soma size plasticity in a mouse model of amyotrophic lateral sclerosis. *Journal of Physiology*, 596(9):1723–1745.

Eftekharzadeh, B., Daigle, J. G., Kapinos, L. E., Coyne, A., Carlomagno, Y., Cook, C., Miller, S. J., Dujardin, S., Ana, S., Grima, J. C., Vanderburgh, C. R., Corjuc, B. T., Devos, S. L., Gonzalez, J. A., Chew, J., Vidensky, S., Gage, F. H., Mertens, J., Troncoso, J., Mandelkow, E., Salvatella, X., Lim, R. Y. H., and Petrucelli, L. (2018). Tau protein disrupts nucleocytoplasmic transport in alzheimer's disease. *Neuron*, 99(5):925–940.

Farg, M. A., Konopka, A., Soo, K. Y., Ito, D., and Atkin, J. D. (2017). The dna damage response (ddr) is induced by the c9orf72 repeat expansion in amyotrophic lateral sclerosis. *Human*

molecular genetics, 26(15):2882–2896.

Farg, M. A., Sundaramoorthy, V., Sultana, J. M., Yang, S., Atkinson, R. A., Levina, V., Halloran, M. A., Gleeson, P. A., Blair, I. P., Soo, K. Y., King, A. E., and Atkin, J. D. (2014). C9orf72, implicated in amytrophic lateral sclerosis and frontotemporal dementia, regulates endosomal trafficking. *Human Molecular Genetics*, 23(13):3579–3595.

Fay, M. M., Anderson, P. J., and Ivanov, P. (2017). Als/ftd-associated c9orf72 repeat rna promotes phase transitions in vitro and in cells. *Cell Reports*, 21(12):3573–3584.

Floeter, M. K. and Gendron, T. F. (2018). Biomarkers for amyotrophic lateral sclerosis and frontotemporal dementia associated with hexanucleotide expansion mutations in c9orf72. *Frontiers in Neurology*, 9(December):1–9.

Flores, B. N., Dulchavsky, M. E., Krans, A., Sawaya, M. R., Paulson, H. L., Todd, P. K., Barmada, S. J., and Ivanova, M. I. (2016). Distinct c9orf72-associated dipeptide repeat structures correlate with neuronal toxicity. *PLoS ONE*, 11(10):1–18.

Fratta, P., Mizielinska, S., Nicoll, A. J., Zloh, M., Fisher, E. M., Parkinson, G., and Isaacs, A. M. (2012). C9orf72 hexanucleotide repeat associated with amyotrophic lateral sclerosis and frontotemporal dementia forms rna g-quadruplexes. *Scientific Reports*, 2:1–6.

Fratta, P., Poulter, M., Lashley, T., Rohrer, J. D., Polke, J. M., Beck, J., Ryan, N., Hensman, D., Mizielinska, S., Waite, A. J., Lai, M. C., Gendron, T. F., Petrucelli, L., Fisher, E. M., Revesz, T., Warren, J. D., Collinge, J., Isaacs, A. M., and Mead, S. (2013). Homozygosity for the c9orf72 ggggcc repeat expansion in frontotemporal dementia. *Acta Neuropathologica*, 126(3):401–409.

Freibaum, B. D., Lu, Y., Lopez-Gonzalez, R., Kim, N. C., Almeida, S., Lee, K. H., Badders, N., Valentine, M., Miller, B. L., Wong, P. C., Petrucelli, L., Kim, H. J., Gao, F. B., and Taylor, J. P. (2015). Ggggcc repeat expansion in c9orf72 compromises nucleocytoplasmic transport. *Nature*, 525(7567):129–133.

Frick, P., Sellier, C., Mackenzie, I. R., Cheng, C. Y., Tahraoui-Bories, J., Martinat, C., Pasterkamp, R. J., Prudlo, J., Edbauer, D., Oulad-Abdelghani, M., Feederle, R., Charlet-Berguerand, N., and Neumann, M. (2018). Novel antibodies reveal presynaptic localization of c9orf72 protein and reduced protein levels in c9orf72 mutation carriers. *Acta neuropathologica communications*, 6(1):72.

Gallardo, G. and Holtzman, D. M. (2017). Antibody therapeutics targeting a and tau. *Cold Spring Harbor Perspectives in Medicine*, 7(10):1–17.

Gasset-rosa, F., Chillon-marinas, C., Goginashvili, A., Atwal, S., Artates, J. W., Tabet, R., Wheeler, V. C., Anne, G., Cleveland, D. W., and Lagier-tourenne, C. (2017). Polyglutamine-

expanded huntingtin exacerbates age-related disruption of nuclear integrity and nucleocytoplasmic transport. *Neuron*, 94(1):48–57.

Gendron, T. F., Bieniek, K. F., Zhang, Y. J., Jansen-West, K., Ash, P. E., Caulfield, T., Daughrity, L., Dunmore, J. H., Castanedes-Casey, M., Chew, J., Cosio, D. M., Van Blitterswijk, M., Lee, W. C., Rademakers, R., Boylan, K. B., Dickson, D. W., and Petrucelli, L. (2013). Antisense transcripts of the expanded c9orf72 hexanucleotide repeat form nuclear rna foci and undergo repeat-associated non-atg translation in c9ftd/als. *Acta Neuropathologica*, 126(6):829–844.

Gendron, T. F., Chew, J., Stankowski, J. N., and Al., E. (2017). Poly(gp) proteins are a useful pharmacodynamic marker for c9orf72-associated amyotrophic lateral sclerosis. *Sci Transl Med.*, 9(383).

Gijselinck, I., Van Langenhove, T., van der Zee, J., Sleegers, K., Philtjens, S., Kleinberger, G., Janssens, J., Bettens, K., Van Cauwenberghe, C., Pereson, S., Engelborghs, S., Sieben, A., De Jonghe, P., Vandenberghe, R., Santens, P., De Bleecker, J., Maes, G., Bäumer, V., Dillen, L., Joris, G., Cuijt, I., Corsmit, E., Elinck, E., Van Dongen, J., Vermeulen, S., Van den Broeck, M., Vaerenberg, C., Mattheijssens, M., Peeters, K., Robberecht, W., Cras, P., Martin, J. J., De Deyn, P. P., Cruts, M., and Van Broeckhoven, C. (2012). A c9orf72 promoter repeat expansion in a flanders-belgian cohort with disorders of the frontotemporal lobar degeneration-amyotrophic lateral sclerosis spectrum: A gene identification study. *The Lancet Neurology*, 11(1):54–65.

Gijselinck, I., Van Mossevelde, S., Van Der Zee, J., Sieben, A., Engelborghs, S., De Bleecker, J., Ivanoiu, A., Deryck, O., Edbauer, D., Zhang, M., Heeman, B., Bäumer, V., Van Den Broeck, M., Mattheijssens, M., Peeters, K., Rogaeva, E., De Jonghe, P., Cras, P., Martin, J. J., De Deyn, P. P., Cruts, M., and Van Broeckhoven, C. (2016). The c9orf72 repeat size correlates with onset age of disease, dna methylation and transcriptional downregulation of the promoter. *Molecular Psychiatry*, 21(8):1112–1124.

Gomez-Deza, J., Lee, Y. B., Troakes, C., Nolan, M., Al-Sarraj, S., Gallo, J. M., and Shaw, C. E. (2015). Dipeptide repeat protein inclusions are rare in the spinal cord and almost absent from motor neurons in c9orf72 mutant amyotrophic lateral sclerosis and are unlikely to cause their degeneration. *Acta neuropathologica communications*, 3:38.

Goodman, L. D., Prudencio, M., Kramer, N. J., Martinez-Ramirez, L. F., Srinivasan, A. R., Lan, M., Parisi, M. J., Zhu, Y., Chew, J., Cook, C. N., Berson, A., Gitler, A. D., Petrucelli, L., and Bonini, N. M. (2019). Toxic expanded ggggcc repeat transcription is mediated by the paf1 complex in c9orf72-associated ftd. *Nature Neuroscience*, 22(6):863–874.

Green, K. M., Glineburg, M. R., Kearse, M. G., Flores, B. N., Linsalata, A. E., Fedak, S. J., Goldstrohm, A. C., Barmada, S. J., and Todd, P. K. (2017). Ran translation at c9orf72-associated repeat expansions is selectively enhanced by the integrated stress response. *Nature Communications*, 8(1).

Grima, J. C., Daigle, J. G., Arbez, N., Cunningham, K. C., Ochaba, J., Geater, C., Morozko, E., Stocksdale, J., Glatzer, C., Pham, J. T., Berson, Ahmed, I., Peng, Q., Wadhwa, H., Troncoso, J. C., Duan, W., Snyder, S. H., Laura, P. W., Thompson, L. M., Lloyd, T. E., Ross, C. A. A., Gitler, A. D., Petrucelli, L., and Bonini, N. M. (2017). Mutant huntingtin disrupts the nuclear pore complex. *Neuron*, 94(1):93–107.

Guo, Q., Lehmer, C., Martínez-Sánchez, A., Rudack, T., Beck, F., Hartmann, H., Frottin, M. P.-B. F., Hipp, M. S., Hartl, F. U., Edbauer, D., Baumeister, W., and Fernández-Busnadiego, R. (2018). In situ structure of neuronal c9orf72 poly-ga aggregates reveals proteasome recruitment. *Cell*, 172(4):696–705.

Haeusler, A. R., Donnelly, C. J., Periz, G., Simko, E. A. J., Shaw, P. G., Kim, M. S., Maragakis, N. J., Troncoso, J. C., Pandey, A., Sattler, R., Rothstein, J. D., and Wang, J. (2014). C9orf72 nucleotide repeat structures initiate molecular cascades of disease. *Nature*, 507:195–200.

Hao, Z., Liu, L., Tao, Z., Wang, R., Ren, H., Sun, H., Lin, Z., Zhang, Z., Mu, C., Zhou, J., and Wang, G. (2019). Motor dysfunction and neurodegeneration in a c9orf72 mouse line expressing poly-pr. *Nature Communications*, 10(1).

Harms, M., Cadya, J., Zaidmana, C., Coopera, P., Balia, T., Allreda, P., Cruchagab, C., Baughnd, M., Pestronka, A., Goateb, A., Ravits, J., and Balohe, R. (2013). Lack of c9orf72 coding mutations supports a gain of function for repeat expansions in als. *Neurobiology of Aging*, 34(9):2234–2234.

Hartmann, H., Hornburg, D., Czuppa, M., Bader, J., Michaelsen, M., Farny, D., Arzberger, T., Mann, M., Meissner, F., and Edbauer, D. (2018). Proteomics and c9orf72 neuropathology identify ribosomes as poly-gr/pr interactors driving toxicity. *Life Science Alliance*, 1(2):1–13.

Hautbergue, G. M., Castelli, L. M., Ferraiuolo, L., Sanchez-Martinez, A., Cooper-Knock, J., Higginbottom, A., Lin, Y. H., Bauer, C. S., Dodd, J. E., Myszczynska, M. A., Alam, S. M., Garneret, P., Chandran, J. S., Karyka, E., Stopford, M. J., Smith, E. F., Kirby, J., Meyer, K., Kaspar, B. K., Isaacs, A. M., El-Khamisy, S. F., De Vos, K. J., Ning, K., Azzouz, M., Whitworth, A. J., and Shaw, P. J. (2017). Srsf1-dependent nuclear export inhibition of c9orf72 repeat transcripts prevents neurodegeneration and associated motor deficits. *Nature Communications*, 8(May):1–18.

Heidenreich (2016). Applications of crispr-cas systems in neuroscience. *Nat Rev Neurosci.*, 17(1):36–44.

Ho, R., Workman, M. J., Mathkar, P., Wu, K., Kim, K. J., O'Rourke, J. G., Kellogg, M., Montel, V., Banuelos, M. G., Aladesuyi, O., Garcia Diaz, S., Oheb, D., Huang, S., Khrebtukova, I., Watson, L., Ravits, J., Taylor, K., Baloh, R. H., and Svendsen, C. N. (2020). Single-cell rna-seq analysis of human ipsc-derived motor neurons resolves early and predictive als signatures. *bioRxiv*.

Ho, W. Y., Tai, Y. K., Chang, J. C., Liang, J., Tyan, S. H., Chen, S., Guan, J. L., Zhou, H., Shen, H. M., Koo, E., and Ling, S. C. (2019). The als-ftd-linked gene product, c9orf72, regulates neuronal morphogenesis via autophagy. *Autophagy*, 15(5):827–842.

Hock, E. M. and Polymenidou, M. (2016). Prion-like propagation as a pathogenic principle in frontotemporal dementia. *Journal of Neurochemistry*, 138:163–183.

Hu, J., Rigo, F., Prakash, T. P., and Corey, D. R. (2017). Recognition of c9orf72 mmutant rna by single-stranded silencing rnas. *Nucleic Acid Therapeutics*, 27(2):87–94.

Hua, Y., Vickers, T. A., Baker, B. F., Bennett, C. F., and Krainer, A. R. (2007). Enhancement of smn2 exon 7 inclusion by antisense oligonucleotides targeting the exon. *PLoS Biology*, 5(4):729–744.

Hutten, S. and Dormann, D. (2019). Seminars in cell developmental biology nucleocytoplasmic transport defects in neurodegeneration — cause or consequence? *Seminars in Cell and Developmental Biology*, (May):1–12.

Hübers, A., Marroquin, N., Schmoll, B., Vielhaber, S., Just, M., Mayer, B., Högel, J., Dorst, J., Mertens, T., Just, W., Aulitzky, A., Wais, V., Ludolph, A. C., Kubisch, C., Weishaupt, J. H., and Volk, A. E. (2014). Polymerase chain reaction and southern blot-based analysis of the c9orf72 hexanucleotide repeat in different motor neuron diseases. *Neurobiology of Aging*, 35(5):1214.e1–1214.e6.

Ishiura, H., Takahashi, Y., Mitsui, J., Yoshida, S., Kihira, T., Kokubo, Y., Kuzuhara, S., Ranum, L. P., Tamaoki, T., Ichikawa, Y., Date, H., Goto, J., and Tsuji, S. (2012). C9orf72 repeat expansion in amyotrophic lateral sclerosis in the kii peninsula of japan. *Archives of Neurology*, 69(9):1154–1158.

Jain, A. and Vale, R. D. (2017). Rna phase transitions in repeat expansion disorders. *Nature*, 546(7657):243–247.

Jiang, J., Zhu, Q., Gendron, T. F., Saberi, S., McAlonis-Downes, M., Seelman, A., Stauffer, J. E., Jafar-nejad, P., Drenner, K., Schulte, D., Chun, S., Sun, S., Ling, S. C., Myers, B., Engelhardt, J., Katz, M., Baughn, M., Platoshyn, O., Marsala, M., Watt, A., Heyser, C. J., Ard, M. C., De Muynck, L., Daughrity, L. M., Swing, D. A., Tessarollo, L., Jung, C. J., Delpoux, A., Utzschneider, D. T., Hedrick, S. M., de Jong, P. J., Edbauer, D., Van Damme, P., Petrucelli, L., Shaw, C. E., Bennett, C. F., Da Cruz, S., Ravits, J., Rigo, F., Cleveland, D. W., and Lagier-Tourenne, C. (2016). Gain of toxicity from als/ftd-linked repeat expansions in c9orf72 is alleviated by antisense oligonucleotides targeting ggggcc-containing rnas. *Neuron*, 90(3):535–550.

Jovičič, A., Mertens, J., Boeynaems, S., Bogaert, E., Chai, N., Yamada, S. B., Paul, J. W., Sun, S., Herdy, J. R., Bieri, G., Kramer, N. J., Gage, F. H., Van Den Bosch, L., Robberecht, W., and

Gitler, A. D. (2015). Modifiers of c9orf72 dipeptide repeat toxicity connect nucleocytoplasmic transport defects to ftd/als. *Nature Neuroscience*, 18(9):1226–1229.

Jung, J., Nayak, A., Schaeffer, V., Starzetz, T., Kirsch, A. K., Müller, S., Dikic, I., Mittelbronn, M., and Behrends, C. (2017). Multiplex image-based autophagy rnai screening identifies smcr8 as ulk1 kinase activity and gene expression regulator. *eLife*, 6(2011):1–32.

Kanekura, K., Yagi, T., Cammack, A. J., Mahadevan, J., Kuroda, M., Harms, M. B., Miller, T. M., and Urano, F. (2016). Poly-dipeptides encoded by the c9orf72 repeats block global protein translation. *Human Molecular Genetics*, 25(9):1803–1813.

Kato, M., Han, T., Xie, S., Shi, K., Du, X., Wu, L., Mirzaei, H., Goldsmith, E., Longgood, J., Pei, J., Grishin, N., Frantz, D., Schneider, J., Chen, S., Li, L., Sawaya, M., Eisenberg, D., Tycko, R., McKnight, and McKnight, S. L. (2012). Cell-free formation of rna granules: low complexity sequence domains form dynamic fibers within hydrogels. *Cell*, 149(4).

Knockenhauer, K. E. and Schwartz, T. U. (2016). The nuclear pore complex as a flexible and dynamic gate. *Cell*, 164(6):1162–1171.

Koppers, M., Blokhuis, A. M., Westeneng, H. J., Terpstra, M. L., Zundel, C. A., Vieira De Sá, R., Schellevis, R. D., Waite, A. J., Blake, D. J., Veldink, J. H., Van Den Berg, L. H., and Pasterkamp, R. J. (2015). C9orf72 ablation in mice does not cause motor neuron degeneration or motor deficits. *Annals of Neurology*, 78(3):426–438.

Kovanda, A., Zalar, M., Šket, P., Plavec, J., and Rogelj, B. (2015). Anti-sense dna d(ggcccc)n expansions in c9orf72 form i-motifs and protonated hairpins. *Scientific Reports*, 5(November):3–9.

Kramer, N. J., Carlomagno, Y., Zhang, Y.-j., Almeida, S., Casey, N., Gendron, T. F., Prudencio, M., Blitterswijk, M. V., Couthouis, J., West, J., Iii, P., Goodman, L. D., Daughrity, L., Chew, J., Garrett, A., Pregent, L., Jansen-west, K., Tabassian, L. J., Rademakers, R., Boylan, K., Graff-radford, N. R., Josephs, K. A., Joseph, E., Knopman, D. S., Petersen, R. C., Boeve, B. F., Deng, N., Cheng, T.-h., Dickson, D. W., Cohen, S. N., Bonini, N. M., Link, C. D., Gao, F.-b., Petrucelli, L., and Gitler, A. D. (2016). Spt4 selectively regulates the expression of c9orf72 sense and antisense mutant transcripts associated with c9ftd/als. *Science*, 353(6300):708–712.

Kramer, N. J., Haney, M. S., Morgens, D. W., Jovičić, A., Li, A., Ousey, J., Ma, R., Bieri, G., Tsui, C. K., Shi, Y., Hertz, N. T., Tessier-lavigne, M., Ichida, J. K., Michael, C., and Gitler, A. D. (2018). Crispr-cas9 screens in human cells and primary neurons identify modifiers of c9orf72 dipeptide repeat protein toxicity nicholas. *Nature Genetics*, 50(4):603–612.

Krishnan, G., Zhang, Y., Gu, Y., Kankel, M. W., Gao, F. B., and Almeida, S. (2020). Crispr deletion of the c9orf72 promoter in als/ftd patient motor neurons abolishes production of dipeptide repeat proteins and rescues neurodegeneration. *Acta Neuropathologica*, 3(0123456789):6–9.

Lagier-Tourenne, C., Baughn, M., Rigo, F., Sun, S., Liu, P., Li, H.-R., Jiang, J., Watt, A. T., Chun, S., Katz, M., Qiu, J., Sun, Y., Ling, S.-C., Zhu, Q., Polymenidou, M., Drenner, K., Artates, J. W., McAlonis-Downes, M., Markmiller, S., Hutt, K. R., Pizzo, D. P., Cady, J., Harms, M. B., Baloh, R. H., Vandenberg, S. R., Yeo, G. W., Fu, X.-D., Bennett, C. F., Cleveland, D. W., and Ravits, J. (2013). Targeted degradation of sense and antisense c9orf72 rna foci as therapy for als and frontotemporal degeneration. 110:E4530–E4539.

Lee, K. H., Zhang, P., Kim, H. J., Mitrea, D. M., Sarkar, M., Freibaum, B. D., Cika, J., Coughlin, M., Messing, J., Molliex, A., Maxwell, B. A., Kim, N. C., Temirov, J., Moore, J., Kolaitis, R. M., Shaw, T. I., Bai, B., Peng, J., Kriwacki, R. W., and Taylor, J. P. (2016). C9orf72 dipeptide repeats impair the assembly, dynamics, and function of membrane-less organelles. *Cell*, 167(3):774–788.e17.

Lee, Y. B., Chen, H. J., Peres, J. N., Gomez-Deza, J., Attig, J., Štalekar, M., Troakes, C., Nishimura, A. L., Scotter, E. L., Vance, C., Adachi, Y., Sardone, V., Miller, J. W., Smith, B. N., Gallo, J. M., Ule, J., Hirth, F., Rogelj, B., Houart, C., and Shaw, C. E. (2013). Hexanucleotide repeats in als/ftd form length-dependent rna foci, sequester rna binding proteins, and are neurotoxic. *Cell Reports*, 5(5):1178–1186.

Lehmer, C., Oeckl, P., Weishaupt, J. H., Volk, A. E., Diehl-Schmid, J., Schroeter, M. L., Lauer, M., Kornhuber, J., Levin, J., Fassbender, K., Landwehrmeyer, B., Schludi, M. H., Arzberger, T., Kremmer, E., Flatley, A., Feederle, R., Steinacker, P., Weydt, P., Ludolph, A. C., Edbauer, D., Otto, M., Danek, A., Feneberg, E., Anderl-Straub, S., Arnim, C., Jahn, H., Schneider, A., Maler, M., Polyakova, M., Riedl, L., Wiltfang, J., and Ziegler, G. (2017). Poly- gp in cerebrospinal fluid links c9orf72 -associated dipeptide repeat expression to the asymptomatic phase of als / ftd. *EMBO Molecular Medicine*, 9(7):859–868.

Levine, T. P., Daniels, R. D., Gatta, A. T., Wong, L. H., and Hayes, M. J. (2013). The product of c9orf72, a gene strongly implicated in neurodegeneration, is structurally related to denn rab-gefs. *Bioinformatics*, 29(4):499–503.

Li, Y. R., King, O. D., Shorter, J., and Gitler, A. D. (2013). Stress granules as crucibles of als pathogenesis. *Journal of Cell Biology*, 201(3):361–372.

Ling, S. C., Polymenidou, M., and Cleveland, D. W. (2013). Converging mechanisms in als and ftd: Disrupted rna and protein homeostasis. *Neuron*, 79(3):416–438.

Liu, E. Y., Russ, J., Wu, K., Neal, D., Suh, E., McNally, A. G., Irwin, D. J., Van Deerlin, V. M., and Lee, E. B. (2014). C9orf72 hypermethylation protects against repeat expansion-associated pathology in als/ftd. *Acta Neuropathologica*, 128(4):525–541.

Liu, F., Liu, Q., Lu, C. X., Cui, B., Guo, X. N., Wang, R. R., Liu, M. S., Li, X. G., Cui, L. y., and Zhang, X. (2016a). Identification of a novel loss-of-function c9orf72 splice site mutation in a patient with amyotrophic lateral sclerosis. *Neurobiology of Aging*, 47:219.e1–219.e5.

Liu, Y., Pattamatta, A., Zu, T., Reid, T., Bardhi, O., Borchelt, D. R., Yachnis, A. T., and Ranum, L. P. (2016b). C9orf72 bac mouse model with motor deficits and neurodegenerative features of als/ftd. *Neuron*, 90(3):521–534.

Liu-Yesucevitz, L., Bilgutay, A., Zhang, Y. J., Vanderwyde, T., Citro, A., Mehta, T., Zaarur, N., McKee, A., Bowser, R., Sherman, M., Michael, Petrucelli, L., and Wolozin, B. (2010). Tar dna binding protein-43 (tdp-43) associates with stress granules: Analysis of cultured cells and pathological brain tissue. *PLoS ONE*, 5(10).

Lo, S. J., Lee, C. C., and Lai, H. J. (2006). The nucleolus: Reviewing oldies to have new understandings. *Cell Research*, 16(6):530–538.

Lopez-Gonzalez, R., Lu, Y., Gendron, T. F., Karydas, A., Tran, H., Yang, D., Petrucelli, L., Miller, B. L., Almeida, S., and Gao, F. B. (2016). Poly(gr) in c9orf72-related als/ftd compromises mitochondrial function and increases oxidative stress and dna damage in ipsc-derived motor neurons. *Neuron*, 92(2):383–391.

Lopez-Gonzalez, R., Yang, D., Pribadi, M., Kim, T. S., Krishnan, G., Choi, S. Y., Lee, S., Coppola, G., and Gao, F. B. (2019). Partial inhibition of the overactivated ku80-dependent dna repair pathway rescues neurodegeneration in c9orf72-als/ftd. *Proceedings of the National Academy of Sciences of the United States of America*, 116(19):9628–9633.

MacKenzie, I. R., Arzberger, T., Kremmer, E., Troost, D., Lorenzl, S., Mori, K., Weng, S. M., Haass, C., Kretzschmar, H. A., Edbauer, D., and Neumann, M. (2013). Dipeptide repeat protein pathology in c9orf72 mutation cases: Clinico-pathological correlations. *Acta Neuropathologica*, 126(6):859–879.

Mackenzie, I. R., Frick, P., Grässer, F. A., Gendron, T. F., Petrucelli, L., Cashman, N. R., Edbauer, D., Kremmer, E., Prudlo, J., Troost, D., and Neumann, M. (2015). Quantitative analysis and clinico-pathological correlations of different dipeptide repeat protein pathologies in c9orf72 mutation carriers. *Acta Neuropathologica*, 130(6):845–861.

Maharjan, N., Künzli, C., Buthey, K., and Saxena, S. (2017). C9orf72 regulates stress granule formation and its deficiency impairs stress granule assembly, hypersensitizing cells to stress. *Molecular Neurobiology*, 54(4):3062–3077.

Martier, R., Liefhebber, J. M., García-osta, A., Miniarikova, J., Cuadrado-tejedor, M., Espelosin, M., Ursua, S., Petry, H., Deventer, S. J. V., and Evers, M. M. (2019a). Targeting rna-mediated toxicity in c9orf72 als and/or ftd by rnai-based gene therapy. *Molecular Therapy: Nucleic Acid*, 16(June):26–37.

Martier, R., Liefhebber, J. M., Miniarikova, J., Zon, T. V. D., Snapper, J., Kolder, I., Petry, H., Deventer, S. J. V., Evers, M. M., and Konstantinova, P. (2019b). Artificial micrornas targeting c9orf72 can reduce accumulation of intra-nuclear transcripts in als and ftd patients. *Nucleic*

Acids, 14(March).

May, S., Hornburg, D., Schludi, M. H., Arzberger, T., Rentzsch, K., Schwenk, B. M., Grässer, F. A., Mori, K., Kremmer, E., Banzhaf-Strathmann, J., Mann, M., Meissner, F., and Edbauer, D. (2014). C9orf72 ftld/als-associated gly-ala dipeptide repeat proteins cause neuronal toxicity and unc119 sequestration. *Acta Neuropathologica*, 128(4):485–503.

McCombe, P. A. and Henderson, R. D. (2010). Effects of gender in amyotrophic lateral sclerosis. *Gender Medicine*, 7(6):557–570.

McMillan, C. T., Russ, J., Wood, E. M., Irwin, D. J., Grossman, M., McCluskey, L., Elman, L., Van Deerlin, V., and Lee, E. B. (2015). C9orf72 promoter hypermethylation is neuroprotective. *Neurology*, 84(16):1622–1630.

Mierzejewska-Krzyzowska, B., Bukowska, D., Taborowska, M., and Celichowski, J. (2014). Sex differences in the number and size of motoneurons innervating rat medial gastrocnemius muscle. *Journal of Veterinary Medicine Series C: Anatomia Histologia Embryologia*, 43(3):182–189.

Miller, T., Pestronk, A., David, W., Rothstein, J., Simpson, E., Appel, S. H., Andres, P. L., Mahoney, K., Allred, P., Alexander, K., Ostrow, L. W., Schoenfeld, D., Macklin, E. A., Norris, D. A., Manousakis, G., Crisp, M., Smith, R., Bennett, C., Bishop, K., and Cudkowicz, M. E. (2013). A phase i, randomised, first-in-human study of an antisense oligonucleotide directed against sod1 delivered intrathecally in sod1-familial als patients. *Lancet Neurology*, 12(5):435–442.

Miller, Z. A., Sturm, V. E., Camsari, G. B., Karydas, A., Yokoyama, J. S., Grinberg, L. T., Boxer, A. L., Rosen, H. J., Rankin, K. P., Tempini, M. L. G., Coppola, G., Geschwind, D. H., Rademakers, R., Seeley, W. W., Graff-Radford, N. R., and Miller, B. L. (2016). Increased prevalence of autoimmune disease within c9 and ftd/mnd cohorts. *Neurology: Neuroimmunology and NeuroInflammation*, 3(6):1–8.

Mizielinska, S., Grönke, S., Niccoli, T., Ridler, C. E., Clayton, E. L., Devoy, A., Moens, T., Norona, F. E., Woollacott, I. O. C., Pietrzyk, J., Cleverley, K., Nicoll, A. J., Pickering-brown, S., Dols, J., Cabecinha, M., Hendrich, O., Fratta, P., Fisher, E. M. C., Partridge, L., and Isaacs, A. M. (2014). C9orf72 repeat expansions cause neurodegeneration in drosophila through arginine-rich proteins. *Science*, 345(6201):1192–1195.

Mizielinska, S., Lashley, T., Norona, F. E., Clayton, E. L., Ridler, C. E., Fratta, P., and Isaacs, A. M. (2013). C9orf72 frontotemporal lobar degeneration is characterised by frequent neuronal sense and antisense rna foci. *Acta Neuropathologica*, 126(6):845–857.

Mizielinska, S., Ridler, C. E., Balendra, R., Thoeng, A., Woodling, N. S., Grässer, F. A., Plagnol, V., Lashley, T., Partridge, L., and Isaacs, A. M. (2017). Bidirectional nucleolar dysfunction in

c9orf72 frontotemporal lobar degeneration. *Acta neuropathologica communications*, 5(1):29.

Molliex, A., Temirov, J., Lee, J., Coughlin, M., Kanagaraj, A. P., Kim, H. J., Mittag, T., and Taylor, J. P. (2015). Phase separation by low complexity domains promotes stress granule assembly and drives pathological fibrillization. *Cell*, 163(1):123–133.

Molteni, M. and Rossetti, C. (2017). Neurodegenerative diseases: The immunological perspective. *Journal of Neuroimmunology*, 313(October):109–115.

Mori, K., Lammich, S., Mackenzie, I. R., Forné, I., Zilow, S., Kretzschmar, H., Edbauer, D., Janssens, J., Kleinberger, G., Cruts, M., Herms, J., Neumann, M., Van Broeckhoven, C., Arzberger, T., and Haass, C. (2013a). Hnrnp a3 binds to ggggcc repeats and is a constituent of p62-positive/tdp43-negative inclusions in the hippocampus of patients with c9orf72 mutations. *Acta Neuropathologica*, 125(3):413–423.

Mori, K., Weng, S.-M., Arzberger, T., May, S., Rentzsch, K., Kremmer, E., Schmid, B., Kretzschmar, H. A., Cruts, M., Van Broeckhoven, C., Haass, C., and Edbauer, D. (2013b). Bidirectional transcripts of the expanded c9orf72 hexanucleotide repeat are translated into aggregating dipeptide repeat proteins. *Acta Neuropathologica*, 126(6):881–893.

Mori, K., Weng, S.-M., Arzberger, T., May, S., Rentzsch, K., Kremmer, E., Schmid, B., Kretzschmar, H. A., Cruts, M., Van Broeckhoven, C., Haass, C., and Edbauer, D. (2013c). The c9orf72 ggggcc repeat is translated into aggregating dipeptide-repeat proteins in ftld/als. *Science*, 126:1335–1338.

Murakami, T., Qamar, S., Lin, J. Q., Schierle, G. S., Rees, E., Miyashita, A., Costa, A. R., Dodd, R. B., Chan, F. T., Michel, C. H., Kronenberg-Versteeg, D., Li, Y., Yang, S. P., Wakutani, Y., Meadows, W., Ferry, R. R., Dong, L., Tartaglia, G. G., Favrin, G., Lin, W. L., Dickson, D. W., Zhen, M., Ron, D., Schmitt-Ulms, G., Fraser, P. E., Shneider, N. A., Holt, C., Vendruscolo, M., Kaminski, C. F., and St George-Hyslop, P. (2015). Als/ftd mutation-induced phase transition of fus liquid droplets and reversible hydrogels into irreversible hydrogels impairs rnp granule function. *Neuron*, 88(4):678–690.

Naguib, A., Sandmann, T., Yi, F., Watts, R. J., Lewcock, J. W., and Dowdle, W. E. (2019). Supt4h1 depletion leads to a global reduction in rna. *Cell Reports*, 26(1):45–53.e4.

Nalabothula, N., Indig, F. E., and Carrier, F. (2010). The nucleolus takes control of protein trafficking under cellular stress. *Molecular and cellular pharmacology*, 2(5):203–212.

Nana, A. L., Sidhu, M., Gaus, S. E., Hwang, J. H. L., Li, L., Park, Y., Kim, E. J., Pasquini, L., Allen, I. E., Rankin, K. P., Toller, G., Kramer, J. H., Geschwind, D. H., Coppola, G., Huang, E. J., Grinberg, L. T., Miller, B. L., and Seeley, W. W. (2019). Neurons selectively targeted in frontotemporal dementia reveal early stage tdp-43 pathobiology. *Acta Neuropathologica*, 137(1):27–46.

Nguyen, H. P., Van Broeckhoven, C., and van der Zee, J. (2018). Als genes in the genomic era and their implications for ftd. *Trends in Genetics*, 34(6):404–423.

Nguyen, L., Montrasio, F., Pattamatta, A., Tusi, S. K., Bardhi, O., Meyer, K. D., Hayes, L., Nakamura, K., Banez-Coronel, M., Coyne, A., Guo, S., Laboissonniere, L. A., Gu, Y., Narayanan, S., Smith, B., Nitsch, R. M., Kankel, M. W., Rushe, M., Rothstein, J., Zu, T., Grimm, J., and Ranum, L. P. (2020). Antibody therapy targeting ran proteins rescues c9 als/ftd phenotypes in c9orf72 mouse model. *Neuron*, 105(4):645–662.e11.

Nordin, A., Akimoto, C., Wuolikainen, A., Alstermark, H., Jonsson, P., Birve, A., Marklund, S. L., Graffmo, K. S., Forsberg, K., Brännström, T., and Andersen, P. M. (2014). Extensive size variability of the ggggcc expansion in c9orf72 in both neuronal and non-neuronal tissues in 18 patients with als or ftd. *Human Molecular Genetics*, 24(11):3133–3142.

Ohki, Y., Wenninger-Weinzierl, A., Hruscha, A., Asakawa, K., Kawakami, K., Haass, C., Edbauer, D., and Schmid, B. (2017). Glycine-alanine dipeptide repeat protein contributes to toxicity in a zebrafish model of c9orf72 associated neurodegeneration. *Molecular Neurodegeneration*, 12(1):1–11.

Olney, N. T., Spina, S., and Miller, B. L. (2017). Frontotemporal dementia. *Neurologic Clinics*, 35(2):339–374.

O'Rourke, J. G., Bogdanik, L., Muhammad, A. K., Gendron, T. F., Kim, K. J., Austin, A., Cady, J., Liu, E. Y., Zarrow, J., Grant, S., Ho, R., Bell, S., Carmona, S., Simpkinson, M., Lall, D., Wu, K., Daughrity, L., Dickson, D. W., Harms, M. B., Petrucelli, L., Lee, E. B., Lutz, C. M., and Baloh, R. H. (2015). C9orf72 bac transgenic mice display typical pathologic features of als/ftd. *Neuron*, 88(5):892–901.

O'Rourke, J. G., Bogdanik, L., Yáñez, A., Lall, D., Wolf, A. J., Muhammad, A. K., Ho, R., Carmona, S., Vit, J. P., Zarrow, J., Kim, K. J., Bell, S., Harms, M. B., Miller, T. M., Dangler, C. A., Underhill, D. M., Goodridge, H. S., Lutz, C. M., and Baloh, R. H. (2016). C9orf72 is required for proper macrophage and microglial function in mice. *Science*, 351(6279):1324–1329.

Patel, A., Lee, H. O., Jawerth, L., Maharana, S., Jahnel, M., Hein, M. Y., Stoynov, S., Mahamid, J., Saha, S., Franzmann, T. M., Pozniakovski, A., Poser, I., Maghelli, N., Royer, L. A., Weigert, M., Myers, E. W., Grill, S., Drechsel, D., Hyman, A. A., and Alberti, S. (2015). A liquid-to-solid phase transition of the als protein fus accelerated by disease mutation. *Cell*, 162(5):1066–1077.

Peters, O. M., Cabrera, G. T., Tran, H., Gendron, T. F., McKeon, J. E., Metterville, J., Weiss, A., Wightman, N., Salameh, J., Kim, J., Sun, H., Boylan, K. B., Dickson, D., Kennedy, Z., Lin, Z., Zhang, Y. J., Daughrity, L., Jung, C., Gao, F. B., Sapp, P. C., Horvitz, H. R., Bosco, D. A., Brown, S. P., de Jong, P., Petrucelli, L., Mueller, C., and Brown, R. H. (2015). Human c9orf72 hexanucleotide expansion reproduces rna foci and dipeptide repeat proteins but not

neurodegeneration in bac transgenic mice. *Neuron*, 88(5):902–909.

Pinto, B. S., Saxena, T., Oliveira, R., Méndez-Gómez, H. R., Cleary, J. D., Denes, L. T., McConnell, O., Arboleda, J., Xia, G., Swanson, M. S., and Wang, E. T. (2017). Impeding transcription of expanded microsatellite repeats by deactivated cas9. *Mol Cell.*, 68(3):479–490.e5.

Pribadi, M., Yang, Z., Kim, T. S., Swartz, E. W., Huang, A. Y., Chen, J. A., Dokuru, D., Baek, J., Gao, F., Fua, A. T., Wojta, K., Wang, Q., Lezcano, E., Ng, S., Chehab, F. F., Karydas, A., Fong, J., Vinters, H. V., Miller, B. L., and Coppola, G. (2016). Crispr-cas9 targeted deletion of the c9orf72 repeat expansion mutation corrects cellular phenotypes in patient-derived ips cells. *bioRxiv*, page 051193.

Proudfoot, M., Gutowski, N. J., Edbauer, D., Hilton, D. A., Stephens, M., Rankin, J., and Mackenzie, I. R. (2014). Early dipeptide repeat pathology in a frontotemporal dementia kindred with c9orf72 mutation and intellectual disability. *Acta Neuropathologica*, 127(3):451–458.

Qin, R., Zhang, H., Li, S., Jiang, W., and Liu, D. (2014). Three major nucleolar proteins migrate from nucleolus to nucleoplasm and cytoplasm in root tip cells of vicia faba l. exposed to aluminum. *Environmental Science and Pollution Research*, 21(18):10736–10743.

Rahimov, F. and Kunkel, L. M. (2013). Cellular and molecular mechanisms underlying muscular dystrophy. *Journal of Cell Biology*, 201(4):499–510.

Ravits, J. (2014). Focality, stochasticity and neuroanatomic propagation in als pathogenesis. *Experimental Neurology*, 262(Part B):121–126.

Reddy, K., Zamiri, B., Stanley, S. Y., Macgregor, R. B., and Pearson, C. E. (2013). The disease-associated r(ggggcc)n repeat from the c9orf72 gene forms tract length-dependent uni- and multimolecular rna g-quadruplex structures. *Journal of Biological Chemistry*, 288(14):9860–9866.

Renton, A. E., Majounie, E., Waite, A., Simón-Sánchez, J., Rollinson, S., Gibbs, J. R., Schymick, J. C., Laaksovirta, H., van Swieten, J. C., Myllykangas, L., Kalimo, H., Paetau, A., Abramzon, Y., Remes, A. M., Kaganovich, A., Scholz, S. W., Duckworth, J., Ding, J., Harmer, D. W., Hernandez, D. G., Johnson, J. O., Mok, K., Ryten, M., Trabzuni, D., Guerreiro, R. J., Orrell, R. W., Neal, J., Murray, A., Pearson, J., Jansen, I. E., Sondervan, D., Seelaar, H., Blake, D., Young, K., Halliwell, N., Callister, J. B., Toulson, G., Richardson, A., Gerhard, A., Snowden, J., Mann, D., Neary, D., Nalls, M. A., Peuralinna, T., Jansson, L., Isoviita, V. M., Kaivorinne, A. L., Hölttä-Vuori, M., Ikonen, E., Sulkava, R., Benatar, M., Wuu, J., Chiò, A., Restagno, G., Borghero, G., Sabatelli, M., Heckerman, D., Rogaeva, E., Zinman, L., Rothstein, J. D., Sendtner, M., Drepper, C., Eichler, E. E., Alkan, C., Abdullaev, Z., Pack, S. D., Dutra, A., Pak, E., Hardy, J., Singleton, A., Williams, N. M., Heutink, P., Pickering-Brown, S., Morris, H. R., Tienari, P. J., and Traynor, B. J. (2011). A hexanucleotide repeat expansion in c9orf72 is the cause of chromosome 9p21-linked als-ftd. *Neuron*, 72(2):257–268.

Russ, J., Liu, E. Y., Wu, K., Neal, D., Suh, E. R., Irwin, D. J., McMillan, C. T., Harms, M. B., Cairns, N. J., Wood, E. M., Xie, S. X., Elman, L., McCluskey, L., Grossman, M., Van Deerlin, V. M., and Lee, E. B. (2015). Hypermethylation of repeat expanded c9orf72 is a clinical and molecular disease modifier. *Acta Neuropathologica*, 129(1):39–52.

Ryan, S., Hobbs, E., Rollinson, S., and Pickering-Brown, S. M. (2019). Crispr/cas9 does not facilitate stable expression of long c9orf72 dipeptides in mice. *Neurobiology of Aging*, 84:235.e1–235.e8.

Saberi, S., Stauffer, J. E., Jiang, J., Garcia, S. D., Taylor, A. E., Schulte, D., Ohkubo, T., Schloffman, C. L., Maldonado, M., Baughn, M., Rodriguez, M. J., Pizzo, D., Cleveland, D., and Ravits, J. (2017). Sense-encoded poly-gr dipeptide repeat proteins correlate to neurodegeneration and uniquely co-localize with tdp-43 in dendrites of repeat-expanded c9orf72 amyotrophic lateral sclerosis. *Acta Neuropathologica*, page 1–16.

Sakae, N., Bieniek, K. F., Zhang, Y. J., Ross, K., Gendron, T. F., Murray, M. E., Rademakers, R., Petrucelli, L., and Dickson, D. W. (2018). Poly-gr dipeptide repeat polymers correlate with neurodegeneration and clinicopathological subtypes in c9orf72-related brain disease. *Acta neuropathologica communications*, 6(1):63.

Santillo, A. F., Nilsson, C., and Englund, E. (2013). von economo neurones are selectively targeted in frontotemporal dementia. *Neuropathology and Applied Neurobiology*, 39(5):572–579.

Sareen, D., O'Rourke, J. G., Meera, P., Muhammad, A. K. M. G., Grant, S., Simpkinson, M., Bell, S., Carmona, S., Ornelas, L., Sahabian, A., Gendron, T., Petrucelli, L., Baughn, M., Ravits, J., Harms, M. B., Rigo, F., Bennett, C. F., Otis, T. S., Svendsen, C. N., and Baloh, R. H. (2013). Targeting rna foci in ipsc-derived motor neurons from als patients with a c9orf72 repeat expansion. *Science Translational Medicine*, 5(208):208ra149 LP–208ra149.

Schipper, L. J., Raaphorst, J., Aronica, E., Baas, F., de Haan, R., de Visser, M., and Troost, D. (2016). Prevalence of brain and spinal cord inclusions, including dipeptide repeat proteins, in patients with the c9orf72 hexanucleotide repeat expansion: a systematic neuropathological review. *Neuropathology and Applied Neurobiology*, 42(6):547–560.

Schludi, M. H., Becker, L., Garrett, L., Gendron, T. F., Zhou, Q., Schreiber, F., Popper, B., Dimou, L., Strom, T. M., Winkelmann, J., von Thaden, A., Rentzsch, K., May, S., Michaelsen, M., Schwenk, B. M., Tan, J., Schoser, B., Dieterich, M., Petrucelli, L., Hölter, S. M., Wurst, W., Fuchs, H., Gailus-Durner, V., de Angelis, M. H., Klopstock, T., Arzberger, T., and Edbauer, D. (2017). Spinal poly-ga inclusions in a c9orf72 mouse model trigger motor deficits and inflammation without neuron loss. *Acta Neuropathologica*, 134(2):241–254.

Schludi, M. H., May, S., Grässer, F. A., Rentzsch, K., Kremmer, E., Küpper, C., Klopstock, T., Ceballos-Baumann, A., Danek, A., Diehl-Schmid, J., Fassbender, K., Förstl, H., Kornhuber, J., Otto, M., Dieterich, M., Feuerecker, R., Giese, A., Klünemann, H., Kurz, A., Levin, J., Lorenzl,

S., Meyer, T., Nübling, G., and Roeber, S. (2015). Distribution of dipeptide repeat proteins in cellular models and c9orf72 mutation cases suggests link to transcriptional silencing. *Acta Neuropathologica*, 130(4):537–555.

Sellier, C., Campanari, M., Julie Corbier, C., Gaucherot, A., Kolb-Cheynel, I., Oulad-Abdelghani, M., Ruffenach, F., Page, A., Ciura, S., Kabashi, E., and Charlet-Berguerand, N. (2016). Loss of c9 orf 72 impairs autophagy and synergizes with polyq ataxin-2 to induce motor neuron dysfunction and cell death. *The EMBO Journal*, 35(12):1276–1297.

Shang, J., Yamashita, T., Nakano, Y., Morihara, R., Li, X., Feng, T., Liu, X., Huang, Y., Fukui, Y., Hishikawa, N., Ohta, Y., and Abe, K. (2017). Aberrant distributions of nuclear pore complex proteins in als mice and als patients. *Neuroscience*, 350:158–168.

Shao, Q., Liang, C., Chang, Q., Zhang, W., Yang, M., and Chen, J. F. (2019). C9orf72 deficiency promotes motor deficits of a c9als/ftd mouse model in a dose-dependent manner. *Acta neuropathologica communications*, 7(1):32.

Shi, K. Y., Mori, E., Nizami, Z. F., Lin, Y., Kato, M., Xiang, S., Wu, L. C., Ding, M., Yu, Y., Gall, J. G., and McKnight, S. L. (2017). Toxic prn poly-dipeptides encoded by the c9orf72 repeat expansion block nuclear import and export. *Proceedings of the National Academy of Sciences of the United States of America*, 114(7):E1111–E1117.

Shi, Y., Lin, S., Staats, K. A., Li, Y., Chang, W. H., Hung, S. T., Hendricks, E., Linares, G. R., Wang, Y., Son, E. Y., Wen, X., Kisler, K., Wilkinson, B., Menendez, L., Sugawara, T., Woolwine, P., Huang, M., Cowan, M. J., Ge, B., Koutsodendris, N., Sandor, K. P., Komberg, J., Vangoor, V. R., Senthilkumar, K., Hennes, V., Seah, C., Nelson, A. R., Cheng, T. Y., Lee, S. J. J., August, P. R., Chen, J. A., Wisniewski, N., Hanson-Smith, V., Belgard, T. G., Zhang, A., Coba, M., Grunseich, C., Ward, M. E., Van Den Berg, L. H., Pasterkamp, R. J., Trotti, D., Zlokovic, B. V., and Ichida, J. K. (2018). Haploinsufficiency leads to neurodegeneration in c9orf72 als/ftd human induced motor neurons. *Nature Medicine*, 24(3):313–325.

Spada, A. R. L. and Taylor, J. P. (2010). Repeat expansion disease: Progress and puzzles in disease pathogenesis. *Nature reviews Genetics*, 11(4):247–258.

Su, Z., Zhang, Y., Gendron, T. F., Bauer, P. O., Yang, W.-y., Fostvedt, E., Jansen-west, K., Belzil, V. V., Desaro, P., Johnston, A., Overstreet, K., Oh, S.-y., Todd, P. K., Berry, J. D., Cudkowicz, M. E., Boeve, B. F., Dickson, D., Kay, M., Traynor, B. J., Morelli, C., Ratti, A., and Silani, V. (2014). Discovery of a biomarker and lead small molecules to target r(ggggcc)-associated defects in c9ftd/als. *Neuron*, 83(5):1043–1050.

Sudria-Lopez, E., Koppers, M., de Wit, M., van der Meer, C., Westeneng, H. J., Zundel, C. A., Youssef, S. A., Harkema, L., de Bruin, A., Veldink, J. H., van den Berg, L. H., and Pasterkamp, R. J. (2016). Full ablation of c9orf72 in mice causes immune system-related pathology and neoplastic events but no motor neuron defects. *Acta Neuropathologica*, 132(1):145–147.

Suh, E., Lee, E. B., Neal, D., Wood, E. M., Toledo, J. B., Irwin, D. J., Mcmillan, C. T., Krock, B., Elman, L. B., Leo, F., Grossman, M., Xie, S. X., Trojanowski, J. Q., and Vivianna, M. (2015). Semi-automated quantification of c9orf72 expansion size reveals inverse correlation between hexanucleotide repeat number and disease duration in frontotemporal degeneration eunran. *Neuropathology*, 130(3):363–372.

Sullivan, P. M., Zhou, X., Robins, A. M., Paushter, D. H., Kim, D., Smolka, M. B., and Hu, F. (2016). The als/ftld associated protein c9orf72 associates with smcr8 and wdr41 to regulate the autophagy-lysosome pathway. *Acta neuropathologica communications*, 4(1):51.

Suzuki, M., Tork, C., Shelley, B., Mchugh, J., Wallace, K., Klein, S., Lindstrom, M., and Svendsen, C. (2007). Sexual dimorphism in disease onset and progression of a rat model of als. *Amyotrophic Lateral Sclerosis*, 8(1):20–25.

Swaminathan, A., Bouffard, M., Liao, M., Ryan, S., Callister, J. B., Pickering-Brown, S. M., Armstrong, G. A. B., and Drapeau, P. (2018). Expression of c9orf72-related dipeptides impairs motor function in a vertebrate model. *Human Molecular Genetics*, 27(10):1754–1762.

Swinnen, B., Bento-Abreu, A., Gendron, T. F., Boeynaems, S., Bogaert, E., Nuyts, R., Timmers, M., Scheveneels, W., Hersmus, N., Wang, J., Mizielinska, S., Isaacs, A. M., Petrucelli, L., Lemmens, R., Van Damme, P., Van Den Bosch, L., and Robberecht, W. (2018). A zebrafish model for c9orf72 als reveals rna toxicity as a pathogenic mechanism. *Acta Neuropathologica*, 135(3):427–443.

Tabet, R., Schaeffer, L., Freyermuth, F., Jambeau, M., Workman, M., Lee, C. Z., Lin, C. C., Jiang, J., Jansen-West, K., Abou-Hamdan, H., Désaubry, L., Gendron, T., Petrucelli, L., Martin, F., and Lagier-Tourenne, C. (2018). Cug initiation and frameshifting enable production of dipeptide repeat proteins from als/ftd c9orf72 transcripts. *Nature Communications*, 9(1):1–14.

Tabrizi, S. J., Leavitt, B. R., Landwehrmeyer, G. B., Wild, E. J., Saft, C., Barker, R. A., Blair, N. F., Craufurd, D., Priller, J., Rickards, H., Rosser, A., Kordasiewicz, H. B., Czech, C., Swayze, E. E., Norris, D. A., Baumann, T., Gerlach, I., Schobel, S. A., Paz, E., Smith, A. V., Bennett, C. F., and Lane, R. M. (2019). Targeting huntingtin expression in patients with huntington's disease. *New England Journal of Medicine*, 380(24):2307–2316.

Tao, Z., Wang, H., Xia, Q., Li, K., Li, K., Jiang, X., Xu, G., Wang, G., and Ying, Z. (2015). Nucleolar stress and impaired stress granule formation contribute to c9orf72 ran translation-induced cytotoxicity. *Human Molecular Genetics*, 24(9):2426–2441.

Taylor, J. P., Brown, R. H., and Cleveland, D. W. (2016). Decoding als: From genes to mechanism. *Nature*, 539(7628):197–206.

Therrien, M., Rouleau, G. A., Dion, P. A., and Parker, J. A. (2013). Deletion of c9orf72 results in motor neuron degeneration and stress sensitivity in c. elegans. *PLoS ONE*, 8(12):1–10.

Tran, H., Almeida, S., Moore, J., Gendron, T. F., Chalasani, U. D., Lu, Y., Du, X., Nickerson, J. A., Petrucelli, L., Weng, Z., and Gao, F. B. (2015). Differential toxicity of nuclear rna foci versus dipeptide repeat proteins in a drosophila model of c9orf72 ftd/als. *Neuron*, 87(6):1207–1214.

Ugolino, J., Ji, Y. J., Conchina, K., Chu, J., Nirujogi, R. S., Pandey, A., Brady, N. R., Hamacher-Brady, A., and Wang, J. (2016). Loss of c9orf72 enhances autophagic activity via deregulated mtor and tfeb signaling. *PLoS Genetics*, 12(11):1–26.

Van Blitterswijk, M., Gendron, T. F., Baker, M. C., DeJesus-Hernandez, M., Finch, N. C. A., Brown, P. H., Daughrity, L. M., Murray, M. E., Heckman, M. G., Jiang, J., Lagier-Tourenne, C., Edbauer, D., Cleveland, D. W., Josephs, K. A., Parisi, J. E., Knopman, D. S., Petersen, R. C., Petrucelli, L., Boeve, B. F., Graff-Radford, N. R., Boylan, K. B., Dickson, D. W., and Rademakers, R. (2015). Novel clinical associations with specific c9orf72 transcripts in patients with repeat expansions in c9orf72. *Acta Neuropathologica*, 130(6):863–876.

Van Mossevelde, S., Van Der Zee, J., Gijselinck, I., Sleegers, K., De Bleecker, J., Sieben, A., Vandenberghe, R., Van Langenhove, T., Baets, J., Deryck, O., Santens, P., Ivanoiu, A., Willems, C., Bäumer, V., Van Den Broeck, M., Peeters, K., Mattheijssens, M., De Jonghe, P., Cras, P., Martin, J. J., Cruts, M., De Deyn, P. P., Engelborghs, S., and Van Broeckhoven, C. (2017). Clinical evidence of disease anticipation in families segregating a c9orf72 repeat expansion. *JAMA Neurology*, 74(4):445–452.

Vatsavayai, S. C., Nana, A. L., Yokoyama, J. S., and Seeley, W. W. (2018). C9orf72-ftd/als pathogenesis: evidence from human neuropathological studies. *Acta Neuropathologica*, page 1–26.

Vatsavayai, S. C., Yoon, S. J., Gardner, R. C., Gendron, T. F., Vargas, J. N. S., Trujillo, A., Pribadi, M., Phillips, J. J., Gaus, S. E., Hixson, J. D., Garcia, P. A., Rabinovici, G. D., Coppola, G., Geschwind, D. H., Petrucelli, L., Miller, B. L., and Seeley, W. W. (2016). Timing and significance of pathological features in c9orf72 expansion-associated frontotemporal dementia. *Brain*, page aww250.

Waite, A. J., Bäumer, D., East, S., Neal, J., Morris, H. R., Ansorge, O., and Blake, D. J. (2014). Reduced c9orf72 protein levels in frontal cortex of amyotrophic lateral sclerosis and frontotemporal degeneration brain with the c9orf72 hexanucleotide repeat expansion. *Neurobiology of Aging*, 35(7):1779.e5–1779.e13.

Wang, D., Tai, P. W. L., Gao, G., Systems, P., and Tai, P. W. L. (2019). Adeno-associated virus vector as a platform for gene therapy delivery. *Nature Review Drug Discovery*, 18(5):358–378.

Wang, X., Hao, L., Saur, T., Joyal, K., Zhao, Y., Zhai, D., Li, J., Pribadi, M., Coppola, G., Cohen, B. M., and Buttner, E. A. (2016). Forward genetic screen in caenorhabditis elegans suggests f57a10.2 and acp-4 as suppressors of c9orf72 related phenotypes. *Frontiers in Molecular*

Neuroscience, 9(November):1–10.

Wang, Z.-f., Ursu, A., Childs-disney, J. L., Guertler, R., Yang, W.-y., Bernat, V., Rzuczek, S. G., Fuerst, R., Zhang, Y.-j., Tania, F., Yildirim, I., Dwyer, B. G., Rice, J. E., Petrucelli, L., and Disney, M. D. (2020). The hairpin form of r(g4c2)exp in c9als/ftd is repeat- associated non-atg translated and a target for bioactive small molecules. *CellnChem Biol*, 26(2):179–190.

Webster, C. P., Smith, E. F., Bauer, C. S., Moller, A., Hautbergue, G. M., Ferraiuolo, L., Myszczynska, M. A., Higginbottom, A., Walsh, M. J., Whitworth, A. J., Kaspar, B. K., Meyer, K., Shaw, P. J., Grierson, A. J., and De Vos, K. J. (2016). The c9orf72 protein interacts with rab1a and the ulk1 complex to regulate initiation of autophagy. *The EMBO Journal*, 35(15):1656–1676.

Wen, X., Tan, W., Westergard, T., Krishnamurthy, K., Markandaiah, S. S., Shi, Y., Lin, S., Shneider, N. A., Monaghan, J., Pandey, U. B., Pasinelli, P., Ichida, J. K., and Trotti, D. (2014). Antisense proline-arginine ran dipeptides linked to c9orf72-als/ftd form toxic nuclear aggregates that initiate invitro and invivo neuronal death. *Neuron*, 84(6):1213–1225.

White, M. R., Mitrea, D. M., Zhang, P., Tolbert, M., Taylor, J. P., Kriwacki, R. W., White, M. R., Mitrea, D. M., Zhang, P., Stanley, C. B., Cassidy, D. E., Nourse, A., Phillips, A. H., Tolbert, M., Taylor, J. P., and Kriwacki, R. W. (2019). C9orf72 poly (pr) dipeptide repeats disturb biomolecular phase separation and disrupt nucleolar function c9orf72 poly (pr) dipeptide repeats disturb biomolecular phase separation and disrupt nucleolar function. *Molecular Cell*, 74(4):713–728.e6.

Wojciechowska, M., Olejniczak, M., Galka-Marciniak, P., Jazurek, M., and Krzyzosiak, W. J. (2014). Ran translation and frameshifting as translational challenges at simple repeats of human neurodegenerative disorders. *Nucleic Acids Research*, 42(19):11849–11864.

Xi, Z., Zhang, M., Bruni, A. C., Maletta, R. G., Colao, R., Fratta, P., Polke, J. M., Sweeney, M. G., Mudanohwo, E., Nacmias, B., Sorbi, S., Tartaglia, M. C., Rainero, I., Rubino, E., Pinessi, L., Galimberti, D., Surace, E. I., McGoldrick, P., McKeever, P., Moreno, D., Sato, C., Liang, Y., Keith, J., Zinman, L., Robertson, J., and Rogaeva, E. (2015). The c9orf72 repeat expansion itself is methylated in als and ftld patients. *Acta Neuropathologica*, 129(5):715–727.

Xi, Z., Zinman, L., Moreno, D., Schymick, J., Liang, Y., Sato, C., Zheng, Y., Ghani, M., Dib, S., Keith, J., Robertson, J., and Rogaeva, E. (2013). Hypermethylation of the cpg island near the g4c2 repeat in als with a c9orf72 expansion. *American Journal of Human Genetics*, 92(6):981–989.

Xiao, S., MacNair, L., McGoldrick, P., McKeever, P. M., McLean, J. R., Zhang, M., Keith, J., Zinman, L., Rogaeva, E., and Robertson, J. (2015). Isoform-specific antibodies reveal distinct subcellular localizations of c9orf72 in amyotrophic lateral sclerosis. *Annals of Neurology*, 78(4):568–583.

Xu, Z., Poidevina, M., Li, X., Li, Y., Shua, L., Nelsonc, D. L., Li, H., Hales, C. M., Gearing, M., Wingo, T. S., and Jin, P. (2013). Expanded ggggcc repeat rna associated with amyotrophic lateral sclerosis and frontotemporal dementia causes neurodegeneration. *Proceedings of the National Academy of Sciences*, 110(19):7778–7783.

Yamakawa, M., Ito, D., Honda, T., Kubo, K. I., Noda, M., Nakajima, K., and Suzuki, N. (2015). Characterization of the dipeptide repeat protein in the molecular pathogenesis of c9ftd/als. *Human Molecular Genetics*, 24(6):1630–1645.

Yang, D., Abdallah, A., Li, Z., Lu, Y., Almeida, S., and Gao, F. B. (2015a). Ftd/als-associated poly(gr) protein impairs the notch pathway and is recruited by poly(ga) into cytoplasmic inclusions. *Acta Neuropathologica*, 130(4):525–535.

Yang, D., Abdallah, A., Li, Z., Lu, Y., Almeida, S., and Gao, F. B. (2015b). Ftd/als-associated poly(gr) protein impairs the notch pathway and is recruited by poly(ga) into cytoplasmic inclusions. *Acta Neuropathologica*, 130(4):525–535.

Yang, M., Chen, L., Swaminathan, K., Herrlinger, S., Lai, F., Shiekhattar, R., and Chen, J. F. (2016). A c9orf72/smcr8-containing complex regulates ulk1 and plays a dual role in autophagy. *Science Advances*, 2(9):1–17.

Yeh, T. H., Liu, H. F., Li, Y. W., Lu, C. S., Shih, H. Y., Chiu, C. C., Lin, S. J., Huang, Y. C., and Cheng, Y. C. (2018). C9orf72 is essential for neurodevelopment and motility mediated by cyclin g1. *Experimental Neurology*, 304(January):114–124.

Zamiri, B., Reddy, K., Macgregor, R. B., and Pearson, C. E. (2014). Tmpyp4 porphyrin distorts rna g-quadruplex structures of the disease-associated r(ggggcc)n repeat of the c9orf72 gene and blocks interaction of rnabinding proteins. *Journal of Biological Chemistry*, 289(8):4653–4659.

Zhang, D., Iyer, L. M., He, F., and Aravind, L. (2012). Discovery of novel denn proteins: Implications for the evolution of eukaryotic intracellular membrane structures and human disease. *Frontiers in Genetics*, 3(DEC):1–10.

Zhang, K., Daigle, J. G., Cunningham, K. M., Coyne, A. N., Ruan, K., Grima, J. C., Bowen, K. E., Wadhwa, H., Yang, P., Rigo, F., Taylor, J. P., Gitler, A. D., Rothstein, J. D., and Lloyd, T. E. (2018). Stress granule assembly disrupts nucleocytoplasmic transport. *Cell*, 173(4):958–959.e17.

Zhang, K., Donnelly, C. J., Haeusler, A. R., Grima, J. C., Machamer, J. B., Steinwald, P., Daley, E. L., Miller, S. J., Cunningham, K. M., Vidensky, S., Gupta, S., Thomas, M. A., Hong, I., Chiu, S. L., Huganir, R. L., Ostrow, L. W., Matunis, M. J., Wang, J., Sattler, R., Lloyd, T. E., and Rothstein, J. D. (2015). The c9orf72 repeat expansion disrupts nucleocytoplasmic transport. *Nature*, 525(7567):56–61.

Zhang, Y.-J., Gendron, T. F., Ebbert, M. T. W., ORaw, A. D., Yue, M., Jansen-West, K., Zhang, X., Prudencio, M., Chew, J., Cook, C. N., Daughrity, L. M., Tong, J., Song, Y., Pickles, S. R., Kurti, M. C.-C. A., Rademakers, R., Oskarsson, B., Dickson, D. W., Hu, W., Gitler, A. D., Fryer, J. D., and Petrucelli, L. (2017). Poly(gr) impairs protein translation and stress granule dynamics in c9orf72-associated frontotemporal dementia and amyotrophic lateral sclerosisma gillentine, ln berry, rp goin-kochel, ma ali, j ge, d guffey, ja rosenfeld, v hannig, p bader, m proud, m sh. *J Autism Dev Disord*, 47(3):549–562.

Zhang, Y.-j., Gendron, T. F., Grima, J. C., Sasaguri, H., Xu, Y.-f., Katzman, R. B., Gass, J., Murray, M. E., Shinohara, M., Lin, W.-l., Garrett, A., Stankowski, J. N., Tong, J., Perkerson, E. a., Yue, M., and Chew, J. (2016). C9orf72 poly(ga) aggregates sequester and impair hr23 and nucleocytoplasmic transport proteins. 19(5):668–677.

Zhang, Y.-j., Guo, L., Gonzales, P. K., Gendron, T. F., Wu, Y., Raw, A. D. O., Pickles, S. R., Prudencio, M., Gachechiladze, M. A., Ludwig, C., Tian, R., Chew, J., Deture, M., Lin, W.-l., Tong, J., Daughrity, L. M., Yue, M., Andersen, J. W., Castanedes-casey, M., Kurti, A., Antognetti, G., Mccampbell, A., Rademakers, R., Dickson, D. W., Kampmann, M., Ward, M. E., Fryer, J. D., Link, C. D., Shorter, J., and Petrucelli, L. (2019). Heterochromatin anomalies and double-stranded rna accumulation underlie c9orf72 poly(pr) toxicity. 363(6428):1–27.

Zhang, Y. J., Jansen-West, K., Xu, Y. F., Gendron, T. F., Bieniek, K. F., Lin, W. L., Sasaguri, H., Caulfield, T., Hubbard, J., Daughrity, L., Chew, J., Belzil, V. V., Prudencio, M., Stankowski, J. N., Castanedes-Casey, M., Whitelaw, E., Ash, P. E., DeTure, M., Rademakers, R., Boylan, K. B., Dickson, D. W., and Petrucelli, L. (2014). Aggregation-prone c9ftd/als poly(ga) ran-translated proteins cause neurotoxicity by inducing er stress. *Acta Neuropathologica*, 128(4):505–524.

Zhou, Q., Lehmer, C., Michaelsen, M., Mori, K., Alterauge, D., Baumjohann, D., Schludi, M. H., Greiling, J., Farny, D., Flatley, A., Feederle, R., May, S., Schreiber, F., Arzberger, T., Kuhm, C., Klopstock, T., Hermann, A., Haass, C., and Edbauer, D. (2017). Antibodies inhibit transmission and aggregation of c9orf72 poly- ga dipeptide repeat proteins. *EMBO Molecular Medicine*, 9(5):687–702.

Zhu, Q., Jiang, J., Gendron, T. F., McAlonis-Downes, M., Jiang, L., Taylor, A., Diaz Garcia, S., Ghosh Dastidar, S., Rodriguez, M. J., King, P., Zhang, Y., La Spada, A. R., Xu, H., Petrucelli, L., Ravits, J., Da Cruz, S., Lagier-Tourenne, C., and Cleveland, D. W. (2020). Reduced c9orf72 function exacerbates gain of toxicity from als/ftd-causing repeat expansion in c9orf72. *Nature Neuroscience*, 23(5):615–624.

Zu, T., Gibbens, B., Doty, N. S., Gomes-Pereira, M., Huguet, A., Stone, M. D., Margolis, J., Peterson, M., Markowski, T. W., Ingram, M. A., Nan, Z., Forster, C., Low, W. C., Schoser, B., Somia, N. V., Clark, H. B., Schmechel, S., Bitterman, P. B., Gourdon, G., Swanson, M. S., Moseley, M., and Ranum, L. P. (2011). Non-atg-initiated translation directed by microsatellite expansions. *Proceedings of the National Academy of Sciences of the United States of America*,

108(1):260–265.

Zu, T., Liu, Y., Banez-Coronel, M., Reid, T., Pletnikova, O., Lewis, J., Miller, T. M., Harms, M. B., Falchook, A. E., Subramony, S. H., Ostrow, L. W., Rothstein, J. D., Troncoso, J. C., and Ranum, L. P. W. (2013). Ran proteins and rna foci from antisense transcripts in c9orf72 als and frontotemporal dementia. *Proceedings of the National Academy of Sciences*, 110(51):E4968–E4977.